8. ELECTRO-OSMOTIC PUMPING OF CAUSTIC SODA SOLUTIONS WITH DIFFERENT ION-EXCHANGE MEMBRANES

Caustic soda brine concentrations, water flows and current efficiencies were determined at different current densities for different caustic soda feed water concentrations. Membrane permselectivities (apparent transport numbers) were measured at the same concentrations differences as encountered during EOP experiments. The EOP results are summarized in Tables 8.1 to 8.11.

8.1 Brine Concentration

Caustic soda brine concentration (c_b) as a function of current density (I) is shown in Figures 8.1 to 8.3. Initially caustic soda brine concentration increases rapidly and then levels off at higher current densities similar to the results that have been obtained with sodium chloride and hydrochloric acid solutions. Brine concentration increases with increasing current density and increasing feed water concentration. Caustic soda brine concentrations obtained at the highest current densities studied are shown in Table 8.12.

Table 8.12: Caustic soda brine concentrations obtained at the highest current densities investigated for different caustic soda feed water concentrations.

Feed Concentration mol/ℓ	Brine Concentration* (%)		
	Selemion AMV & CMV	Selemion AMP & CMV	Ionac MA-3475 & MC-3470
0,05	14,3	15,4	15,7
0,1	17,7	19,9	18,0
0,5	20,1	22,4	21,7
1,0	24,2	-	16,0

* Data obtained from Tables 8.1 to 8.11.

Very high caustic soda brine concentrations were obtained for all the membranes investigated. Caustic soda brine concentrations of 17,7; 19,9 and 18,0% could be obtained from a 0,1 mol/ℓ caustic soda feed solution with *Selemion* AMV and CMV; *Selemion* AMP and CMV and *Ionac* MA-3475 and MC-3470 membranes, respectively. It is known from the literature that there is presently not an anion-exchange membrane commercially available that is stable at high caustic soda concentrations for long periods[114]. The *Selemion* AMP anion-exchange membrane is claimed by the manufacturers to be more resistant to caustic soda solutions than other commercially

Table 8.1: Electro-osmotic pumping experimental conditions and results for 0,05 mol/ℓ caustic soda (Selemion AMV and CMV).

Current Density	Brine concentration c_b, mol/l		Water flow	Current Efficiency	Effective Current Density	Transport Numbers				
I, mA/cm²	$c_{b\ exp.}$	$c_{b\ calc.}$	J, cm/h	e_p, %	I_{eff}, mA/cm²	Δt^c	Δt^a	$\bar{\Delta}t$	$\bar{t}_1^c$	$\bar{t}_2^a$
10	2,30	3,15	0,0953	58,79	5,88	0,73	0,88	0,80	0,86	0,94
20	2,88	4,08	0,1413	54,43	10,89	0,68	0,87	0,77	0,84	0,94
30	3,18	4,59	0,1854	52,61	15,78	0,65	0,87	0,76	0,82	0,94
40	3,20	5,04	0,2251	48,29	19,31	0,65	0,87	0,76	0,83	0,93
50	3,58	5,50	0,2472	47,39	23,69	0,59	0,87	0,73	0,79	0,94

Electro-osmotic coefficient (2ß) = 0,228 ℓ/F (slope = 0,0085120 mℓ/mAh)
J_{osm} = y-intercept = 0,054571 cm/h
c_b^{max} = 4,39 mol/l
$\Delta t^c = t_1^c - t_2^c$

$\Delta t^a = t_2^a - t_1^a$
$\bar{\Delta}t$ = Average transport number of membrane pair
$\bar{t}_1^c$ = Transport number of cation through cation membrane
$\bar{t}_2^a$ = Transport number of anion through anion membrane.

Table 8.2: Electro-osmotic pumping experimental conditions and results for 0,1 mol/ℓ caustic soda (Selemion AMV and CMV)

Current Density	Brine concentration c_b, mol/l		Water flow	Current Efficiency	Effective Current Density	Transport Numbers				
I, mA/cm²	$c_{b\ exp.}$	$c_{b\ calc.}$	J, cm/h	e_p, %	I_{eff}, mA/cm²	Δt^c	Δt^a	$\bar{\Delta}t$	$\bar{t}_1^c$	$\bar{t}_2^a$
10	2,16	2,67	0,1147	66,46	6,65	0,78	0,86	0,82	0,89	0,93
20	2,78	3,46	0,1721	64,04	12,81	0,74	0,85	0,80	0,87	0,93
30	3,45	4,31	0,1960	60,43	18,13	0,67	0,84	0,75	0,83	0,92
40	3,50		0,2578	60,48	24,19	0,68	0,84	0,76	0,84	0,92
50	3,69	4,63	0,2966	58,69	29,35	0,64	0,84	0,74	0,82	0,92
60	3,82		0,3108	53,04	31,83	0,67	0,81	0,74	0,83	0,90
80	4,33	5,59	0,3567	51,70	41,36	0,62	0,80	0,71	0,81	0,90
100	4,43	6,21	0,4203	49,85	49,85	0,60	0,80	0,70	0,80	0,90

Electro-osmotic coefficient (2ß) = 0,179 ℓ/F (slope = 0,0066710 mℓ/mAh)
J_{osm} = y-intercept = 0,0898921 cm/h
c_b^{max} = 5,59 mol/l
$\Delta t^c = t_1^c - t_2^c$

$\Delta t^a = t_2^a - t_1^a$
$\bar{\Delta}t$ = Average transport number of membrane pair
$\bar{t}_1^c$ = Transport number of cation through cation membrane
$\bar{t}_2^a$ = Transport number of anion through anion membrane.

Table 8.3 : Electro-osmotic pumping experimental conditions and results for 0,5 mol/ℓ caustic soda (Selemion AMV and CMV).

Current Density	Brine concentration c_b, mol/l		Water flow	Current Efficiency	Effective Current	Transport Numbers				
I, mA/cm²	$c_{b\ exp.}$	$c_{b\ calc}$	J, cm/h	ep, %	I_{eff}, mA/cm²	Δt^c	Δt^a	$\bar{\Delta}t$	$\bar{t}_1^c$	$\bar{t}_2^a$
10	2,2	2,02	0,1457	66,39	6,64	0,78	0,80	0,79	0,89	0,90
20	2,33	3,32	0,1748	66,20	13,23	0,77	0,78	0,78	0,89	0,89
30	3,36	3,96	0,2120	63,62	19,89	0,73	0,77	0,75	0,87	0,88
40	3,56		0,2560	61,09	24,28	0,70	0,78	0,74	0,85	0,89
50	3,96	4,97	0,2649	56,24	28,12	0,65	0,76	0,71	0,83	0,88
60	4,13		0,2825	52,07	31,24	0,62	0,77	0,70	0,81	0,89
70	4,39	5,80	0,3072	51,65	36,16	0,59	0,78	0,68	0,79	0,89
80	4,53		0,3355	50,87	40,70	0,60	0,77	0,68	0,80	0,88
100	4,83	6,31	0,3920	50,71	50,71	0,57	0,76	0,66	0,79	0,88
120	5,03	6,40	0,459	51,54	61,85	0,58	0,73	0,66	0,79	0,87

Electro-osmotic coefficient (2ß) = 0,152 ℓ/F (slope = 0,0056728 mℓ/mAh)
J_{osm} = y-intercept = 0,1059033 cm/h
c_b^{max} = 6,58 mol/l
$\Delta t^c = t_1^c - t_2^c$

$\Delta t^a = t_2^a - t_1^a$
$\bar{\Delta}t$ = Average transport number of membrane pair
$\bar{t}_1^c$ = Transport number of cation through cation membrane
$\bar{t}_2^a$ = Transport number of anion through anion membrane.

Table 8.4: Electro-osmotic pumping experimental conditions and results for 1 mol/ℓ NaOH (Selemion AMV and CMV)

Current Density	Brine concentration c_b, mol/l		Water flow	Current Efficiency	Effective Current Density	Transport Numbers				
I, mA/cm²	$c_{b\,exp.}$	$c_{b\,calc.}$	J, cm/h	ϵ_p, %	I_{eff}, mA/cm²	Δt^c	Δt^a	$\bar{\Delta}t$	$\bar{t}_1^c$	$\bar{t}_2^a$
30	4,4	3,5	0,1943	76,37	22,91	0,57	0,75	0,66	0,78	0,87
50	5,2	4,55	0,2649	73,84	36,92	0,56	0,74	0,65	0,77	0,86
70	5,8	5,3	0,3046	67,66	47,36	0,50	0,74	0,62	0,75	0,86
90	6,05	6,3	0,3310	59,66	53,69	0,49	0,75	0,62	0,74	0,87

Electro-osmotic coefficient (2ß) = 0,118 ℓ/F (slope = 0,0044119 mℓ/mAh)
J_{osm} = y-intercept = 0,0962310 cm/h
c_b^{max} = 8,46 mol/l
$\Delta t^c = t_1^c - t_2^c$

$\Delta t^a = t_2^a - t_1^a$
$\bar{\Delta}t$ = Average transport number of membrane pair
$\bar{t}_1^c$ = Transport number of cation through cation membrane
$\bar{t}_2^a$ = Transport number of anion through anion membrane.

Table 8.5 : Electro-osmotic pumping experimental conditions and results for 0,05 mol/ℓ caustic soda (Selemion AMP and CMV)

Current Density	Brine concentration c_b, mol/l		Water flow	Current Efficiency	Effective Current Density	Transport Numbers				
I, mA/cm²	c_b exp.	$c_{b\,calc.}$	J, cm/h	ϵ_p, %	I_{eff}, mA/cm²	Δt^c	Δt^a	$\bar{\Delta}t$	$\bar{t}_1^c$	$\bar{t}_2^a$
10	1,92	2,55	0,118	61,07	6,11	0,74	0,87	0,81	0,87	0,93
20	2,48	3,64	0,172	57,06	11,41	0,82	0,86	0,84	0,91	0,93
30	2,76	3,58	0,235	57,92	17,38	0,67	0,85	0,75	0,84	0,92
40	3,16	3,94	0,268	56,66	22,66	0,57	0,84	0,71	0,79	0,92
50	3,44	4,61	0,293	54,06	27,03	0,61	0,84	0,72	0,80	0,92
60	3,84	5,31	0,297	50,90	30,54	0,59	0,82	0,71	0,79	0,91

Electro-osmotic coefficient (2ß) = 0,176 ℓ/F (slope = 0,0065825 mℓ/mAh)
J_{osm} = y-intercept = 0,1094348 cm/h
$\bar{\Delta}t$ = Average transport number of membrane pair
c_b^{max} = 5,68 mol/l

$\Delta t^a = t_2^a - t_1^a$
$\Delta t^c = t_1^c - t_2^c$
$\bar{t}_1^c$ = Transport number of cation through cation membrane
$\bar{t}_2^a$ = Transport number of anion through anion membrane.

Table 8.6 : Electro-osmotic pumping experimental conditions and results for 0,1 mol/ℓ caustic soda (Selemion AMP and CMV)

Current Density	Brine concentration c_b, mol/l		Water flow	Current Efficiency	Effective Current Density	Transport Numbers				
I, mA/cm²	$c_{b\,exp.}$	$c_{b\,calc.}$	J, cm/h	ϵ_p, %	I_{eff}, mA/cm²	Δt^c	Δt^a	$\bar{\Delta}t$	$\bar{t}_1^c$	$\bar{t}_2^a$
10	2,14	2,53	0,117	67,34	6,73	0,76	0,83	0,79	0,88	0,91
20	2,88	3,33	0,169	65,00	13,00	0,70	0,81	0,76	0,85	0,91
30	3,35	3,69	0,221	66,21	19,86	0,65	0,80	0,73	0,83	0,90
40	3,62		0,248	60,12	24,05	0,59	0,80	0,70	0,80	0,90
50	3,90	4,63	0,282	59,04	29,52	0,59	0,81	0,70	0,80	0,90
60	4,38		0,298	58,32	34,99	0,58	0,79	0,69	0,79	0,89
70	4,41	5,24	0,333	56,20	39,34	0,54	0,79	0,67	0,77	0,90
80	4,61		0,366	56,41	45,13	0,54	0,78	0,66	0,77	0,89
90	4,67	5,61	0,396	55,08	49,57	0,53	0,79	0,66	0,77	0,89
100	4,97	5,82	0,404	53,82	53,82	0,48	0,78	0,63	0,74	0,89

Electro-osmotic coefficient (2ß) = 0,155 ℓ/F (slope = 0,0057673 mℓ/mAh)
J_{osm} = y-intercept = 0,1036958 cm/h
c_b^{max} = 6,45 mol/l
$\Delta t^c = t_1^c - t_2^c$

$\Delta t^a = t_2^a - t_1^a$
$\bar{\Delta}t$ = Average transport number of membrane pair
$\bar{t}_1^c$ = Transport number of cation through cation membrane
$\bar{t}_2^a$ = Transport number of anion through anion membrane.

Table 8.7 : Electro-osmotic pumping experimental conditions and results for 0,50 mol/ℓ caustic soda (Selemion AMP and CMV)

Current Density	Brine concentration c_b, mol/l		Water flow	Current Efficiency	Effective Current Density	Transport Numbers				
I, mA/cm²	$c_{b\ exp.}$	$c_{b\ calc.}$	J, cm/h	ϵ_p, %	I_{eff}, mA/cm²	Δt^c	Δt^a	$\bar{\Delta}t$	$\bar{t}_1^c$	$\bar{t}_2^a$
10	2,29	2,62	0,110	67,75	6,78	0,76	0,79	0,77	0,88	0,89
20	3,02	3,36	0,159	64,33	12,87	0,66	0,78	0,72	0,83	0,89
30	3,57	4,05	0,196	62,63	18,79	0,65	0,77	0,71	0,83	0,88
40	3,98		0,236	62,99	25,20	0,56	0,77	0,67	0,78	0,88
50	4,12	4,71	0,265	58,58	29,29	0,60	0,74	0,67	0,80	0,88
60	4,43	5,02	0,295	58,42	35,05	0,58	0,74	0,66	0,79	0,87
70	4,89		0,282	52,83	36,98	0,47	0,75	0,61	0,74	0,87
80	4,83	5,67	0,331	53,59	42,87	0,53	0,72	0,63	0,77	0,86
100	5,19	5,59	0,399	55,46	55,46	0,48	0,72	0,60	0,74	0,86
120	5,59	6,29	0,419	52,76	63,31	0,47	0,70	0,59	0,74	0,85

Electro-osmotic coefficient (2ß) = 0,137 ℓ/F (slope = 0,0051179 mℓ/mAh)
J_{osm} = y-intercept = 0,1068910 cm/h
c_b^{max} = 7,30 mol/l
$\Delta t^c = t_1^c - t_2^c$

$\Delta t^a = t_2^a - t_1^a$
$\bar{\Delta}t$ = Average transport number of membrane pair
$\bar{t}_1^c$ = Transport number of cation through cation membrane
$\bar{t}_2^a$ = Transport number of anion through anion membrane.

Table 8.8 : Electro-osmotic pumping experimental conditions and results for 0,05 mol/ℓ caustic soda (Ionac MA-3475 and MC-3470)

Current Density	Brine concentration c_b, mol/l		Water flow	Current Efficiency	Effective Current Density	Transport Numbers				
I, mA/cm²	$c_{b\ exp.}$	$c_{b\ calc}$	J, cm/h	ϵ_p, %	I_{eff}, mA/cm²	Δt^c	Δt^c	$\bar{\Delta}t$	$\bar{t}_1^a$	$\bar{t}_2^a$
10	2,77	2,79	0,0927	68,8	0,8196	0,57	0,82	0,69	0,78	0,91
20	3,4	3,61	0,1391	63,37	12,6	0,55	0,80	0,67	0,77	0,90
30	3,76	3,96	0,1854	62,29	18,6	0,51	0,80	0,66	0,76	0,90
40	3,92	4,14	0,2344	61,59	24,63	0,51	0,79	0,65	0,75	0,90

Electro-osmotic coefficient (2ß) = 0,212 ℓ/F (slope = 0,0079229 mℓ/mAh)
J_{osm} = y-intercept = 0,0388302 cm/h
c_b^{max} = 4,72 mol/l
$\Delta t^c = t_1^c - t_2^c$

$\Delta t^a = t_2^a - t_1^a$
$\bar{\Delta}t$ = Average transport number of membrane pair
$\bar{t}_1^c$ = Transport number of cation through cation membrane
$\bar{t}_2^a$ = Transport number of anion through anion membrane.

Table 8.9 : Electro-osmotic pumping experimental conditions and results for 0,1 mol/ℓ caustic soda (Ionac MA-3475 and MC-3470)

Current Density	Brine concentration c_b, mol/l		Water flow,	Current Efficiency	Effective Current Density	Transport Numbers				
I, mA/cm²	$c_{b\ exp.}$	$c_{b\ calc.}$	J, cm/h	ϵ_p, %	I_{eff}, mA/cm²	Δt^c	Δt^a	$\bar{\Delta}t$	$\bar{t}_1^c$	$\bar{t}_2^a$
10	2,63	2,58	0,1033	72,22	7,22	0,61	0,81	0,71	0,81	0,91
20	3,4	3,38	0,1522	69,38	13,88	0,57	0,80	0,69	0,79	0,90
30	3,71	3,69	0,200	66,77	20,03	0,52	0,80	0,66	0,76	0,90
40	4,1		0,247	67,93	27,17	0,48	0,79	0,64	0,74	0,89
50	4,26	4,04	0,279	64,50	32,25	0,43	0,78	0,60	0,71	0,89
60	4,15		0,318	58,93	35,35					
70	4,45	4,37	0,371	63,19	44,23	0,45	0,79	0,62	0,73	0,89
75	4,51		0,371	59,71	44,78	0,43	0,79	0,61	0,71	0,89

Electro-osmotic coefficient (2ß) = 0,193 ℓ/F (slope = 0,0071947 mℓ/mAh)
J_{osm} = y-intercept = 0,0529144 cm/h
c_b^{max} = 5,18 mol/l
$\Delta t^c = t_1^c - t_2^c$

$\Delta t^a = t_2^a - t_1^a$
$\bar{\Delta}t$ = Average transport number of membrane pair
$\bar{t}_1^c$ = Transport number of cation through cation membrane
$\bar{t}_2^a$ = Transport number of anion through anion membrane.

Table 8.10 : Electro-osmotic pumping experimental conditions and results for 0,5 mol/ℓ caustic soda (Ionac MA-3475 and MC-3470)

Current Density	Brine concentration c_b, mol/l		Water flow	Current Efficiency	Effective Current Density	Transport Numbers				
I, mA/cm²	$c_{b\,exp.}$	$c_{b\,calc.}$	J, cm/h	e_p, %	I_{eff}, mA/cm²	Δt^c	Δt^a	$\bar{\Delta}t$	$\bar{t}_1^c$	$\bar{t}_2^a$
10	2,63	2,13	0,0993	70,56	7,06	0,37	0,76	0,57	0,68	0,88
20	3,40	2,86	0,1378	62,77	12,55	0,32	0,73	0,53	0,66	0,87
30	3,98	3,14	0,1854	65,86	19,76	0,32	0,72	0,52	0,66	0,86
40	4,33	3,35	0,2296	66,65	26,66	0,22	0,72	0,47	0,61	0,86
50	4,50		0,2560	61,77	30,88	0,20	0,72	0,46	0,60	0,86
60	4,55		0,3178	64,62	38,77					
70	4,98	3,50	0,3443	65,67	45,97	0,22	0,70	0,46	0,61	0,85
80	5,00		0,3921	65,68	52,55					
90	5,23	3,71	0,4132	64,31	57,88	0,21	0,70	0,46	0,61	0,85
100	5,20		0,4503	62,77	62,77					
110	5,43		0,14768	63,04	69,34					

Electro-osmotic coefficient (2ß) = 0,176 ℓ/F (slope = 0,0065599 mℓ/mAh)
J_{osm} = y-intercept = 0,0526844 cm/h
c_b^{max} = 5,68 mol/l
$\Delta t^c = t_1^c - t_2^c$

$\Delta t^a = t_2^a - t_1^a$
$\bar{\Delta}t$ = Average transport number of membrane pair
$\bar{t}_1^c$ = Transport number of cation through cation membrane
$\bar{t}_2^a$ = Transport number of anion through anion membrane.

Table 8.11: Electro-osmotic pumping experimental conditions and results for 1,0 mol/ℓ caustic soda (Ionac MA-3475 and MC-3470)

Current Density	Brine concentration c_b, mol/l		Water flow	Current Efficiency	Effective Current Density	Transport Numbers				
I, mA/cm²	$c_{b\,exp.}$	$c_{b\,calc.}$	J, cm/h	e_p, %	I_{eff}, mA/cm²	Δt^c	Δt^a	$\bar{\Delta}t$	$\bar{t}_1^c$	$\bar{t}_2^a$
10	2,75	1,80	0,0971	71,60	7,16	0,20	0,73	0,47	0,60	0,87
20	3,44	2,50	0,1378	63,51	12,70	0,21	0,71	0,46	0,61	0,86
30	3,84	2,70	0,1854	63,62	19,09	0,20	0,68	0,44	0,60	0,84
40	4,02	3,40	0,1986	53,52	21,4	0,18	0,73	0,46	0,59	0,87

Electro-osmotic coefficient (2ß) = 0,193 ℓ/F (slope = 0,0072079 mℓ/mAh)
J_{osm} = y-intercept = 0,0459504 cm/h
c_b^{max} = 5,18 mol/l
$\Delta t^c = t_1^c - t_2^c$

$\Delta t^a = t_2^a - t_1^a$
$\bar{\Delta}t$ = Average transport number of membrane pair
$\bar{t}_1^c$ = Transport number of cation through cation membrane
$\bar{t}_2^a$ = Transport number of anion through anion membrane.

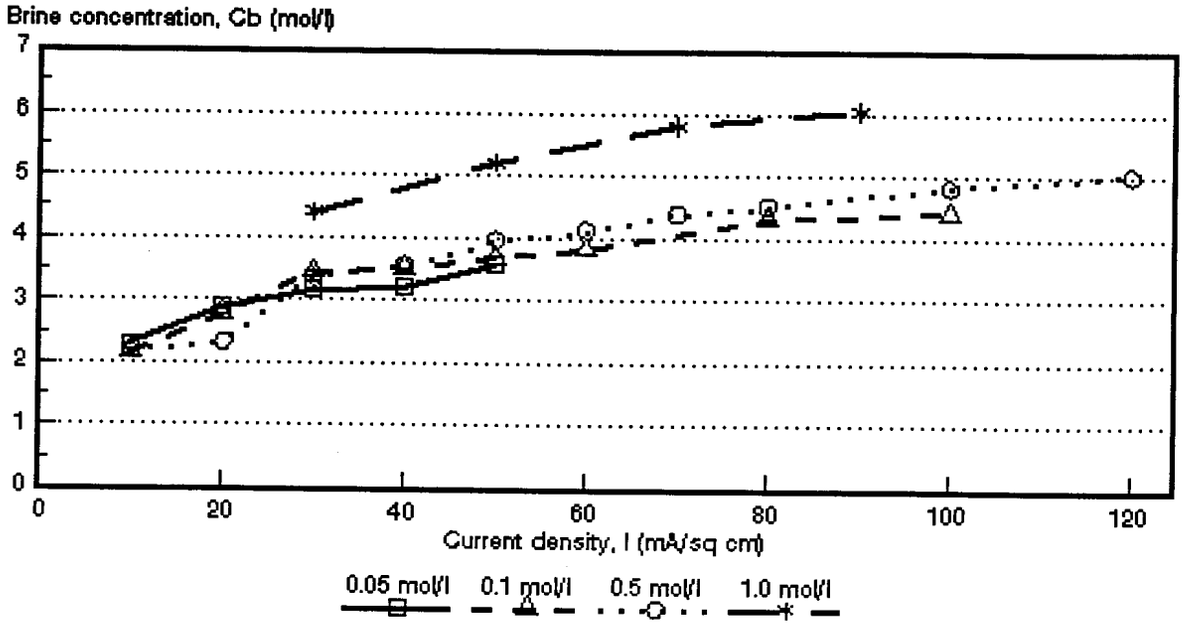

Figure 8.1: **Caustic soda concentration as a function of current density for 4 different NaOH feed water concentrations. *Selemion* AMV and CMV membranes.**

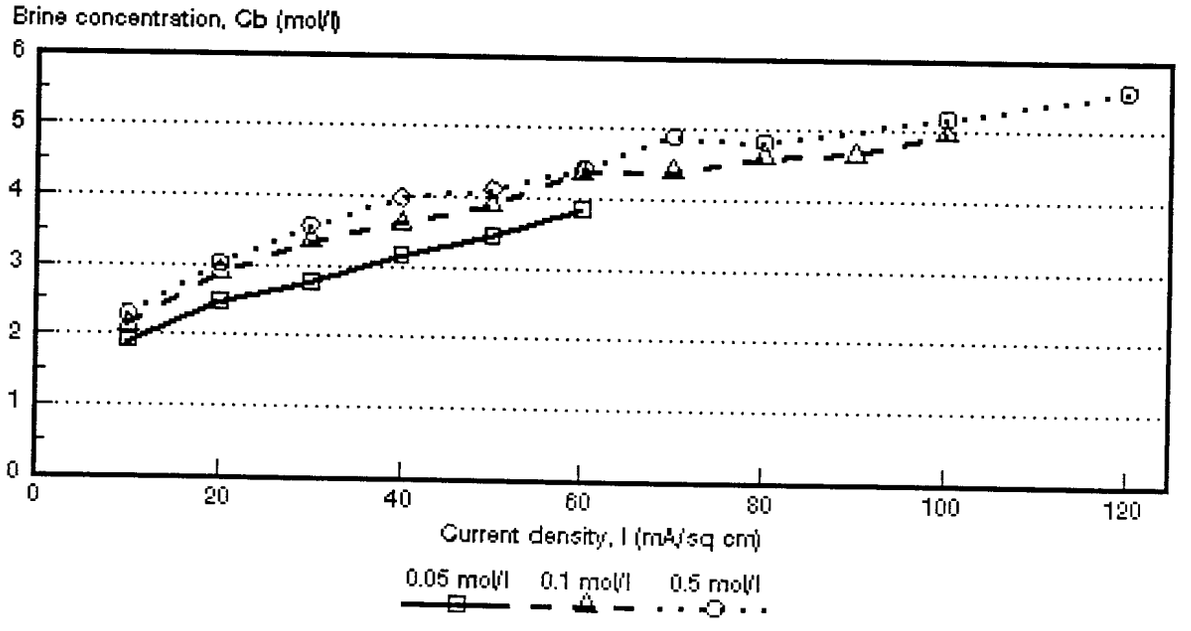

Figure 8.2: **Caustic soda concentration as a function of current density for 3 different NaOH feed water concentrations. *Selemion* AMP and CMV membranes.**

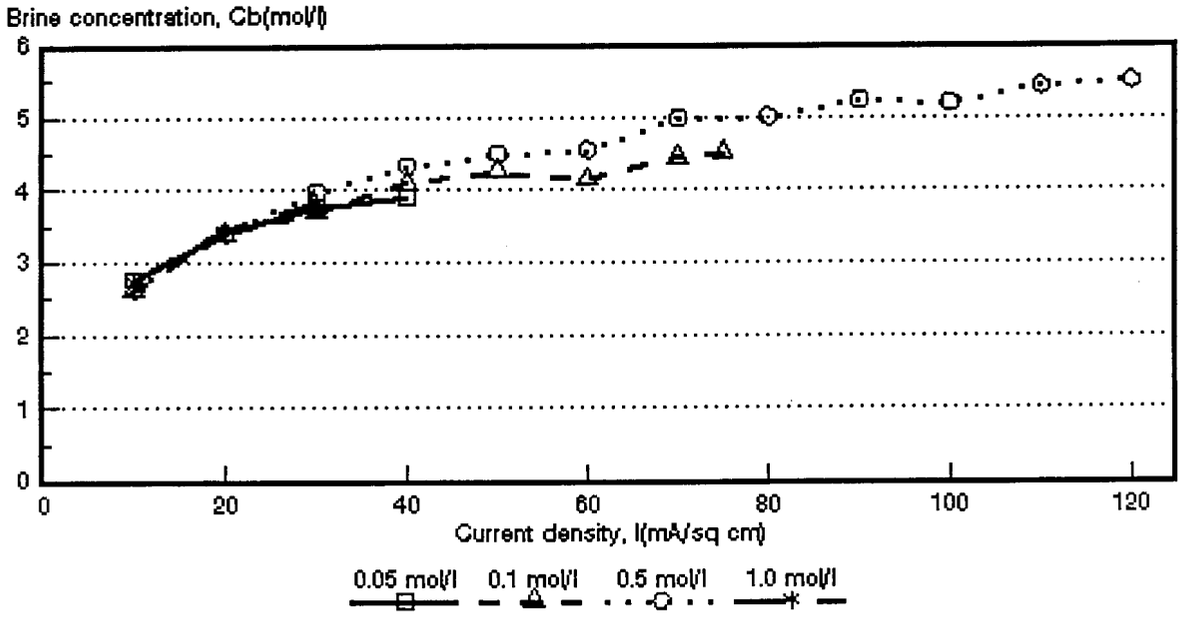

Figure 8.3: **Caustic soda concentration as a function of current density for 4 different NaOH feed water concentrations. *Ionac* MA-3475 and MC-3470 membranes.**

available anion-exchange membranes. Consequently, membrane life time will be a problem when caustic soda solutions are electrodialyzed with conventional ion-exchange membranes. However, the value of the product recovered by ED might be of such a nature that a relatively short membrane life time could be tolerated.

It appears that the caustic soda brine concentration will reach a maximum value, c_b^{max}, as has been experienced with sodium chloride and hydrochloric acid solutions. This maximum value, however, was not reached even at the lowest caustic soda feed concentrations that were used (Figs. 8.1 to 8.3). It appears, however, that the maximum caustic soda brine concentration will be reached at relatively low current densities at the lowest feed water concentrations used. Maximum caustic soda brine concentration for higher caustic soda feed concentrations (0,1 to 1,0 mol/ℓ) will be reached at high current densities.

Maximum caustic soda brine concentration, c_b^{max}, was calculated from the same relationships as used in 6.1. The results are shown in Tables 8.13 and Figures 8.4 to 8.6. Maximum caustic soda brine concentration depends somewhat on feed concentration. The *Selemion* AMV and CMV membranes showed an increase in the maximum brine concentration as a function of feed concentration in the feed

Table 8.13: Maximum caustic soda brine concentration, c_b^{max}, calculated from $c_b^{max} = 1/2\ F\beta$* and $c_b^{max} = c_b\ (1 + J_{osm}/J_{eiosm})$**

Feed Concentration mol/ℓ	Maximum Brine Concentration, c_b^{max}					
	AMV and CMV		AMP and CMV		MA-3475 and MC-3470	
	1	2	1	2	1	2
0,05	4,4	4,6	5,7	5,8	4,7	4,7
0,10	5,6	5,4	6,5	6,4	5,2	5,2
0,50	6,6	6,5	7,3	7,2	5,7	5,7
1,0	8,5	8,5			5,2	5,2

1 : $c_b^{max} = 1/2\ F\beta$
2 : $c_b^{max} = c_b\ (1 + J_{osm}/J_{eiosm})$
* : Calculated from electro-osmotic coefficients (Tables 8.1 - 8.11)
** : Calculated from $J_{eiosm} = J - J_{osm}$ (y-intercept and the corresponding c_b values) (Tables 8.1 - 8.11).

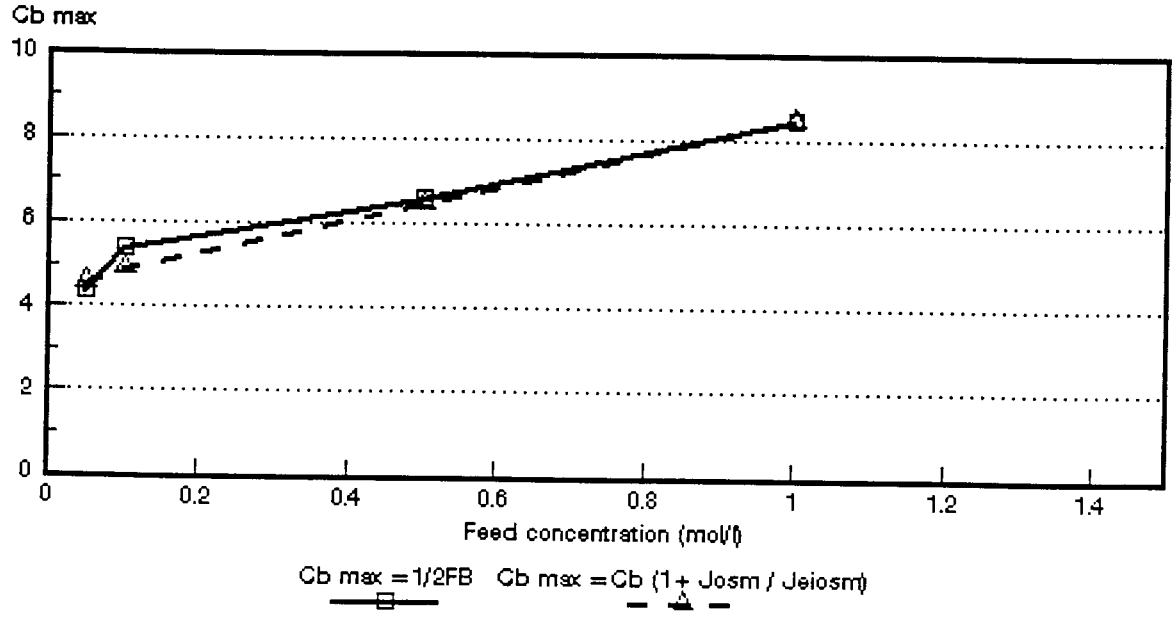

Figure 8.4: Maximum caustic soda brine concentration as a function of feed concentration for different NaOH feed water concentrations. *Selemion* AMV and CMV membranes.

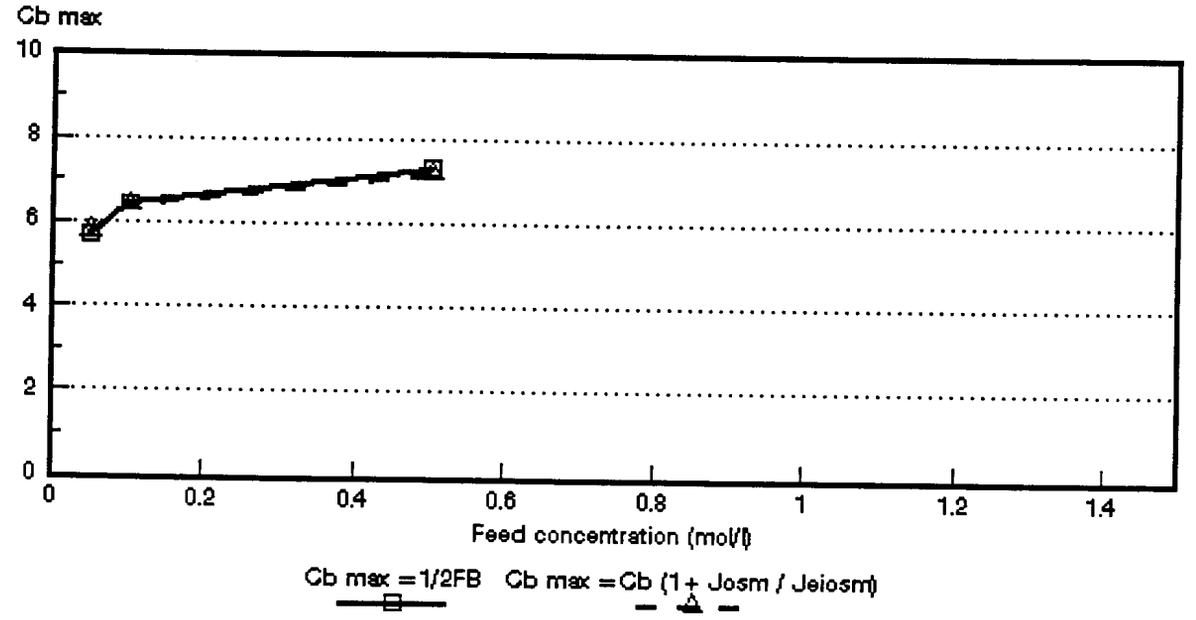

Figure 8.5: **Maximum caustic soda brine concentration as a function of feed concentration for different NaOH feed water concentrations. *Selemion* AMP and CMV membranes.**

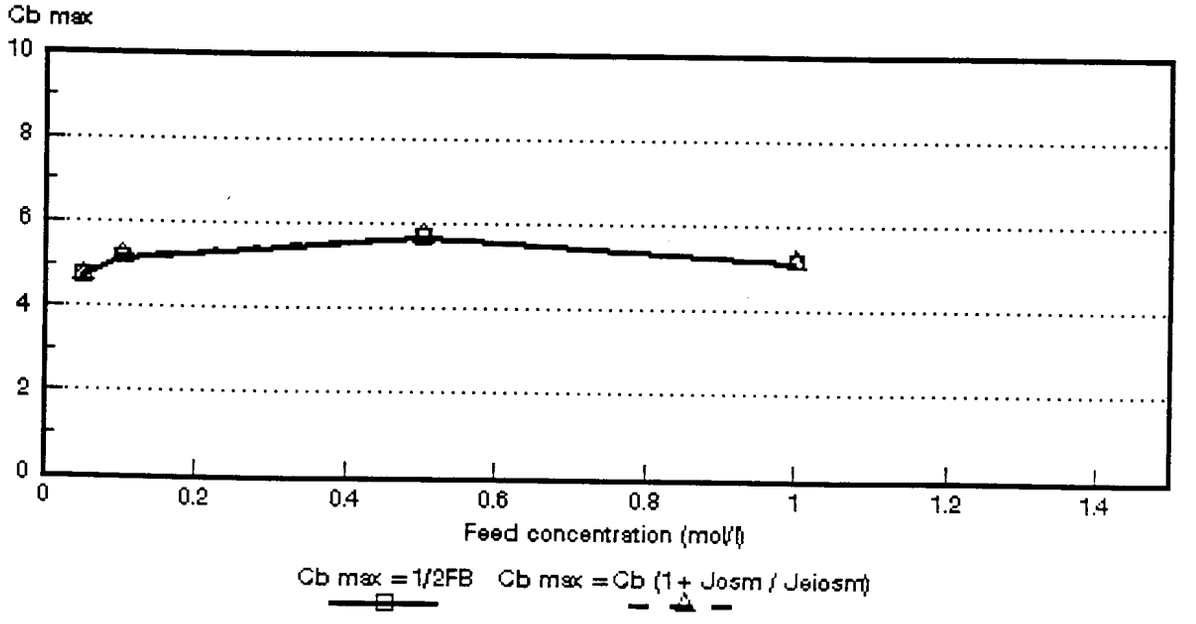

Figure 8.6: **Maximum caustic soda brine concentration as a function of feed concentration for different NaOH feed water concentrations. *Ionac* MA-3475 and MC-3470 membranes.**

concentration range from 0,05 to 1,0 mol/ℓ (Fig. 8.4). A similar trend was observed for the Selemion AMP and CMV membranes (Fig. 8.5) while the *Ionac* membranes first showed an increase and then a slight decrease in c_b^{max} at high feed concentration (Fig. 8.6). A very good correlation was again obtained by the two methods that were used to calculate the maximum caustic soda brine concentration (Table 8.13).

Caustic soda brine concentrations obtained at different current densities and feed water concentrations were predicted from measured transport numbers and volume flows (J) with the same relationship as used in 6.1. The experimental and calculated caustic soda brine concentrations are shown in Tables 8.1 to 8.11. and Figures 8.7 to 8.17. The calculated caustic soda brine concentrations were determined from the average value of the apparent transport number of a membrane pair ($\bar{\Delta}t$) and from water flows. The correlations between the calculated and experimentally determined brine concentrations, expressed as the ratio c_{bcalc}/c_{bexp}, are shown in Table 8.14.

The calculated caustic soda brine concentrations were significantly higher than the experimentally determined brine concentrations at a caustic soda feed concentration of 0,05 mol/ℓ in the case of the *Selemion* AMV and CMV and *Selemion* AMP and CMV membranes (Table 8.14). The calculated caustic soda brine concentration was from 1,36 to 1,54 times higher than the experimentally determined brine concentration in the case of the *Selemion* AMV and CMV membranes and from 1,25 to 1,47 higher in the case of the *Selemion* AMP and CMV membranes. However, a much better correlation was obtained at 0,1 and 0,5 mol/ℓ caustic soda feed concentration for both membrane pairs. The ratio c_{bcalc}/c_{bexp} varied between 1,23 and 1,25 (10 to 50 mA/cm^2, 0,1 mol/ℓ feed) and between 0,92 and 1,25 (10 to 50 mA/cm^2, 0,5 mol/ℓ feed) for the *Selemion* AMV and CMV membranes. The same ratio for the *Selemion* AMP and CMV membranes varied between 1,10 and 1,19 (10 to 50 mA/cm^2, 0,1 mol/ℓ feed) and between 1,11 and 1,14 (10 to 50 mA/cm^2, 0,5 mol/ℓ feed). Therefore, a higher estimation of caustic soda brine concentration can be obtained from measured transport numbers and water flows in this case.

A very good correlation was obtained between the calculated and experimentally determined caustic soda brine concentrations in the case of *Ionac* membranes at 0,05 and 0,1 mol/ℓ feed concentration. The ratio c_{bcalc}/c_{bexp} varied between 1,01 and 1,06 (10 to 40 mA/cm^2, 0,05 mol/ℓ feed) and between 0,95 and 0,99 (10 to 70 mA/cm^2, 0,1 mol/ℓ feed). Therefore, an excellent correlation was obtained. However, the correlations at 0,5 and 1,0 mol/ℓ feed for the same membranes were not very good (Table 8.14).

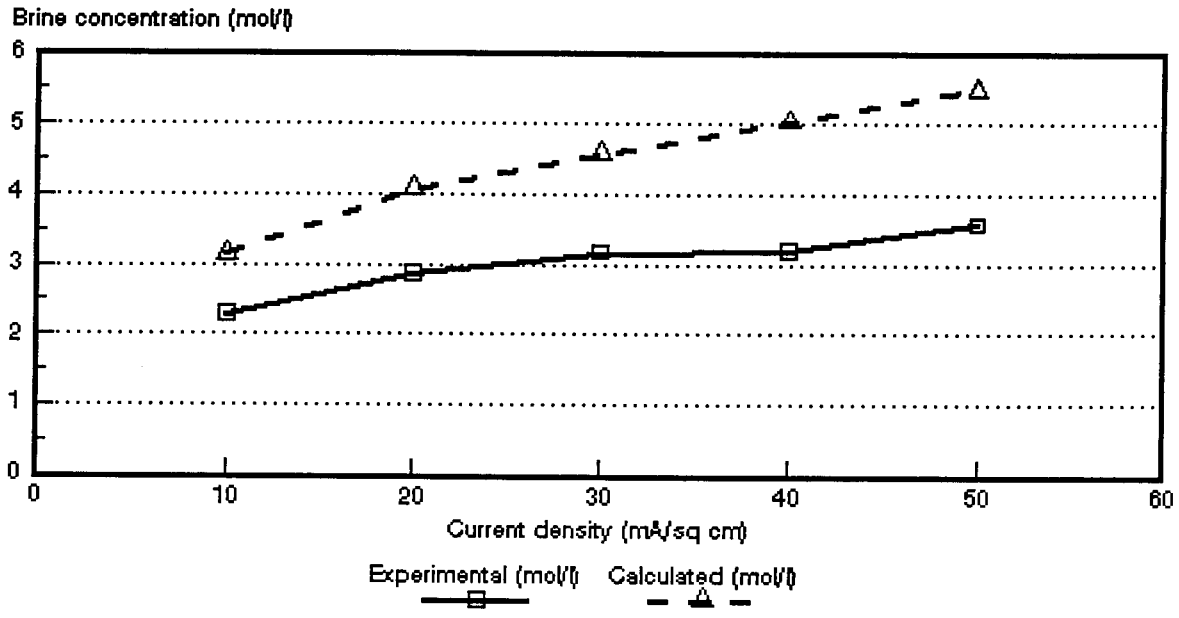

Figure 8.7: **Experimental and calculated caustic soda brine concentrations as a function of current density for 0,05 mol/ℓ NaOH feed solution. *Selemion* AMV and CMV membranes.**

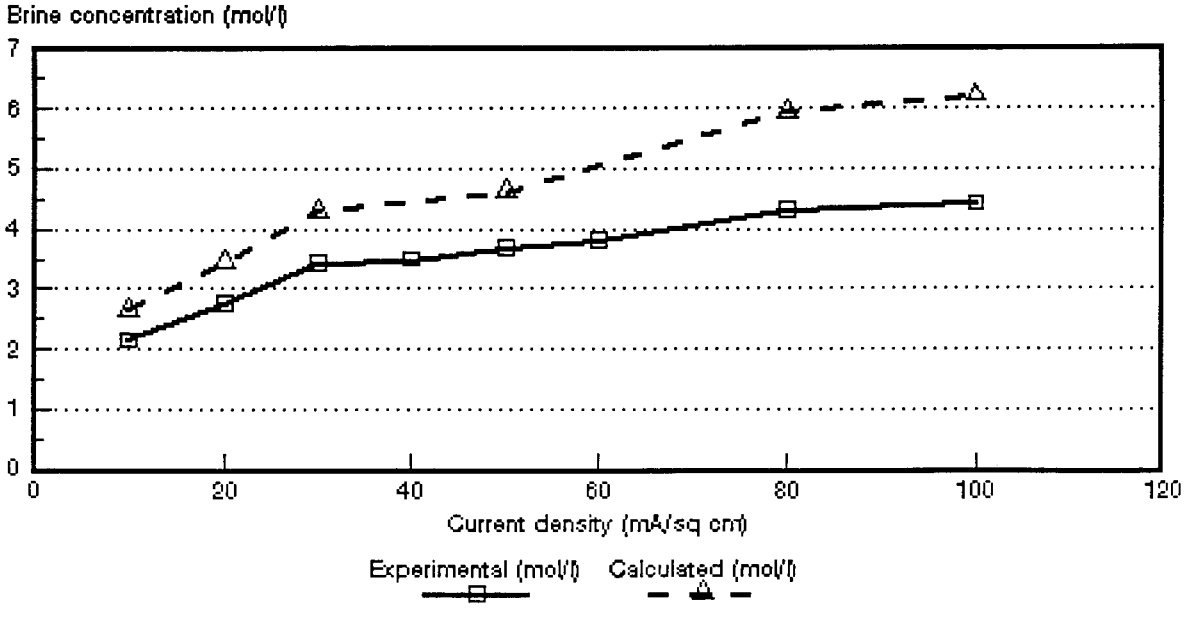

Figure 8.8: **Experimental and calculated caustic soda brine concentrations as a function of current density for 0,1 mol/ℓ NaOH feed solution. *Selemion* AMV and CMV membranes.**

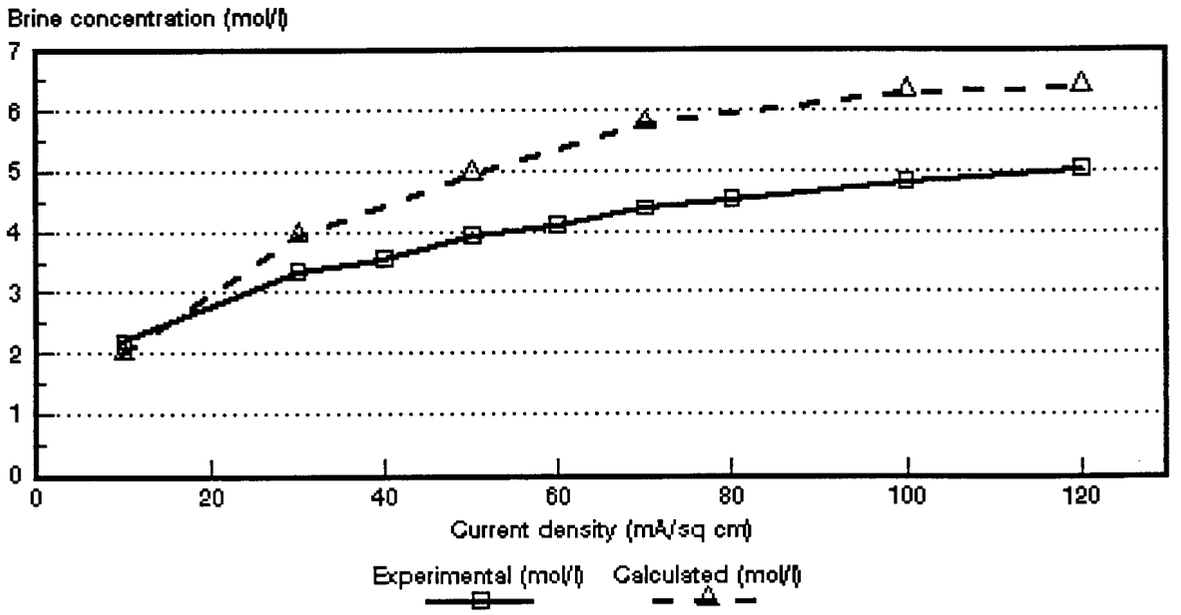

Figure 8.9: **Experimental and calculated caustic soda brine concentrations as a function of current density for 0,5 mol/ℓ NaOH feed solution. *Selemion* AMV and CMV membranes.**

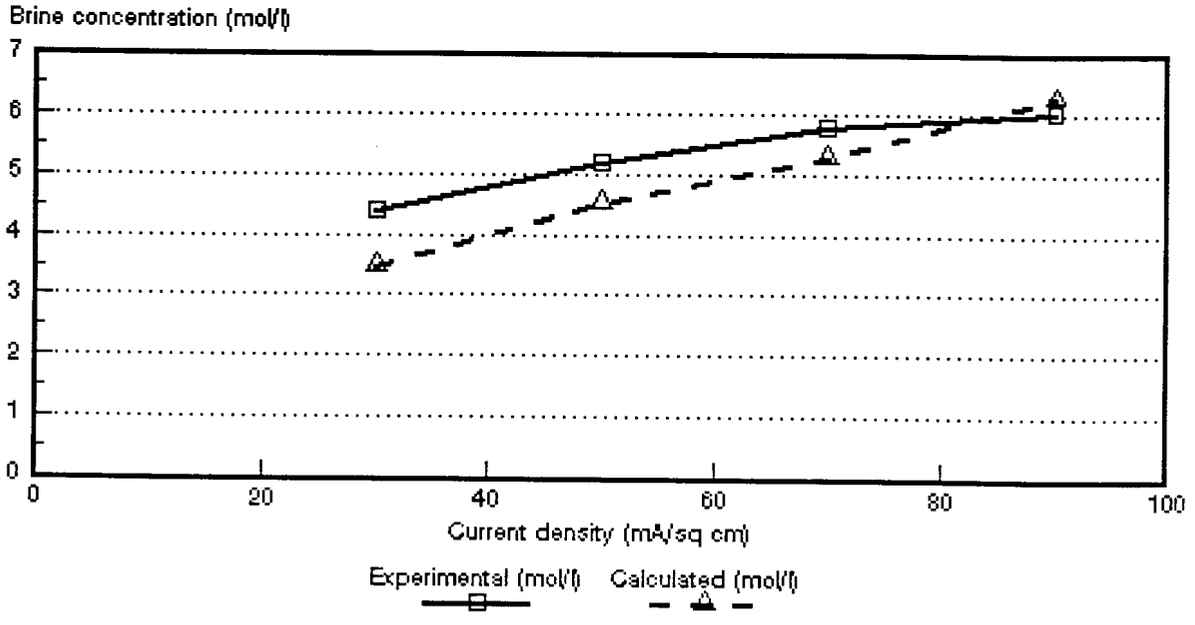

Figure 8.10: **Experimental and calculated caustic soda brine concentrations as a function of current density for 1,0 mol/ℓ NaOH feed solution. *Selemion* AMV and CMV membranes.**

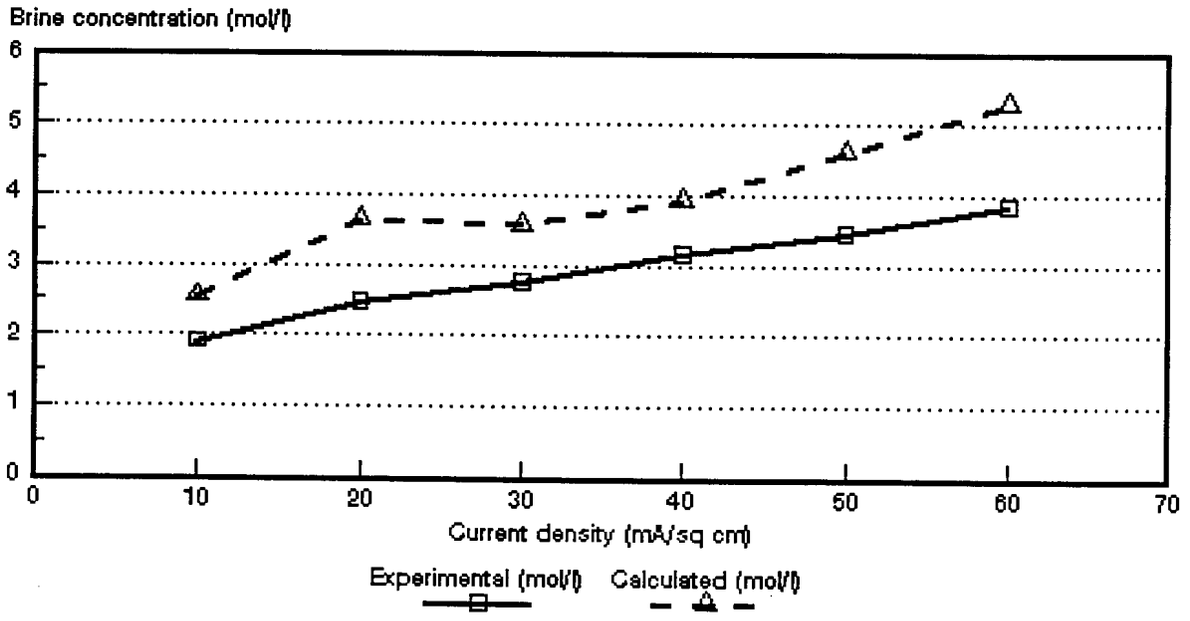

Figure 8.11: **Experimental and calculated caustic soda brine concentrations as a function of current density for 0,05 mol/ℓ NaOH feed solution. *Selemion* AMP and CMV membranes.**

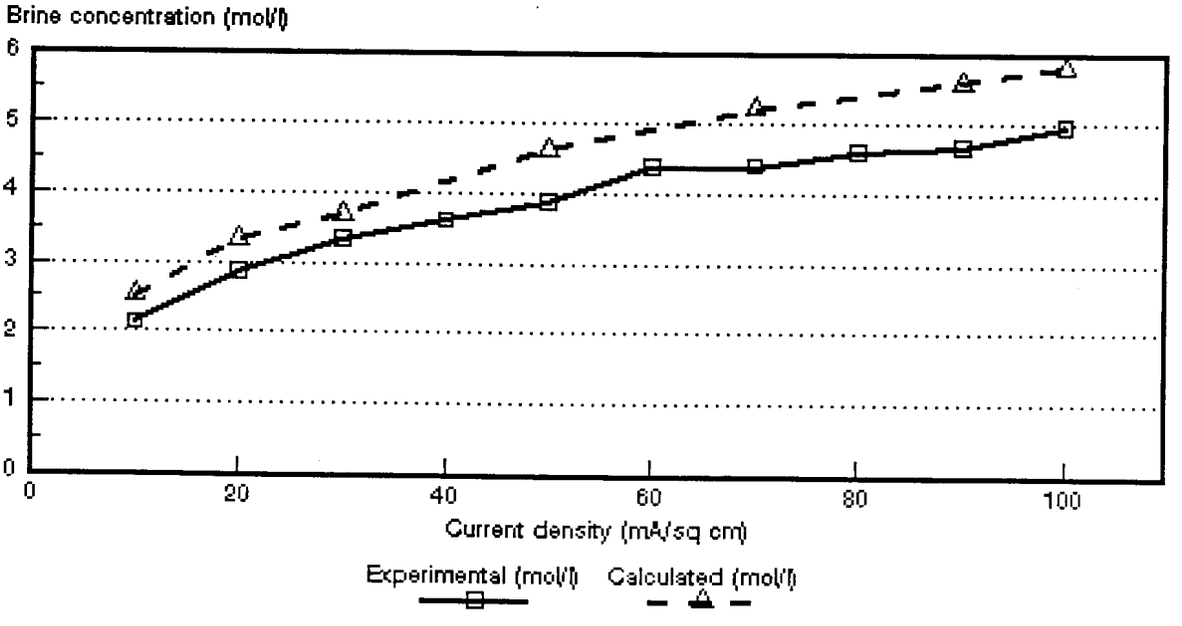

Figure 8.12: **Experimental and calculated caustic soda brine concentrations as a function of current density for 0,1 mol/ℓ NaOH feed solution. *Selemion* AMP and CMV membranes.**

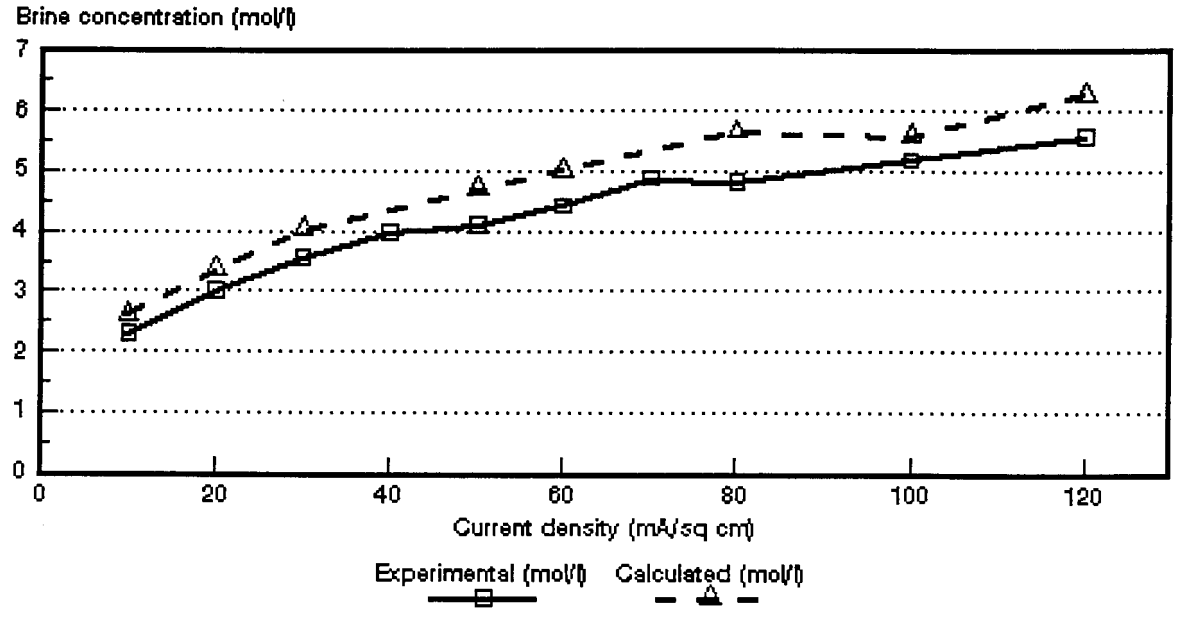

Figure 8.13: **Experimental and calculated caustic soda brine concentrations as a function of current density for 0,5 mol/ℓ NaOH feed solution. *Selemion* AMP and CMV membranes.**

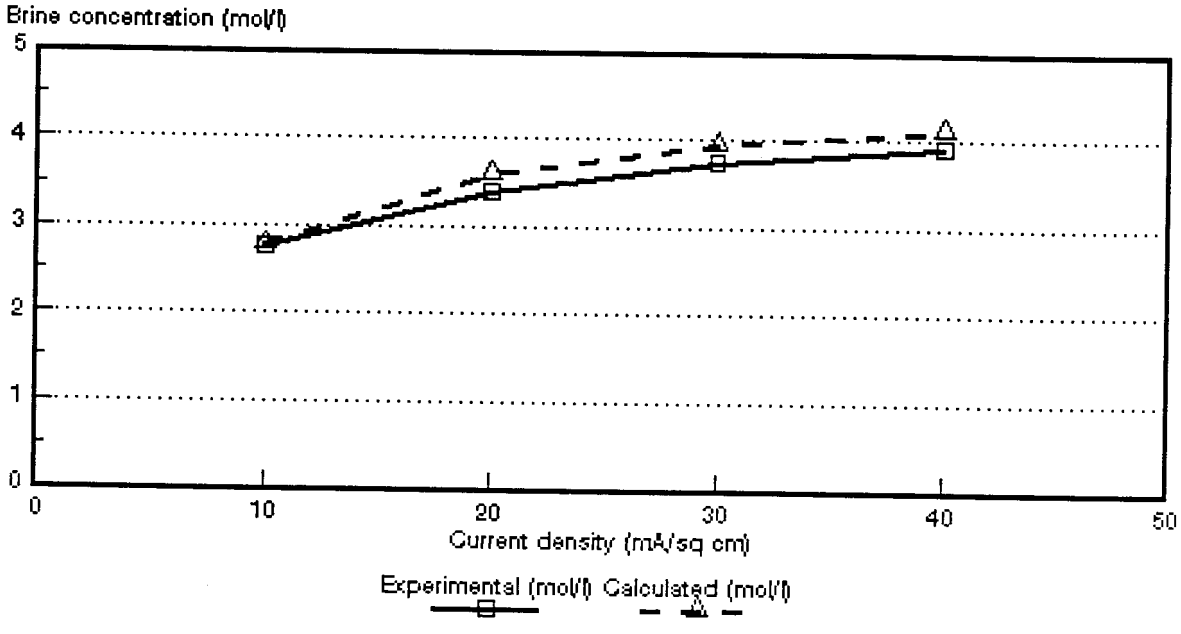

Figure 8.14: **Experimental and calculated caustic soda brine concentrations as a function of current density for 0,05 mol/ℓ NaOH feed solution. *Ionac* MA-3475 and MC-3470 membranes.**

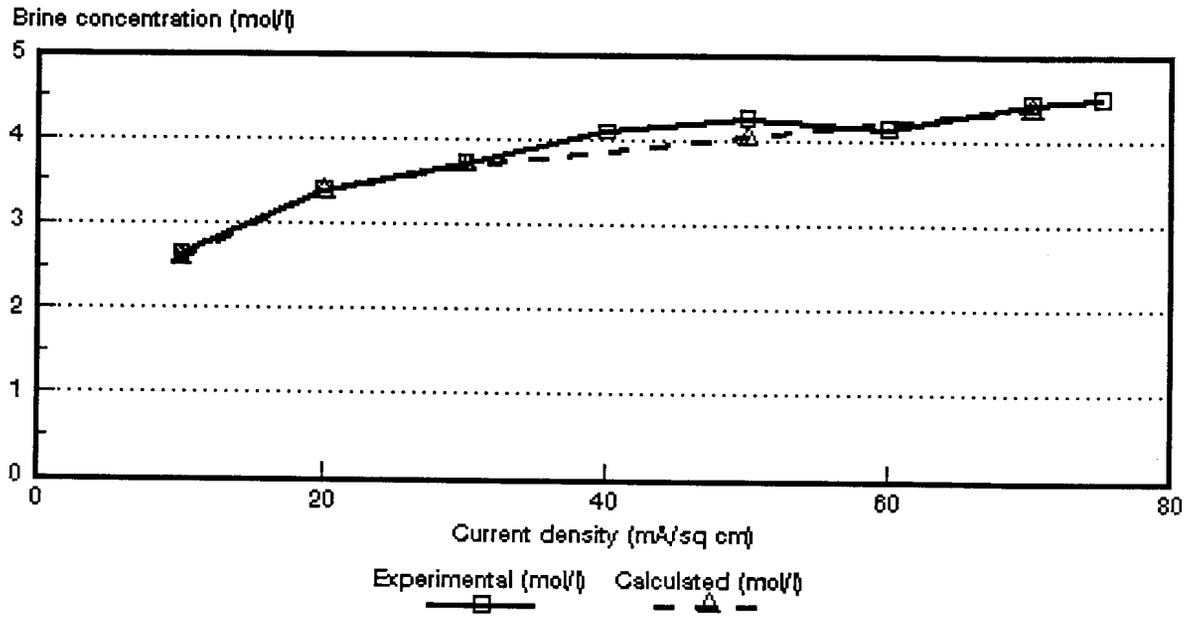

Figure 8.15: **Experimental and calculated caustic soda brine concentrations as a function of current density for 0,1 mol/ℓ NaOH feed solution. *Ionac* MA-3475 and MC-3470 membranes.**

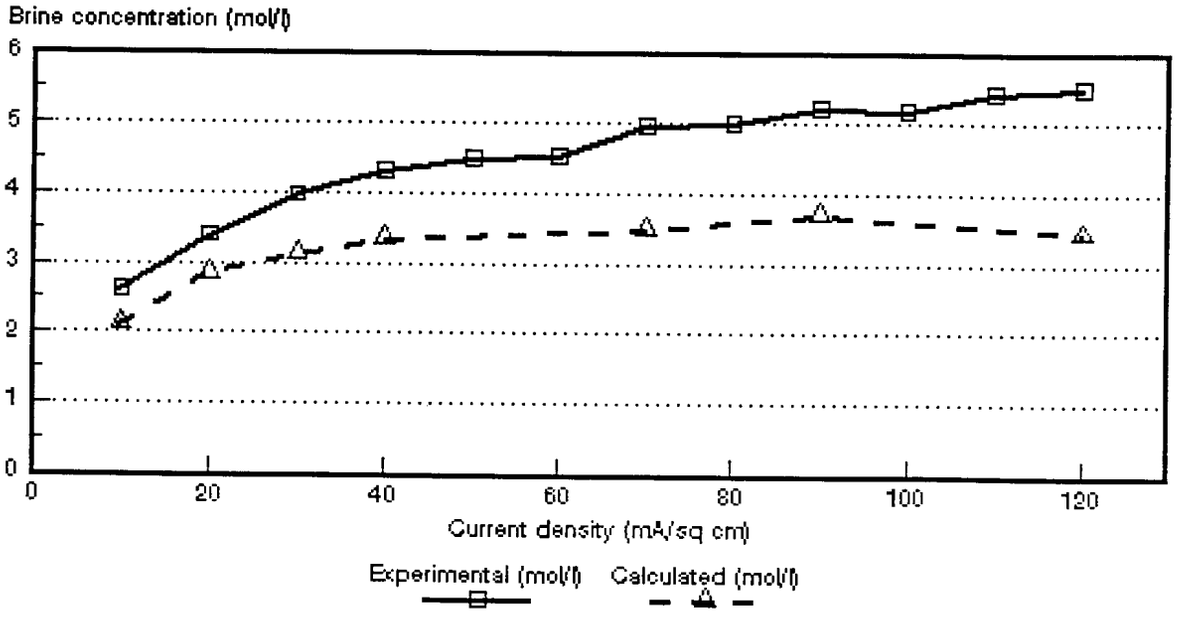

Figure 8.16: **Experimental and calculated caustic soda brine concentrations as a function of current density for 0,5 mol/ℓ NaOH feed solution. *Ionac* MA-3475 and MC-3470 membranes.**

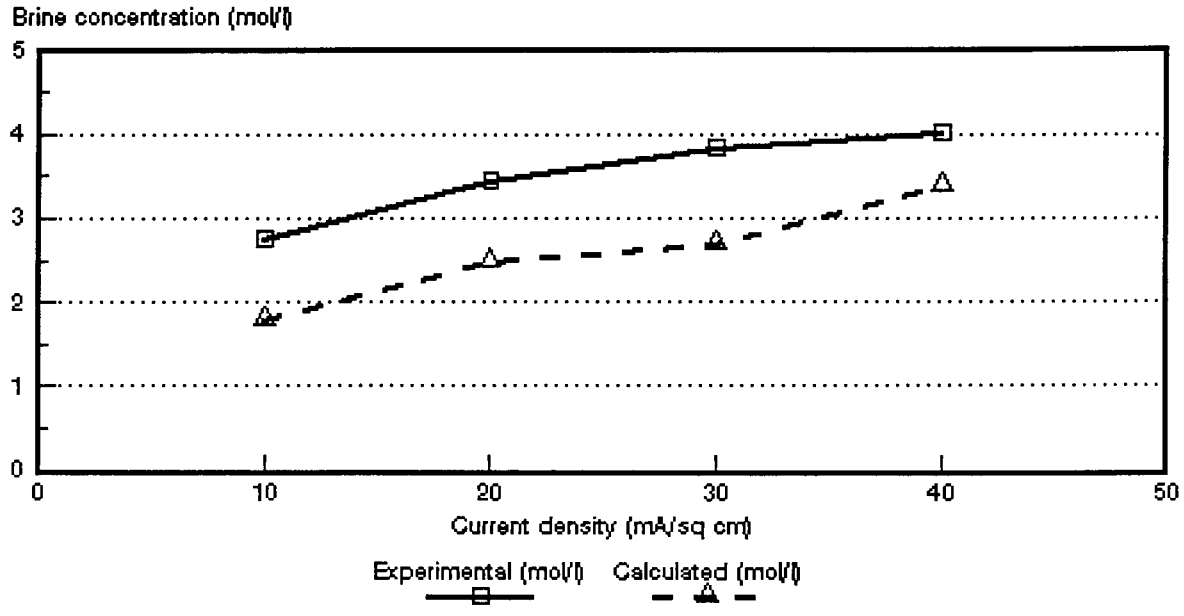

Figure 8.17: **Experimental and calculated caustic soda brine concentrations as a function of current density for 1,0 mol/ℓ NaOH feed solution. *Ionac* MA-3475 and MC-3470 membranes.**

Table 8.14: Correlation between calculated (c_{bcalc}) and experimentally (c_{bexp}) determined brine concentrations.

Current Density	c_{bcalc}/c_{bexp}										
mA/cm²	Selemion AMV & CMV Concentration, mol/ℓ				Selemion AMP & CMV Concentration, mol/ℓ			Ionac MA-3475 & MC-3470 Concentration, mol/ℓ			
	0,05	0,1	0,5	1,0	0,05	0,1	0,5	0,05	0,1	0,5	1,0
10	1,36	1,23	0,92		1,33	1,18	1,14	1,01	0,98	0,81	0,65
20	1,42	1,24	1,42		1,47	1,16	1,11	1,06	0,99	0,84	0,73
30	1,44	1,25	1,18	0,80	1,30	1,10	1,13	1,05	0,99	0,79	0,70
40	1,58				1,25			1,06		0,77	0,85
50	1,54	1,25	1,25	0,88	1,34	1,19	1,14		0,95		
60					1,38		1,13				
70			1,32	0,91		1,19			0,98	0,70	
75											
80		1,29					1,17				
90				1,04		1,20				0,71	
100		1,40	1,30			1,17	1,08				
110											
120							1,13				

8.2 Current Efficiency

Current efficiency (ϵ_p) determined during the EOP experiments as a function of current density and caustic soda feed water concentration is shown in Figures 8.18 to 8.20. Current efficiency increases with increasing feed water concentration in the caustic soda feed concentration range from 0,05 to 1,0 mol/ℓ. However, very little difference in current efficiency was experienced in the 0,1 to 0,5 mol/ℓ feed concentration range. Current efficiency was significantly higher at 1,0 mol/ℓ caustic soda feed concentration in the case of the *Selemion* AMV and CMV membranes (Fig. 8.18). This phenomena was not observed in the case of the *Selemion* AMP and CMV (Fig. 8.19) and the *Ionac* membranes (Fig. 8.20).

Current efficiency decreased slightly with increasing current density. This was observed even at the highest caustic soda feed concentration (1,0 mol/ℓ) in the case of the *Selemion* AMV and CMV membranes (Fig. 8.18). Current efficiency, however, appeared to remain reasonably constant in the 0,1 to 0,5 mol/ℓ feed water concentration range for all the membranes investigated.

The apparent transport numbers ($\bar{\Delta}t$, Δt^a and Δt^c) for a concentration difference similar to that obtained in the EOP experiments are shown in Figures 8.21 to 8.31. The current efficiencies (ϵ_p) as determined by the EOP method and shown in Figures 8.18 to 8.20 are also shown in Figures 8.21 to 8.31. The correlation between the apparent transport numbers ($\bar{\Delta}t$, Δt^a, Δt^c) and the current efficiency is shown in Tables 8.15 to 8.17.

The apparent transport numbers ($\bar{\Delta}t$) were significantly higher than the current efficiencies in the case of the *Selemion* AMV and CMV and *Selemion* AMP and CMV membranes at 0,05 mol/ℓ feed concentration (Table 8.15). The apparent transport numbers were from 1,37 to 1,57 times higher than the current efficiency for the *Selemion* AMV and CMV membranes in the 10 to 40 mA/cm^2 current density range (0,05 mol/ℓ feed). The apparent transport numbers were from 1,30 to 1,48 times higher than current efficiency for the *Selemion* AMP and CMV membranes in the 10 to 60 mA/cm^2 current density range (0,05 mol/ℓ feed). However, better correlations were obtained in the 0,1 and 0,5 mol/ℓ feed concentration range for both membrane types. The apparent transport numbers were approximately 1,2 times higher than the current efficiency in the 0,1 and 0,5 mol/ℓ feed concentration range for the *Selemion* AMV and CMV membranes (10 to 50 mA/cm^2) while the ratio $\bar{\Delta}t/\epsilon_p$ was approximately 0,9 at 1,0

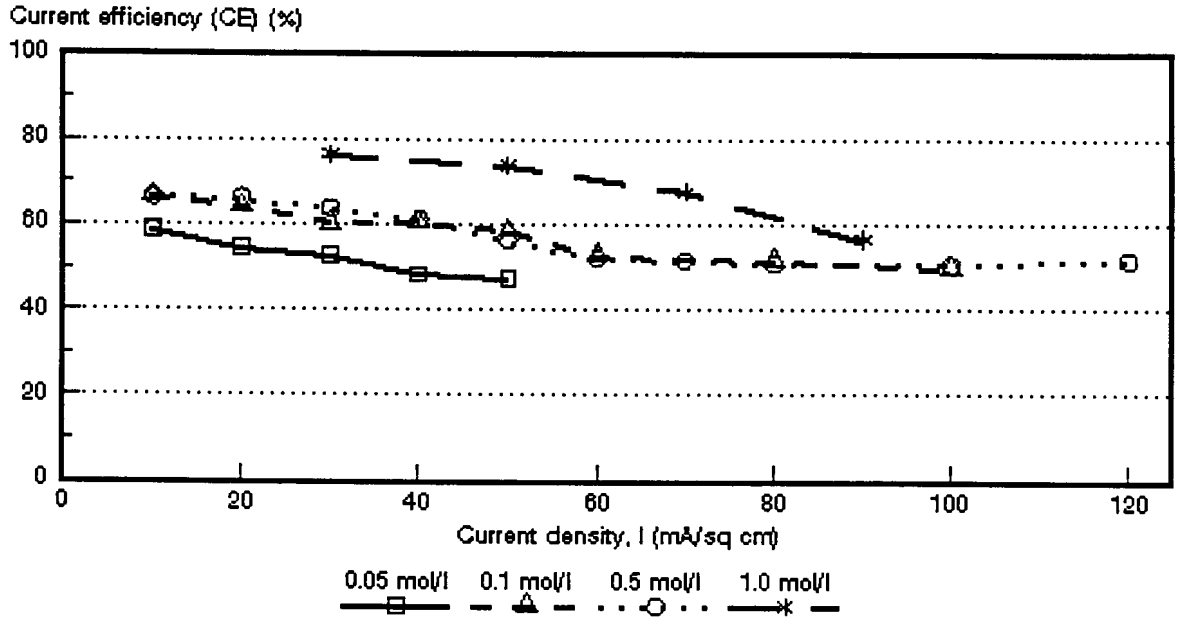

Figure 8.18: **Current efficiency (e_p) as a function of current density for 4 different NaOH feed water concentrations. *Selemion* AMV and CMV membranes.**

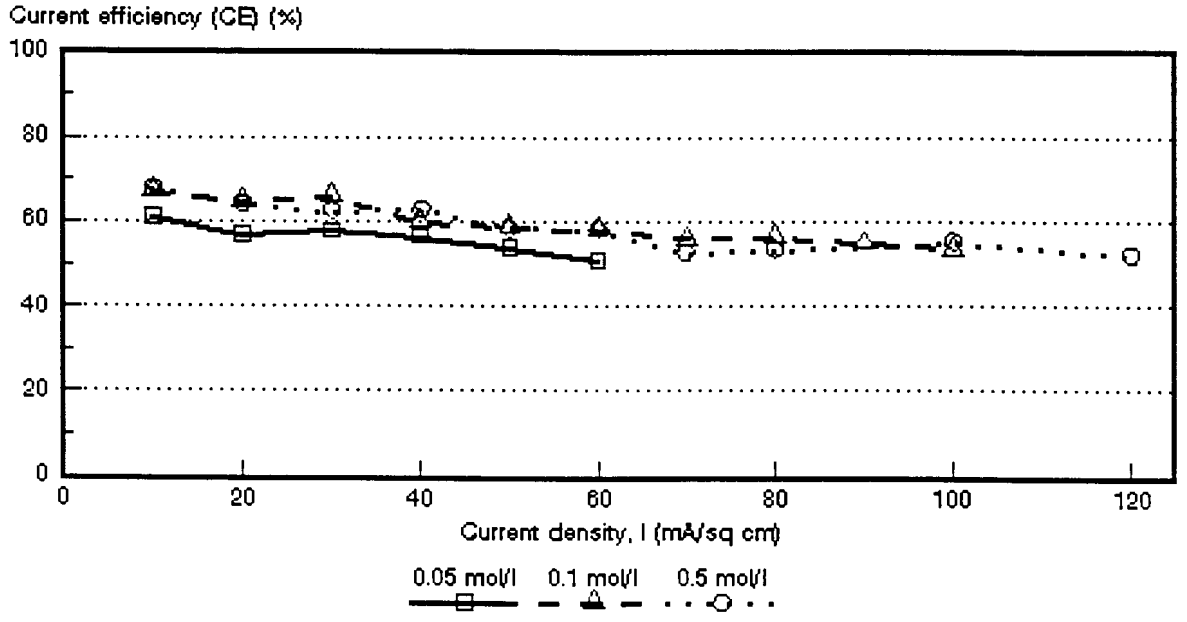

Figure 8.19: **Current efficiency (e_p) as a function of current density for 3 different NaOH feed water concentrations. *Selemion* AMP and CMV membranes.**

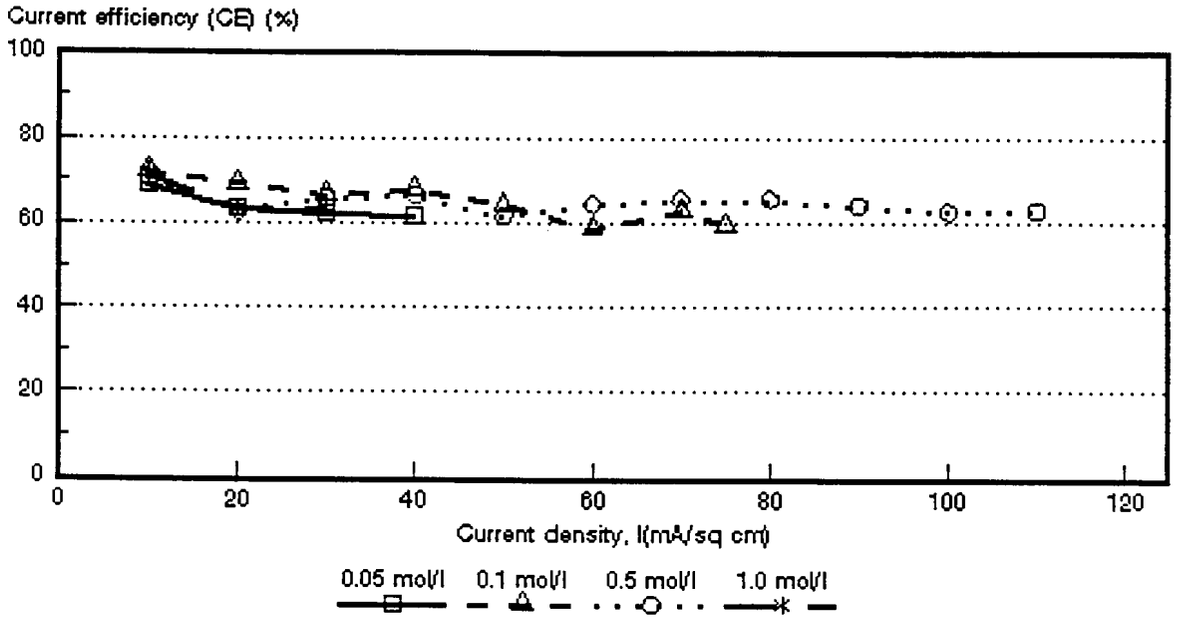

Figure 8.20: **Current efficiency (ϵ_p) as a function of current density for 4 different NaOH feed water concentrations. *Ionac* MA-3475 and MC-3470 membranes.**

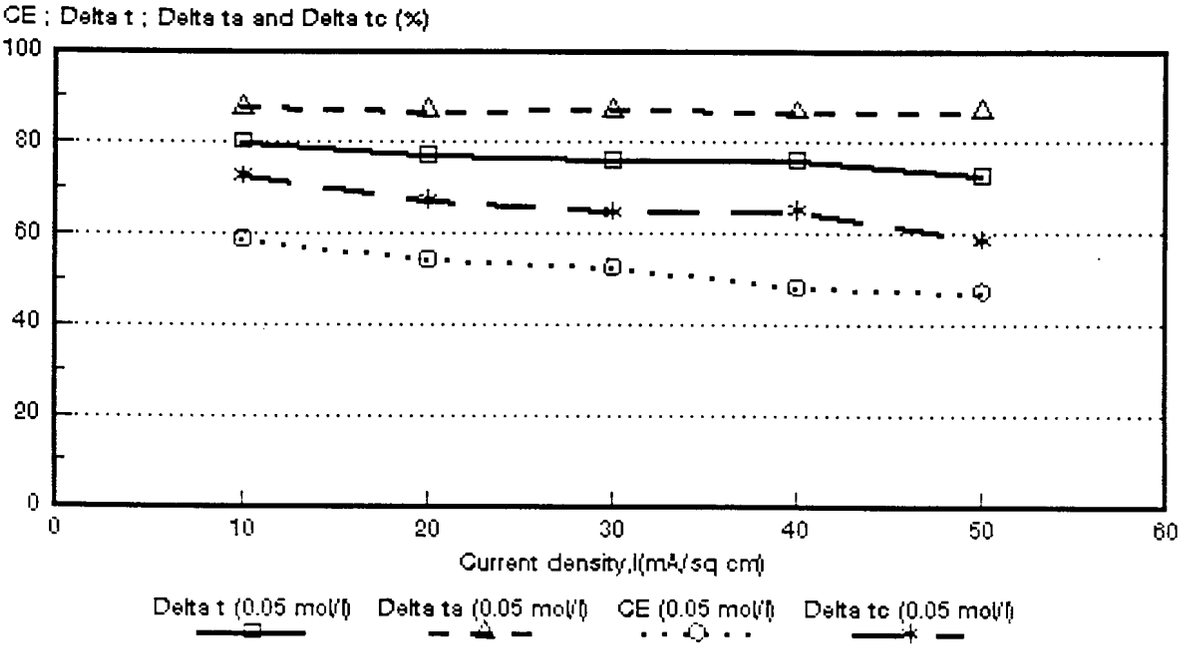

Figure 8.21: **Current efficiency (CE = ϵ_p) as a function of current density for 0,05 mol/ℓ NaOH feed. *Selemion* AMV and CMV membranes. Delta t = $\bar{\Delta}t$; Delta ta = Δt^a; Delta tc = Δt^c.**

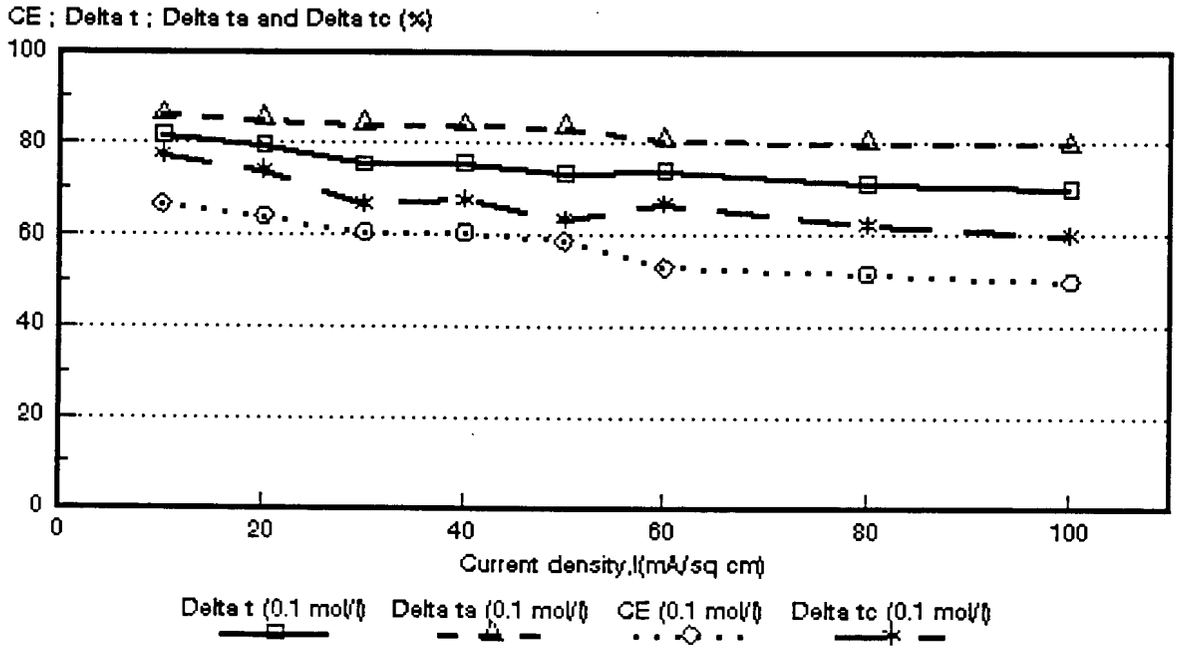

Figure 8.22: **Current efficiency (CE = ϵ_p) as a function of current density for 0,1 mol/ℓ NaOH feed. *Selemion* AMV and CMV membranes. Delta t = $\bar{\Delta}t$; Delta ta = Δt^a; Delta tc = Δt^c.**

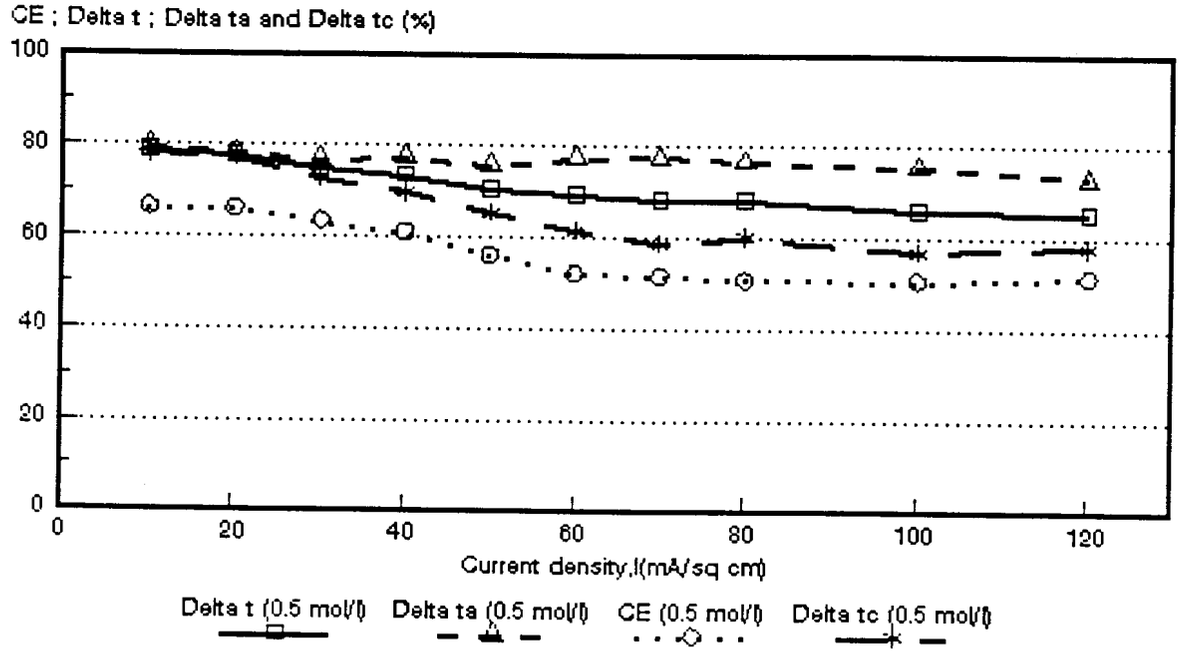

Figure 8.23: **Current efficiency (CE = ϵ_p) as a function of current density for 0,5mol/ℓ NaOH feed. *Selemion* AMV and CMV membranes. Delta t = $\bar{\Delta}t$; Delta ta = Δt^a; Delta = tc = Δt^c.**

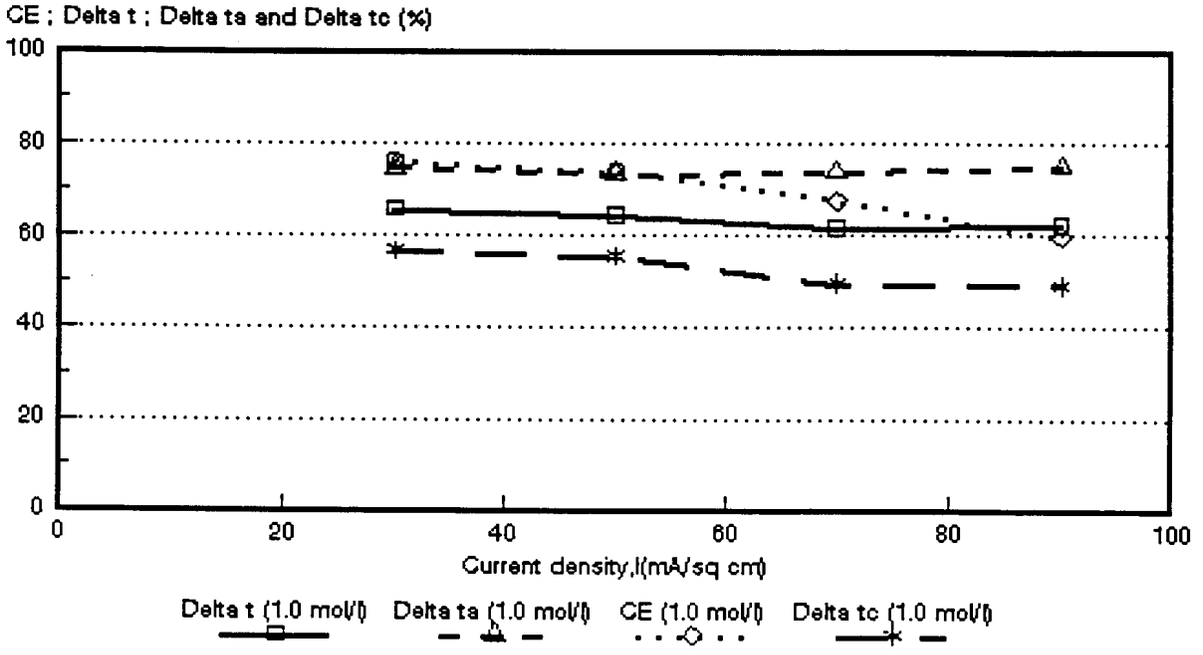

Figure 8.24: **Current efficiency (CE = ϵ_p) as a function of current density for 1,0 mol/ℓ NaOH feed. *Selemion* AMV and CMV membranes. Delta t = $\bar{\Delta}t$; Delta ta = Δt^a; Delta tc = Δt^c.**

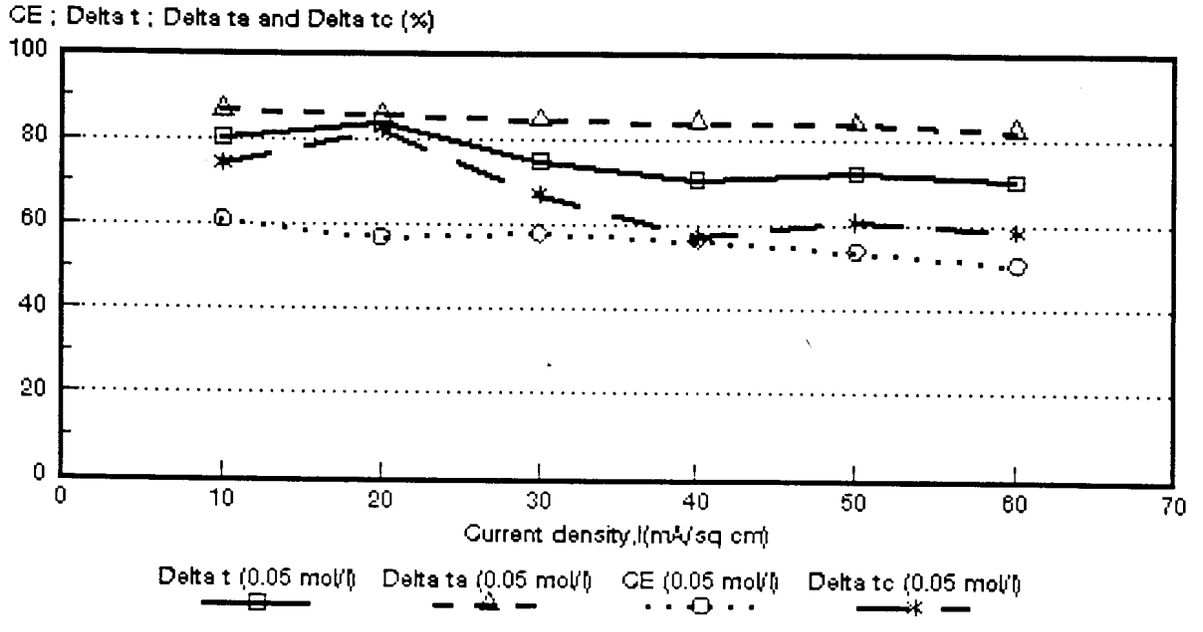

Figure 8.25: **Current efficiency (CE = ϵ_p) as a function of current density for 0,05 mol/ℓ NaOH feed. *Selemion* AMP and CMV membranes. Delta t = $\bar{\Delta}t$; Delta ta = Δt^c; Delta tc = Δt^c.**

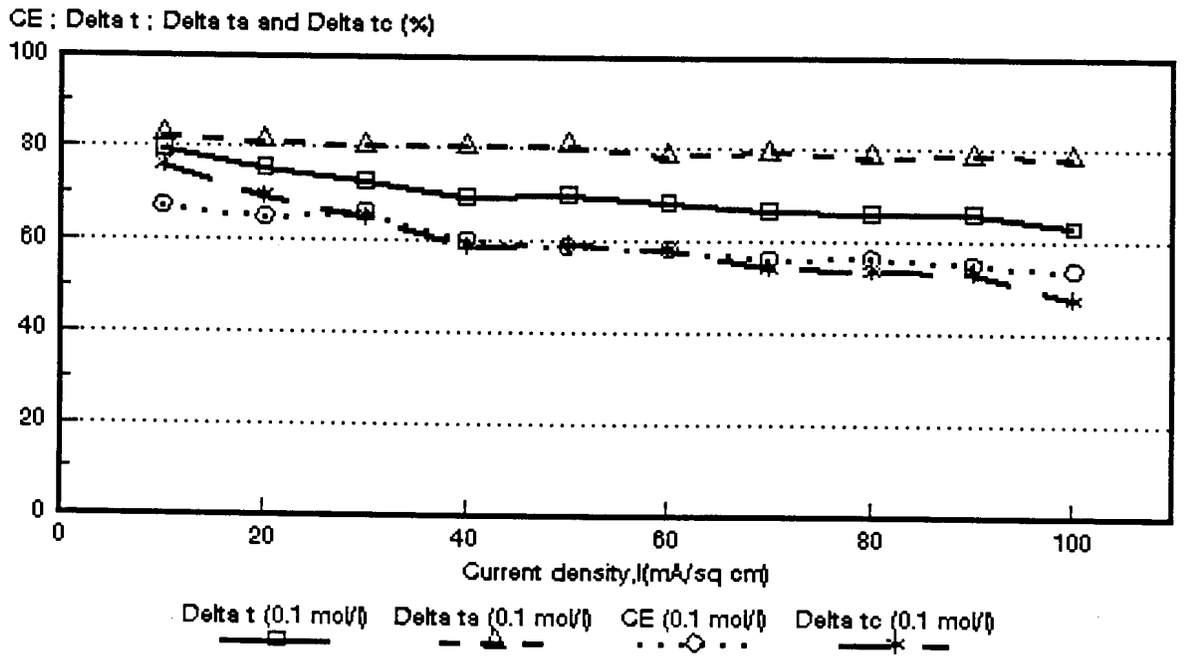

Figure 8.26: Current efficiency (CE = ϵ_p) as a function of current density for 0,1 mol/ℓ NaOH feed. *Selemion* AMP and CMV membranes. Delta t = $\bar{\Delta}t$; Delta tc = Δt^c; Delta ta = Δt^a.

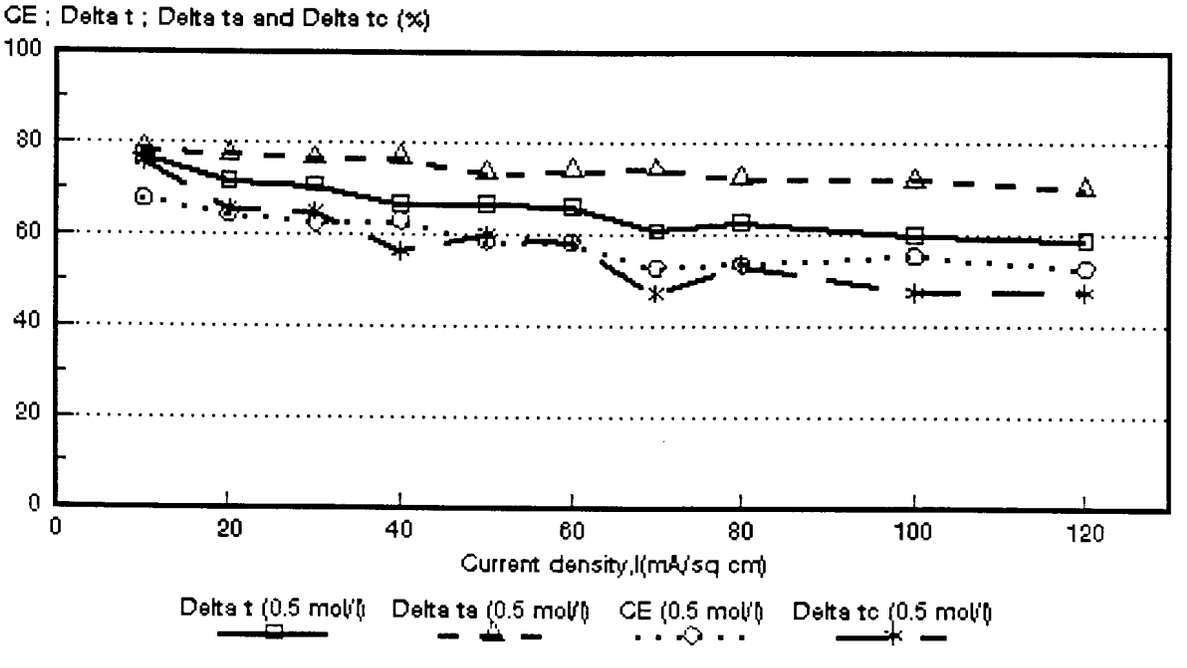

Figure 8.27: Current efficiency (CE = ϵ_p) as a function of current density for 0,5 mol/ℓ NaOH feed. *Selemion* AMP and CMV membranes. Delta t = $\bar{\Delta}t$; Delta tc = Δt^c; Delta ta = Δt^a.

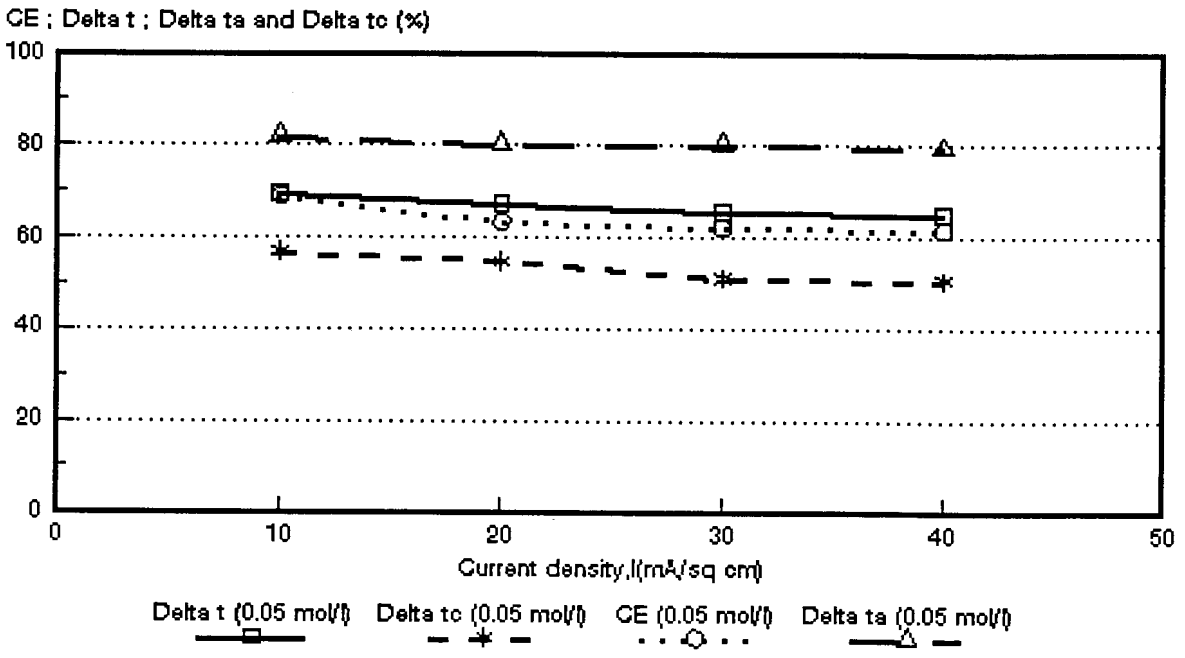

Figure 8.28: **Current efficiency (CE = ϵ_p) as a function of current density for 0,05 mol/ℓ NaOH feed. *Ionac* MA-3470 and MC-3475 membranes. Delta t = $\bar{\Delta}$t; Delta tc = Δt^c; Delta ta = Δt^a.**

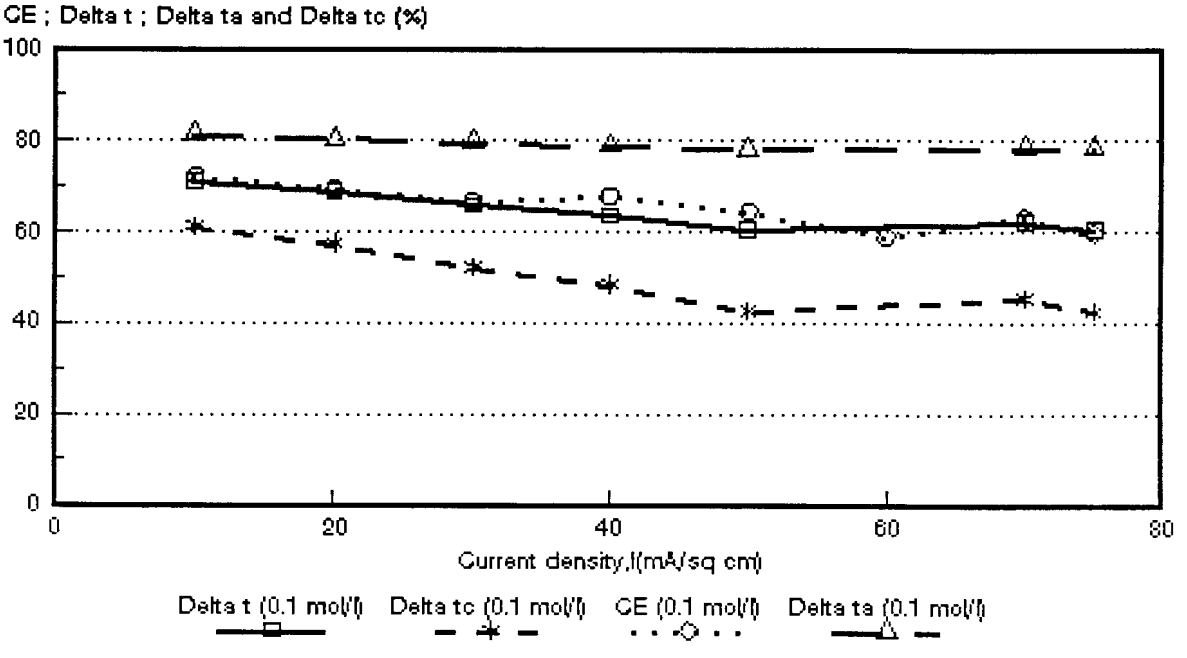

Figure 8.29: **Current efficiency (CE = ϵ_p) as a function of current density for 0,1 mol/ℓ NaOH feed. *Ionac* MA-3470 and MC-3475 membranes. Delta t = $\bar{\Delta}$t; Delta tc = Δt^c; Delta ta = Δt^a.**

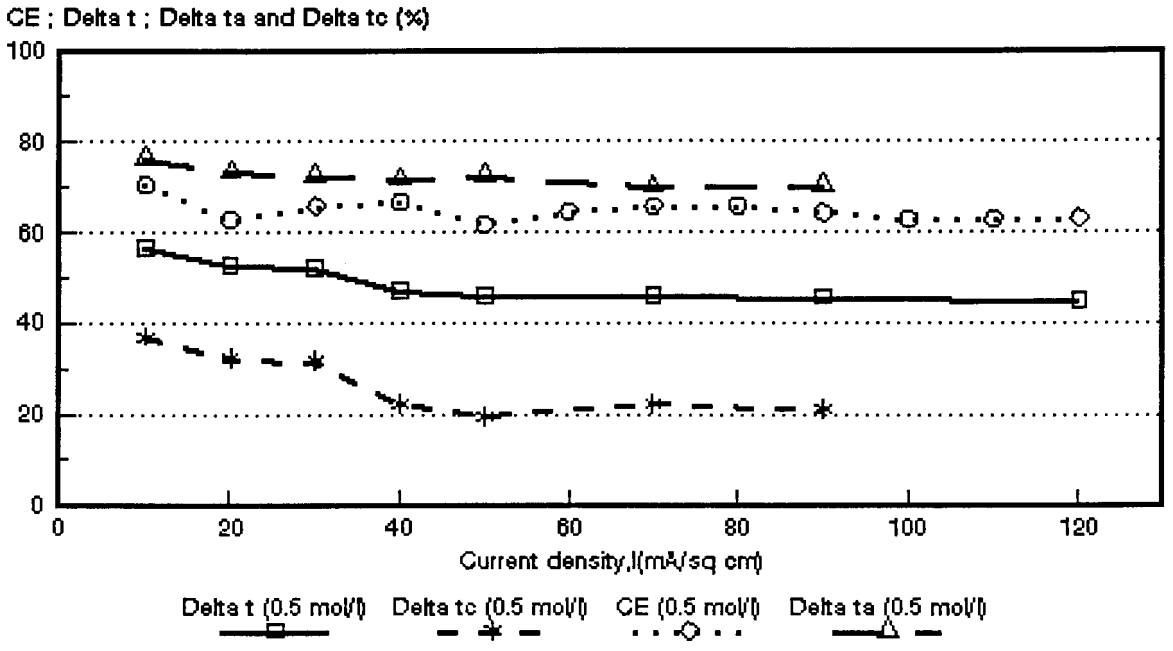

Figure 8.30 **Current efficiency (CE = ϵ_p) as a function of current density for 0,5 mol/ℓ NaOH feed. *Ionac* MA-3470 and MC-3475 membranes. Delta t = $\bar{\Delta}t$; Delta tc = Δ^c; Delta ta = Δt^a.**

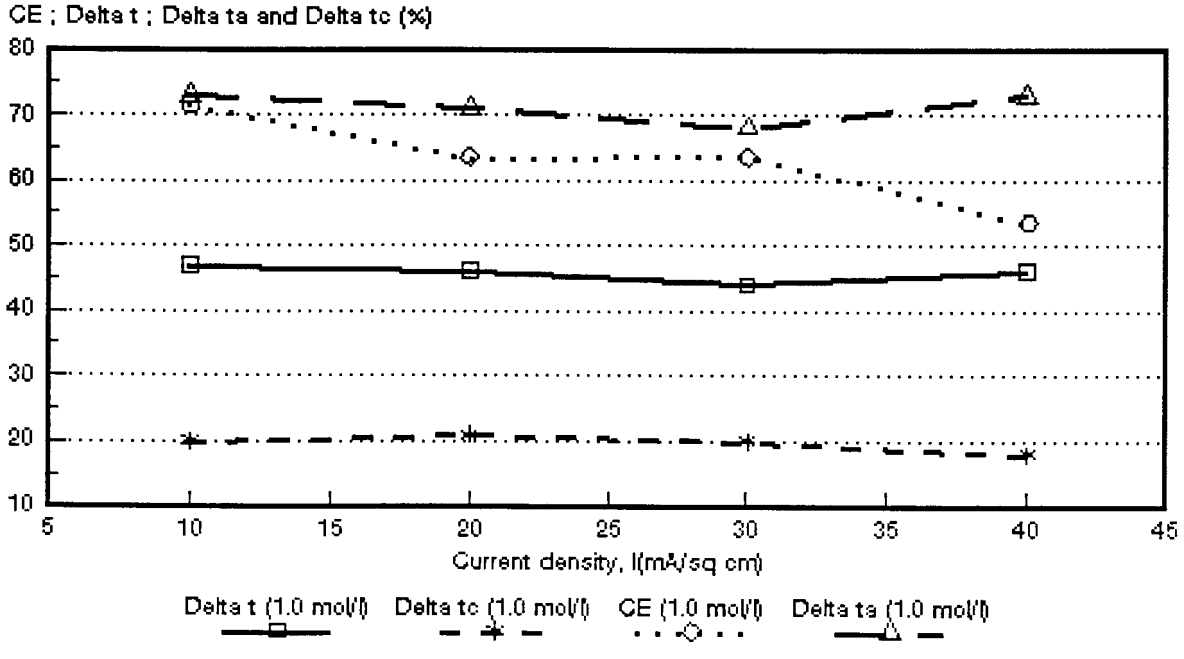

Figure 8.31 **Current efficiency (CE = ϵ_p) as a function of current density for 0,1 mol/ℓ NaOH feed. *Ionac* MA-3470 and MC-3475 membranes. Delta t = $\bar{\Delta}t$; Delta tc = Δt^c; Delta ta = Δt^a.**

Table 8.15: Correlation between apparent transport number of a membrane pair ($\bar{\Delta}t$) and current efficiency (ϵ_p).

Current Density	$\bar{\Delta}t/\epsilon_p$										
mA/cm²	Selemion AMV & CMV Concentration, mol/ℓ				Selemion AMP & CMV Concentration, mol/ℓ			Ionac MA-3475 & MC-3470 Concentration, mol/ℓ			
	0,05	0,1	0,5	1,0	0,05	0,1	0,5	0,05	0,1	0,5	1,0
10	1,37	1,23	1,19		1,31	1,17	1,14	1,00	0,98	0,81	0,65
20	1,42	1,23	1,16		1,47	1,15	1,10	1,06	0,98	0,84	0,72
30	1,45	1,24	1,16	0,85	1,30	1,09	1,12	1,06	0,97	0,79	0,69
40	1,57	1,24	1,19		1,48	1,15	1,05	1,06	0,93	0,71	0,84
50		1,24	1,24	0,87	1,33	1,17	1,13		0,93	0,74	
60		1,38	1,32		1,37	1,17	1,13				
70			1,32	0,90		1,17	1,14		0,98	0,70	
75									1,01		
80		1,37	1,34			1,17	1,16				
90				1,04		1,20				0,70	
100		1,38	1,30			1,17	1,06				
110											
120			1,26				1,10				

Table 8.16: Correlation between apparent transport number of the cation membrane (Δt^c) and current efficiency (e_p).

Current Density	$\Delta t^c/e_p$										
mA/cm²	Selemion AMV & CMV Concentration, mol/ℓ				Selemion AMP & CMV Concentration, mol/ℓ			Ionac MA-3475 & MC-3470 Concentration, mol/ℓ			
	0,05	0,1	0,5	1,0	0,05	0,1	0,5	0,05	0,1	0,5	1,0
10	1,24	1,17	1,17		1,21	1,13	1,12	0,83	0,84	0,52	0,29
20	1,25	1,16	1,16		1,43	1,06	1,03	0,87	0,82	0,51	0,33
30	1,23	1,11	1,15	0,73	1,16	0,98	1,04	0,82	0,78	0,47	0,31
40	1,34	1,12	1,13		1,01	0,98	0,89	0,81	0,70	0,33	0,34
50	1,24	1,09	1,16	0,75	1,11	1,00	1,02		0,65	0,31	
60		1,26	1,17		1,14	0,99	0,99				
70			1,12	0,72		0,96	0,89		0,71	0,33	
75									0,70		
80		1,19	1,18			0,94	0,99				
90				0,82		0,96				0,33	
100		1,20	1,12			0,87	0,85				
110											
120			1,13				0,89				

Table 8.17: Correlation between apparent transport number of the anion membrane (Δt^a) and current efficiency (ϵ_p).

Current Density	$\Delta t^a/\epsilon_p$										
mA/cm²	Selemion AMV & CMV Concentration, mol/ℓ				Selemion AMP & CMV Concentration, mol/ℓ			Ionac MA-3475 & MC-3470 Concentration, mol/ℓ			
	0,05	0,1	0,5	1,0	0,05	0,1	0,5	0,05	0,1	0,5	1,0
10	1,49	1,29	1,19		1,41	1,22	1,17	1,19	1,12	1,08	1,02
20	1,60	1,32	1,18		1,49	1,24	1,20	1,26	1,15	1,16	1,12
30	1,65	1,39	1,21	0,97	1,45	1,21	1,21	1,28	1,18	1,09	1,07
40	1,80	1,39	1,26		1,48	1,33	1,21	1,28	1,15	1,08	1,36
50	1,84	1,43	1,35	0,99	1,53	1,36	1,25		1,21	1,17	
60		1,53	1,48		1,61	1,34	1,27				
70			1,49	1,08		1,41	1,40		1,23	1,06	
75									1,31		
80		1,55	1,49			1,38	1,34				
90				1,26		1,42				1,09	
100		1,58	1,48			1,45	1,30				
110											
120			1,42				1,33				

mol/ℓ feed (30 to 50 mA/cm^2). The ratio $\bar{\Delta}t/\epsilon_p$ for the *Selemion* AMP and CMV membranes varied between 1,1 and 1,2 (0,1 mol/ℓ feed, 10 to 70 mA/cm^2) and was 1,1 at 0,5 mol/ℓ feed concentration (10 to 70 mA/cm^2). Therefore, satisfactory correlations were obtained between the apparent transport numbers and current efficiency in the 0,1 to 0,5 mol/ℓ feed concentration ranges.

Very satisfactory correlations were obtained between $\bar{\Delta}t/\epsilon_p$ in the 0,05 to 0,1 mol/ℓ feed concentration range for the *Ionac* membranes (Fig's 8,28 and 8,29). The ratio $\bar{\Delta}t/\epsilon_p$ varied between 1 and 1,1 (10 to 40 mA/cm^2, 0,05 mol/ℓ) and between 0,9 and 1,0 (10 to 70 mA/cm^2, 0,1 mol/ℓ feed). The correlation, however, at 0,5 and 1,0 mol/ℓ feed concentration was not satisfactory. The ratio $\bar{\Delta}t/\epsilon_p$ varied between 0,7 and 0,8 at 0,5 mol/ℓ feed concentration and between 0,7 and 0,8 at 1,0 mol/ℓ feed concentration. Therefore, it should be possible to predict membrane performance for caustic soda concentration/desalinationwith ED with an accuracy of approximately 20% from the apparent transport numbers of the membrane pair. However, the accuracy of the predictions will depend on the feed concentration used.

Satisfactory correlations were obtained between the apparent transport numbers of the cation membrane (Δt^c) and current efficiency in the case of the *Selemion* and *Ionac* membranes (Table 8.16). The ratio between $\Delta t^c/\epsilon_p$ varied between 1,1 and 1,2 in the 0,1 to 0,5 mol/ℓ feed concentration range (10 to 120 mA/cm^2) for the *Selemion* AMV and CMV membranes (Table 8.16). The same correlation was approximately 1,2 at 0,5 mol/ℓ feed concentration (10 to 50 mA/cm^2) and varied between 0,7 and 0,8 at 1,0 mol/ℓ feed concentration (30 to 90 mA/cm^2). The ratio between $\Delta t^c/\epsilon_p$ varied between 1,1 and 1,2 (0,05 mol/ℓ feed; 10 to 60 mA/cm^2); 1,0 and 1,1 (0,1 mol/ℓ feed; 10 to 90 mA/cm^2) and between 0,9 and 1,1 (0,5 mol/ℓ feed; 10 to 80 mA/cm^2) for the *Selemion* AMP and CMV membranes. The ratio $\Delta t^c/\epsilon_p$ was approximately 0,8 (0,5 mol/ℓ feed; 10 to 40 mA/cm^2) and varied between 0,7 and 0,8 (0,1 mol/ℓ feed; 10 to 70 mA/cm^2) in the case of the *Ionac* membranes. However, a much poorer correlation was obtained at 0,5 and 1,0 mol/ℓ feed concentration as a result of the low selectivity of the cation membrane for sodium ions as a result of the high mobility of the hydroxyl ion[30] (Table 8.16). Therefore, it appears that membrane performance for caustic soda concentration/desalination can also be predicted from the apparent transport number of the cation membrane with an accuracy of approximately 20%.

Satisfactory correlations were obtained between the apparent transport number of the anion membrane (Δt^a) and current efficiency in the case of the *Selemion* AMV and CMV

- (1,0 mol/ℓ feed) and *Ionac* membranes (1,0 mol/ℓ feed) (Table 8.17). The ratio $\Delta t^a/\epsilon_p$ varied between approximately 1 and 1,1 in the case of the *Selemion* AMV and CMV membranes (30 to 70 mA/cm^2). The ratio $\Delta t^a/\epsilon_p$ varied between 1 and 1,1 in the case of the *Ionac* membranes (10 to 30 mA/cm^2). Poorer correlations of $\Delta t^a/\epsilon_p$ were obtained at the other feed concentrations (Table 8.17). Consequently, it should be possible to predict membrane performance for caustic soda concentration/desalination applications with an accuracy of approximately 10% from the apparent transport number of the anion membrane at high (1,0 mol/ℓ) feed concentration.

8.3 Water Flow

Water flow (J) through the membranes as a function of current density and feed water concentration is shown in Figures 8.32 to 8.34. Water flow (J_i) through the membranes relative to the flow at $J_{0,5\ mol/\ell}$ is shown in Table 8.18. Water flow through the membranes increases as a function of current density. Volume flow through the *Selemiom* AMV and CMV membranes increased in the 0,05 to 0,1 mol/ℓ feed concentration range (Table 8.18). However, volume flow decreased slightly in the 0,1 to 0,5 mol/ℓ feed concentration range at higher current densities and volume flow remained approximately constant at 1,0 mol/ℓ feed concentration. Current efficiency increased significantly in the 0,05 to 0,1 mol/ℓ feed concentration range (Fig. 8.18) as a result of the increased water flow. Current efficiency, however, was significantly higher at 1,0 mol/ℓ feed concentration (Fig. 8.18) than at 0,01 and 0,5 mol/ℓ feed, despite a slightly lower volume flow.

Volume flow decreased in the case of the *Selemion* AMP and CMV membranes in the feed concentration range from 0,05 to 0,5 mol/ℓ (Table 8.18). Current efficiencies, however, were approximately the same especially at the two higher feed concentrations (Fig. 8.19).

Volume flow was slightly higher at 0,1 mol/ℓ feed concentration in the case of the *Ionac* membranes in the beginning of the run. It is interesting to note that current efficiency has also been slightly higher at this feed concentration (Fig. 8.20). However, current efficiency was approximately the same in the feed concentration range from 0,05 to 1,0 mol/ℓ. Nevertheless, it also appears with caustic soda solutions as has been the case with sodium chloride solutions that increasing water flow can cause an increase in current efficiency.

Water flow (J) through the membranes as a function of effective current density, I_{eff}, and feed concentration is shown in Figures 8.35 to 8.37. Straight lines were obtained at higher values of I_{eff}. The slope of these lines corresponds to the combined electro-osmotic coefficient (2β) of a membrane pair. The electro-osmotic coefficients as a function of caustic soda feed water concentration is shown in Figures 8.38 to 8.40. The electro-osmotic coefficients decreased sharply with increasing feed concentration in the case of the *Selemion* AMV and CMV membranes (Figs. 8.38). It is interesting to note that the electro-osmotic coefficients have decreased over the entire feed concentration range from 0,05 to 1,0 mol/ℓ. A similar effect was observed with the *Selemion* AMP

and CMV membranes but the decrease in the electro-osmotic coefficients were far less (Fig. 8.39). These membranes, therefore, deswell less than the *Selemion* AMV and CMV membranes with increasing feed concentration. The *Ionac* membranes also showed less deswelling than the *Selemion* AMV and CMV membranes (Fig. 8.40).

The effect of the electro-osmotic coefficient on the maximum caustic soda brine concentration, c_b^{max}, is shown in Table 8.19. Maximum caustic soda brine concentration increases with decreasing electro-osmotic coefficient. The electro-osmotic coefficient of the *Selemion* AMP and CMV membranes were lower than that of the *Selemion* AMV and CMV and *Ionac* membranes. The electro-osmotic coefficient of the *Selemion* AMP and CMV membranes were determined at 0,155 ℓ/Faraday at 0,1 mol/ℓ feed concentration. The coefficients for the *Selemion* AMV and CMV and *Ionac* membranes at the same feed concentration were 0,179 and 0,193 ℓ/Faraday, respectively. Therefore, higher caustic soda brine concentrations could be obtained with the *Selemion* AMP and CMV membranes.

Approximately 8 to 9 mol H_2O/Faraday passed through the *Selemion* AMP and CMV membranes in the feed concentration range between 0,1 and 0,5 mol/ℓ (Table 8.19). Approximately 8 to 10 and 10 to 11 mol H_2O/Faraday passed through the membranes in the case of the *Selemion* AMV and CMV and *Ionac* membranes, respectively (0,1 to 0,5 mol/ℓ feed).

The osmotic flow (J_{osm}) relative to the total flow (J) through the membranes as a function of current density is shown in Table 8.20. The osmotic water flow through the membranes decreases with increasing current density. Osmotic water flow represented 45,9; 46,9 and 26,5% of the total flow through the membranes at a current density of 30 mA/cm^2 in the case of the *Selemion* AMV and CMV; *Selemion* AMP and CMV and *Ionac* membranes, respectively. Therefore, osmosis makes a significant contribution to water flow through the membranes at relative low current density. The osmotic contribution to total flow through the membranes (*Selemion* AMV and CMV and *Selemion* AMP and CMV) at a current density of 100 mA/cm^2 (0,1 mol/ℓ feed) was 21,4 and 25,7%, respectively. The osmotic contribution to the total flow in the case of the *Ionac* membranes at a current density of 70 mA/cm^2 (0,1 mol/ℓ feed) was 14,2%. Therefore, the contribution of osmotic water flow to total water flow through the membranes is much lower at high current density.

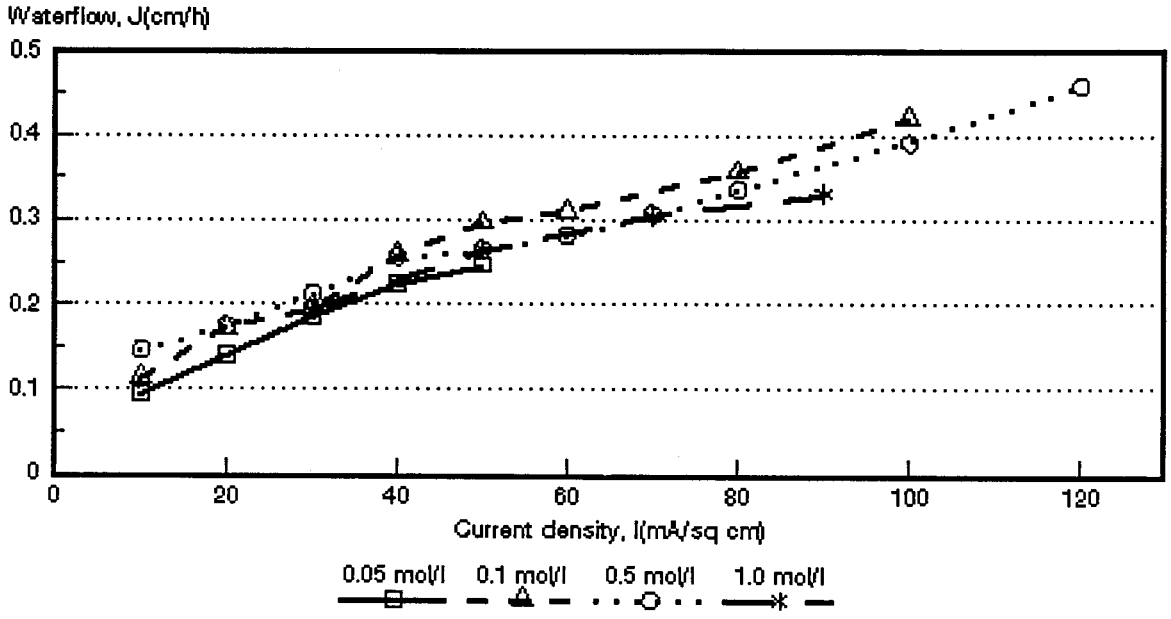

Figure 8.32 **Water flow through the membranes as a function of current density and feed water concentration. *Selemion* AMV and CMV membranes.**

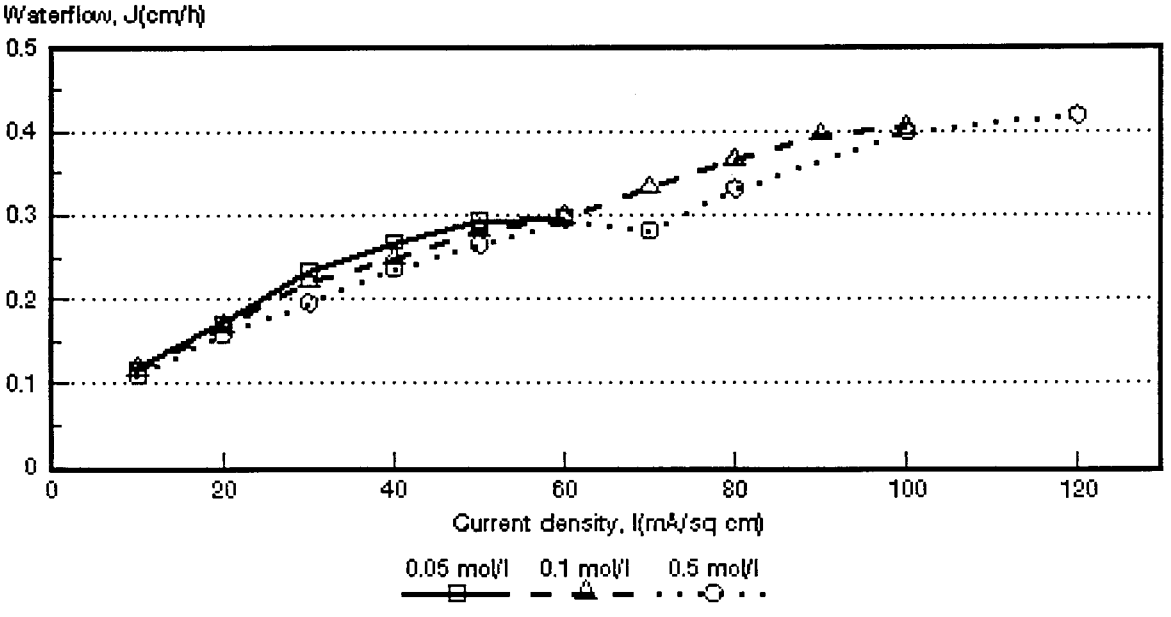

Figure 8.33: **Water flow through the membranes as a function of current density and feed water concentration. *Selemion* AMP and CMV membranes.**

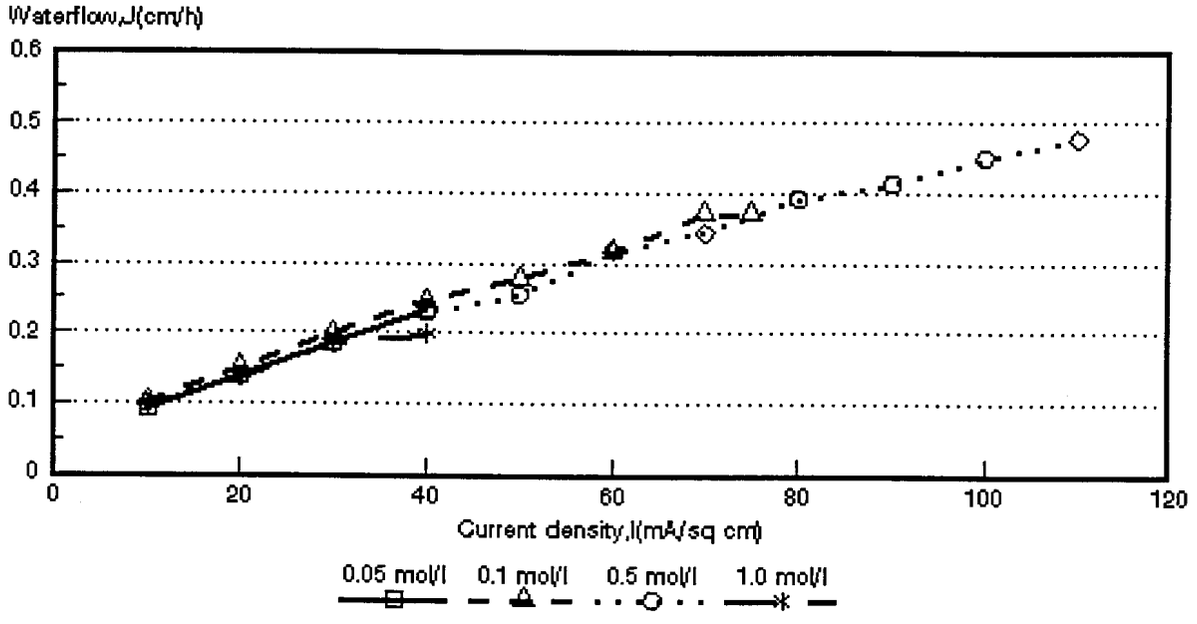

Figure 8.34: **Water flow through the membranes as a function of current density and feed water concentration. *Ionac* MA-3475 and MC-3470 membranes.**

Table 8.18: Water flow (J_i) through the membranes relative to the flow at $J_{0,5\ mol/\ell}$

Current Density mA/cm²	$J_i/J_{0,5\ mol/\ell}$										
	Selemion AMV & CMV Concentration, mol/ℓ				Selemion AMP & CMV Concentration, mol/ℓ			Ionac MA-3475 & MC-3470 Concentration, mol/ℓ			
	0,05	0,1	0,5	1,0	0,05	0,1	0,5	0,05	0,1	0,5	1,0
10	0,65	0,79	1,0		1,07	1,06	1,0	0,93	1,04	1,0	0,98
20	0,81	0,98	1,0		1,08	1,06	1,0	1,01	1,10	1,0	1,00
30	0,87	0,92	1,0	0,92	1,20	1,13	1,0	1,00	1,08	1,0	1,00
40	0,88	1,01	1,0		1,14	1,05	1,0	1,02	1,08	1,0	0,86
50	0,93	1,12	1,0	1,0	1,11	1,06	1,0		1,00	1,0	
60		1,10	1,0		1,01	1,01	1,0		1,08	1,0	
70		1,06	1,0	0,99		1,18	1,0				
75		1,07	1,0				1,0				
80						1,11	1,0				
90							1,0				
100						1,01	1,0				
110											
120											

i = 0,05; 0,1 and 1,0 mol/ℓ

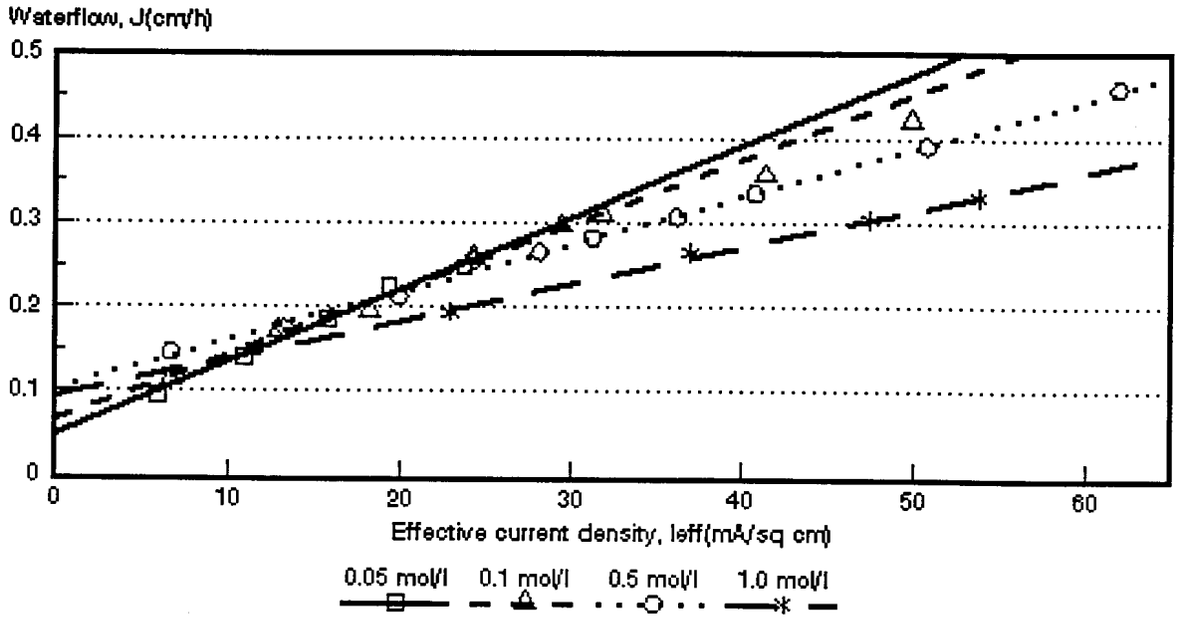

Figure 8.35: **Water flow through the membranes as a function of effective current density and feed water concentration. *Selemion* AMV and CMV membranes.**

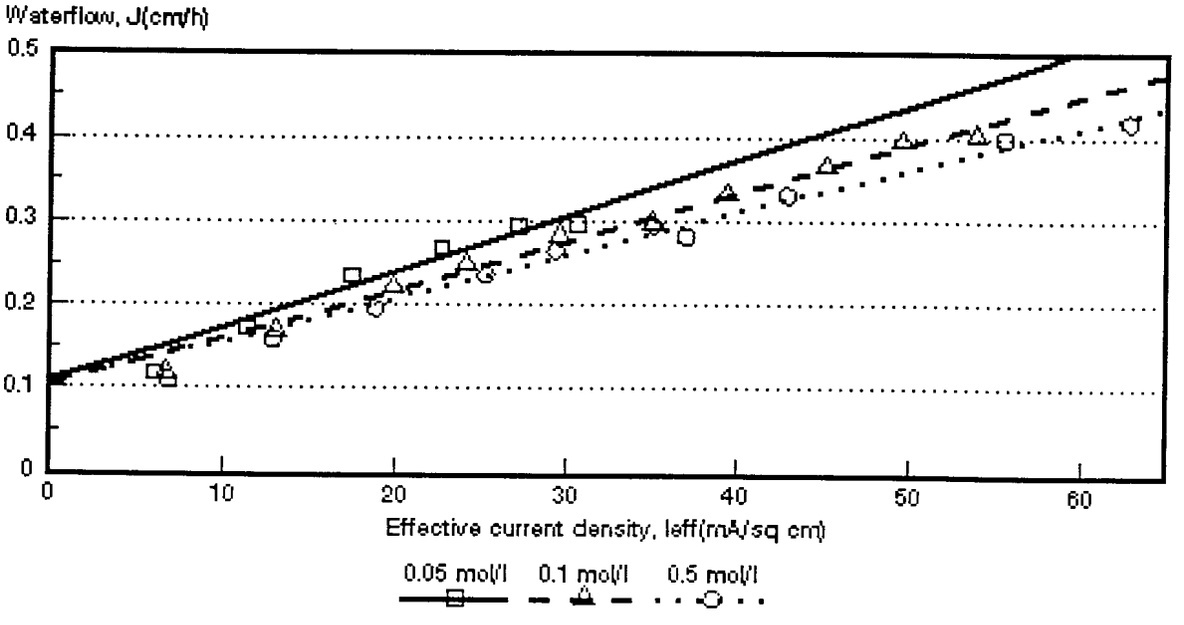

Figure 8.36: **Water flow through the membranes as a function of effective current density and feed water concentration. *Selemion* AMP and CMV membranes.**

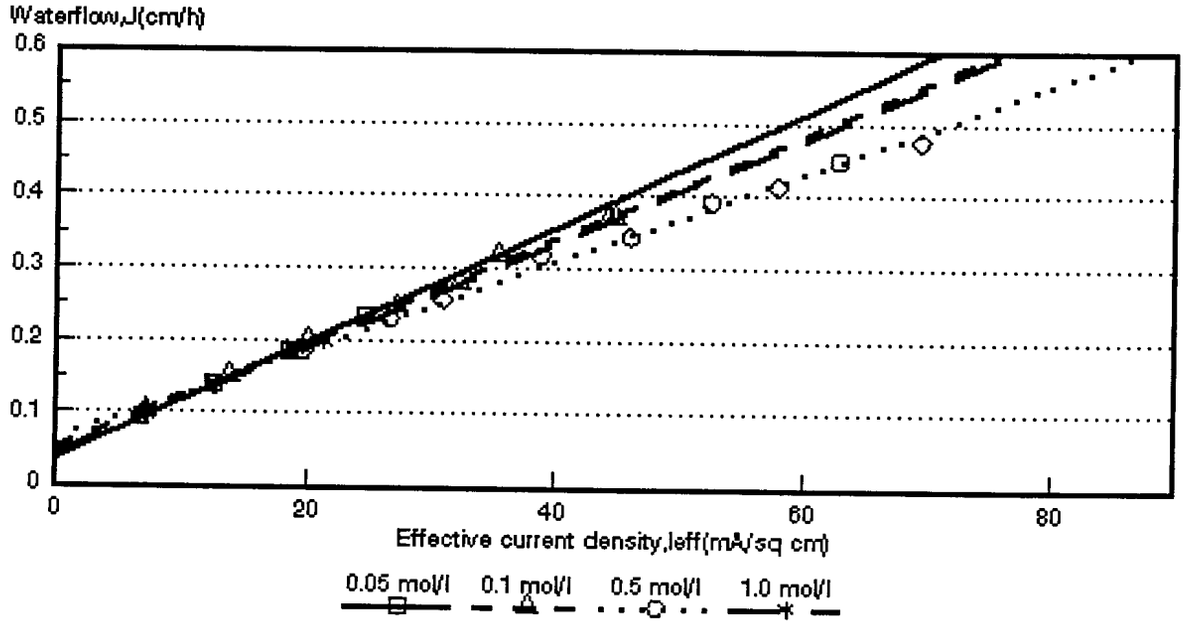

Figure 8.37: **Water flow through the membranes as a function of effective current density and feed water concentration. *Ionac* MA-3475 and MC-3470 membranes.**

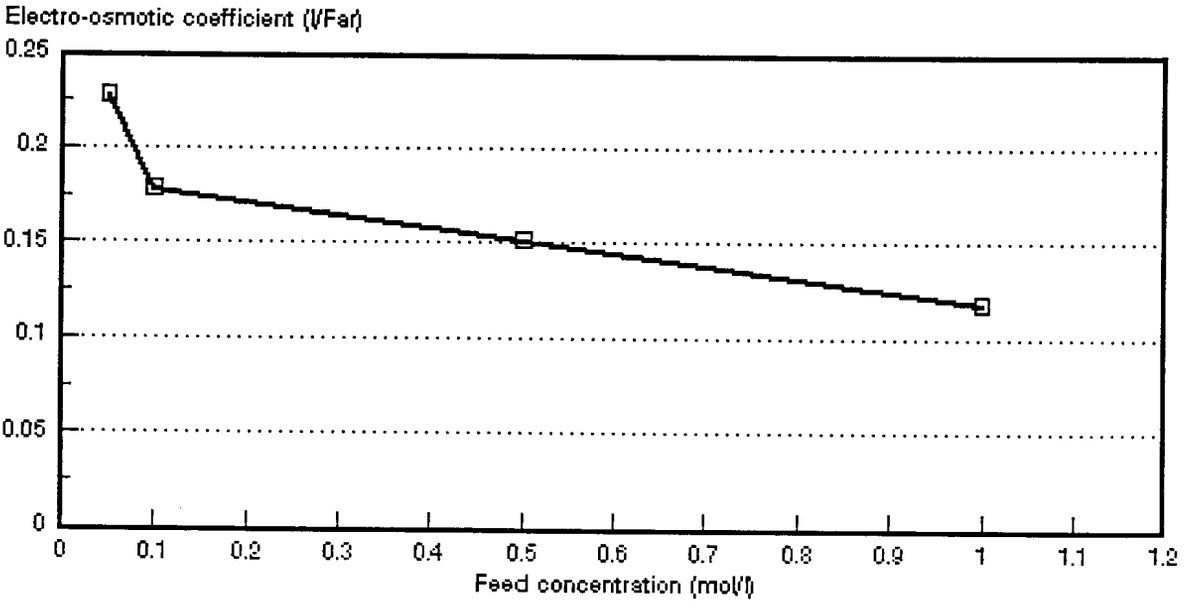

Figure 8.38: **Electro-osmotic coefficient as a function of NaOH feed concentration. *Selemion* AMV and CMV membranes.**

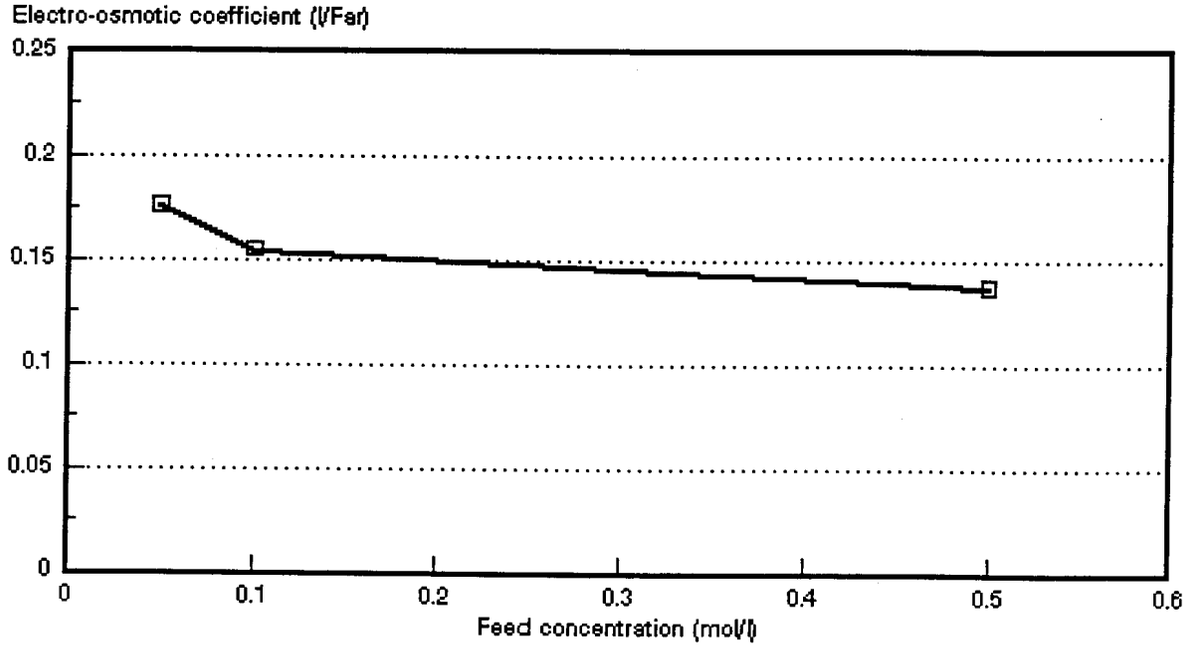

Figure 8.39: **Electro-osmotic coefficient as a function of NaOH feed concentration. *Selemion* AMP and CMV membranes.**

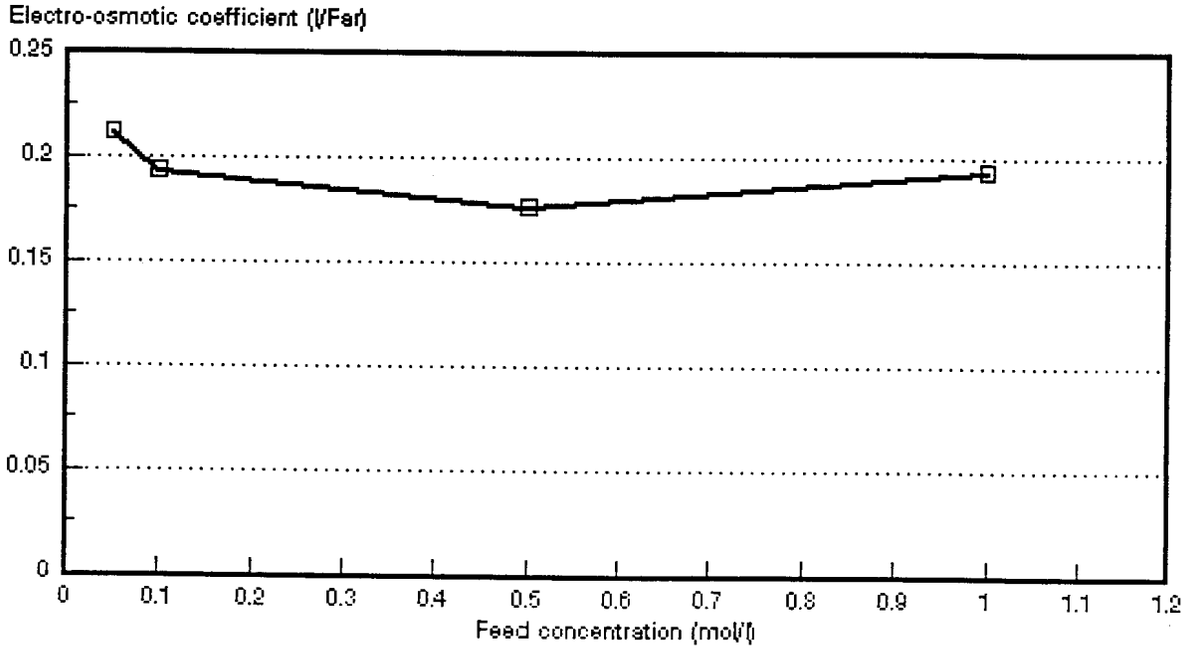

Figure 8.40: **Electro-osmotic coefficient as a function of NaOH feed concentration. *Ionac* MA-3475 and MC-3470 membranes.**

Table 8.19: Effect of the electro-osmotic coefficient (EOC)* on the maximum caustic soda brine concentration, c_b^{max}.

Membranes	Feed Concentration mol/ℓ	EOC ℓ/Faraday	c_b^{max} mol/ℓ	mol H_2O/Faraday
Selemion AMV & CMV	0,05	0,228	4,39	12,7
	0,10	0,179	5,59	9,9
	0,50	0,152	6,58	8,4
	1,0	0,118	8,46	6,6
Selemion AMP & CMV	0,05	0,176	5,68	9,8
	0,10	0,155	6,45	8,6
	0,5	0,137	7,30	7,6
Ionac MA-3470 & MC-3475	0,05	0,212	4,72	11,8
	0,10	0,193	5,18	10,7
	0,50	0,176	5,68	9,8
	1,0	0,193	5,18	10,7

* Data from Tables 8.1 to 8.11.

Table 8.20: Osmotic flow* (J_{osm}) relative to the total flow (J) through the membranes as a function of current density.

Membranes	Current Density mA/cm²	J_{osm}/J (%) Feed concentration (mol/ℓ)			
		0,05	0,1	0,5	1,0
Selemion AMV & CMV	10	57,3	78,4	72,7	
	20	38,6	52,23	60,6	
	30	29,4	45,9	50,0	49,5
	40	24,2	34,9	41,4	
	50	22,1	30,3	40,0	36,3
	60		28,9	37,5	
	70				31,5
	80		25,2	31,6	
	90				29,07
	100		21,4	27,0	
	120			23,1	
Selemion AMP & CMV	10	92,7	88,6	97,1	
	20	63,6	61,4	67,2	
	30	46,6	46,9	54,5	
	40	40,8	41,8	45,3	
	50	37,3	36,8	40,3	
	60	36,8	37,8	36,2	
	70		31,1		
	80		28,3	32,3	
	90		26,2		
	100		25,7	26,7	
Ionac MA-3475 & MC-3470	10	41,9	51,2	53,1	47,3
	20	27,9	34,8	38,2	33,3
	30	20,9	26,5	28,4	24,8
	40	16,6	21,4	22,9	23,1
	50		18,9	20,6	
	60		16,6	16,6	
	70		14,2	15,3	
	80			13,4	
	100			11,7	

* Data from Tables 8.1 to 8.11.

8.4 Membrane Permselectivity

Membrane permselectivity (from membrane potential measurements) as a function of brine concentration at different initial feed water concentrations is shown in Figures 8.41 to 8.43. Membrane permselectivity decreases with increasing caustic soda brine concentration and increasing feed water concentration. It is interesting to note that membrane permselectivity has not been much effected by increasing brine concentration in the case of the *Selemion* AMP and CMV membranes at 0,1 mol/ℓ feed concentration.

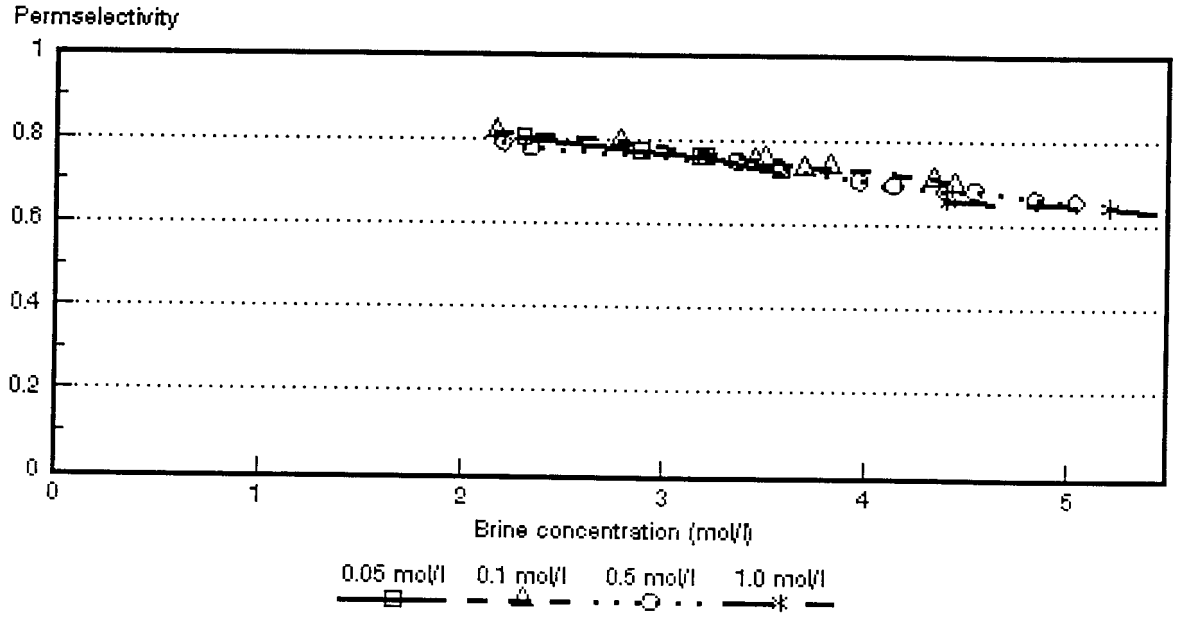

Figure 8.41: Permselectivity ($\bar{\Delta}t$) as a function of brine concentration for different NaOH feed concentrations. *Selemion* AMV and CMV membranes.

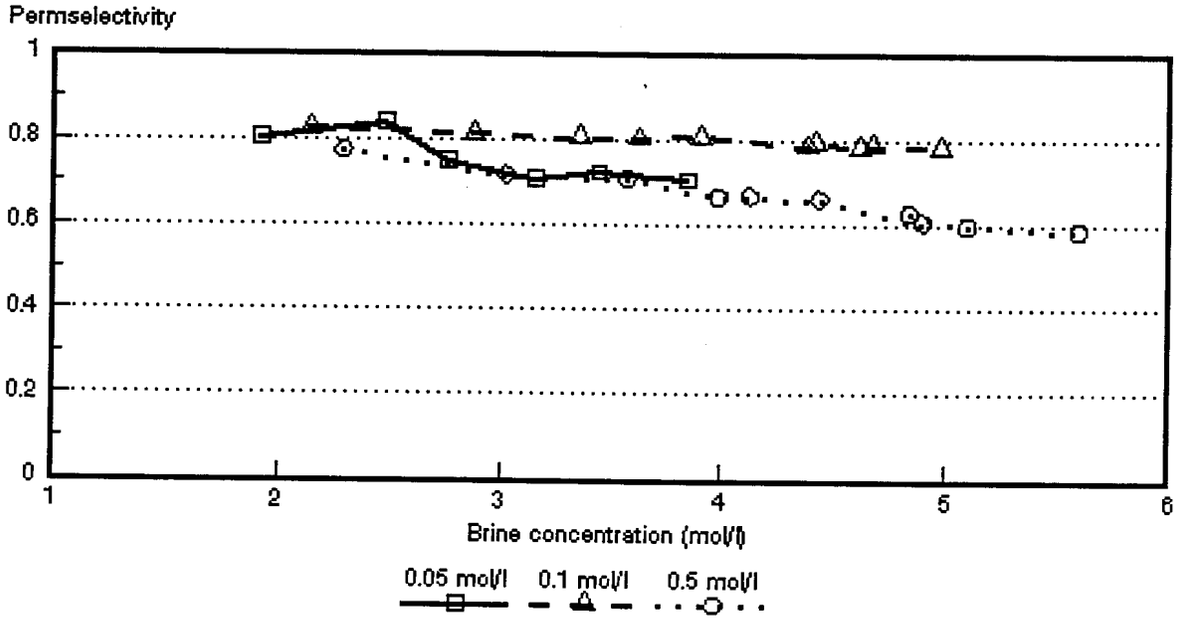

Figure 8.42: **Permselectivity ($\bar{\Delta}t$) as a function of brine concentration for different NaOH feed concentrations. *Selemion* AMP and CMV membranes.**

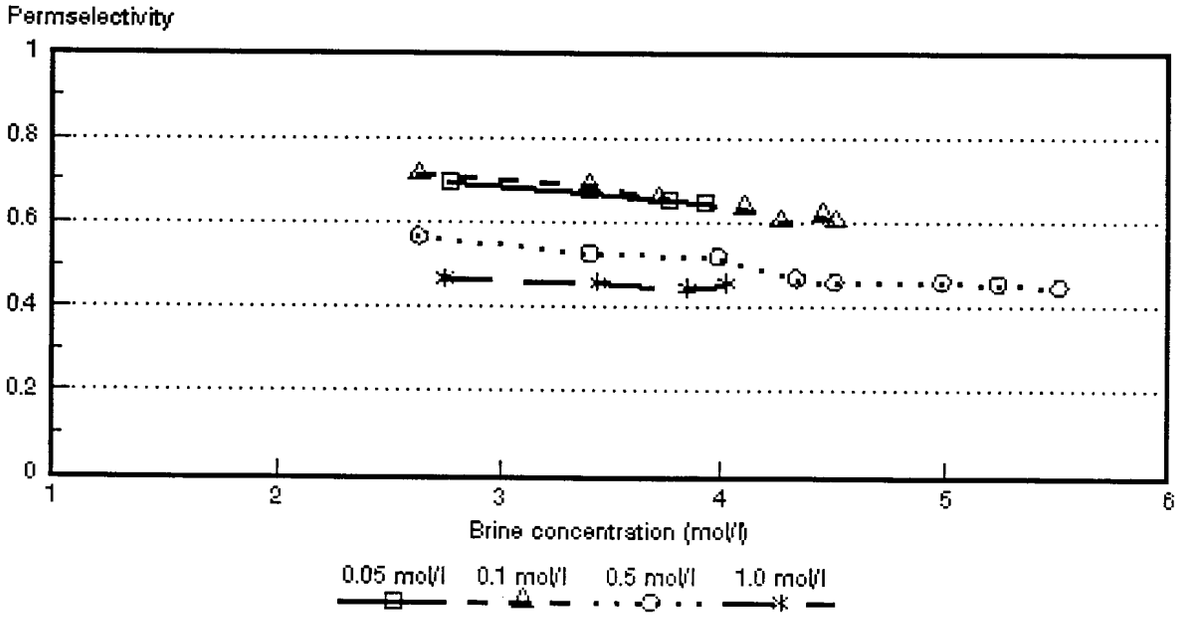

Figure 8.43: **Permselectivity ($\bar{\Delta}t$) as a function of brine concentration for different NaOH feed concentrations. *Ionac* MA-3475 and MC-3470 membranes.**

8.5 Membrane Characteristics

8.5.1 Membrane resistances of membranes used for EOP of caustic soda solutions

Membrane resistances of the membranes used for EOP of caustic soda solutions are summarized in Table 8.21.

Table 8.21: Membrane resistances of the membranes used for EOP of caustic soda solutions.

Membrane	Resistance - ohm·cm²	
	0,1 mol/ℓ	0,5 mol/ℓ
Selemion AMV	4,1	0,5
Selemion AMP	9,6	1,5
Selemion CMV	5,1	1,2
Ionac MA-3475	15,7	7,1
Ionac MC-3470	26,9	15,7

8.5.2 Gel water contents and ion-exchange capacities of the membranes used for EOP of caustic soda solutions.

Gel water contents and ion-exchange capacities of the membranes used for EOP of caustic soda solutions are shown in Table 8.22.

Table 8.22: Gel water contents and ion-exchange capacities of the membranes used for EOP of caustic soda solutions.

Membrane	Gel Water Content	Ion-exchange Capacity
	%	me/dry g
Selemion AMV	18,4	1,3
Selemion CMV	22,7	2,3
Selemion AMP	17,6	1,1
Ionac MA-3475	17,8	1,1
Ionac MC-3470	18,5	1,8

8.5.3 Permselectivities of the membranes used for EOP of caustic soda solutions.

Permselectivities of the membranes used for EOP of caustic soda solutions are shown in Table 8.23.

Table 8.23: Membrane permselectivities of the membranes used for EOP of caustic soda solutions at different salt gradients.

Membrane	$\Delta t(1)^{*}$	$\Delta t(2)^{**}$	$\Delta t(3)^{***}$
Selemion AMV	0,87	0,87	0,83
Selemion CMV	0,98	0,83	0,65
Selemion AMP	0,93	0,87	0,81
Ionac MA-3475	0,87	0,82	0,79
Ionac MC-3470	0,92	0,61	0,46

$(1)^{*}$: 0,1 / 0,2 mol/ℓ NaOH
$(2)^{**}$: 0,5 / 1,0 mol/ℓ NaOH
$(3)^{***}$: 0,1 / 4,0 mol/ℓ NaOH

9. ELECTRO-OSMOTIC PUMPING OF SODIUM CHLORIDE-, HYDROCHLORIC ACID- AND CAUSTIC SODA SOLUTIONS IN A CONVENTIONAL ELECTRODIALYSIS STACK

9.1 Concentration/Desalination of Sodium Chloride Solutions with *Ionac* MA-3475 and MC-3470 Membranes.

The concentration/desalination results of different sodium chloride feed water concentrations at different cell pair voltages are summarized in Table 9.1.

9.1.1 Brine and dialysate concentrations

Dialysate and brine concentrations as a function of time and cell pair voltage for different initial feed water concentrations are shown in Figures 9.1 to 9.8. Brine concentration as a function of feed water concentration and cell pair voltage is shown in Figure 9.9. A typical example of current as a function of time and cell pair voltage for an approximately 3 000 mg/ℓ feed water solution is shown in Figure 9.10.

Desalination/concentration rate increased with increasing cell pair voltage (Figs. 9.1 to 9.8 and 9.10). Brine concentration increased as a function of feed water concentration and cell pair voltage (Table 9.1 and Fig. 9.9). Brine concentrations of 2,1 to 14,0% could be obtained in the feed water concentration range from 1 000 to 10 000 mg/ℓ and cell pair voltage range from 0,5 to 4 volt per cell pair (Table 9.1). Product water concentrations of less than 500 mg/ℓ could be obtained in the same feed water concentration and cell pair voltage range.

The concentration factors (brine/feed) were relatively low (Table 9.1). This could be ascribed to the small volume of feed water (12 ℓ) that was used. Concentration factors decreased with increasing feed concentration. This shows that there is a limit to the brine concentration that can be obtained with ED. Brine concentration that can be obtained with ED depends inter alia on the permselectivity of the ion-exchange membranes and current density used and on the feed water concentration[6, 7]. Ion-exchange membranes tend to lose some of their permselectivity at high concentration.

9.1.2 Brine volume and water recovery

Low brine volume and high water recoveries were obtained (Table 9.1). Brine volume varied between 1,5 and 4% of the treated water volume in the feed water concentration

Table 9.1: Concentration/desalination results of sodium chloride solutions at different feed concentrations and cell pair voltages using Ionac MA-3475 and MC-3470 membranes.

Vcp	c_f mg/ℓ	c_p mg/ℓ	c_b mg/ℓ	CF	CE %	WR %	BV %	EEC kWh/m³	OP m³/m²·d	d_{eff} mm	R_{cp} ohm·cm²
0,5	992	212	21 981	22,2	93,6	98,1	1,9	0,192	0,37		
	2 906	488	73 460	25,3	84,3	97,1	2,9	0,662	0,28	4,23	49,2
1,0	933	193	30 814	33	81,8	98,5	1,5	0,417	0,45		
	3 224	503	82 025	25,4	81,1	97,2	2,8	1,55	0,35	6,76	80,2
	5 132	451	99 786	19,4	91,4	96,0	4,0	2,358	0,30	6,56	69,2
1,5	1 033	196	42 805	41,4	75,2	98,5	1,5	0,769	0,48		
	3 349	435	83 738	25,0	79,9	97,3	2,7	2,52	0,37	11,83	62,9
	3 045	450	86 893	28,5	81,3	97,6	2,4	2,21	0,55*	5,66	99,75
	3 058	433	104 475	34,16	83,01	97,6	2,4	2,18	0,67**	4,81	75,5
2	4 959	372	107 630	21,7	78,9	96,3	3,7	5,35	0,36	10,18	77,1
	10 709	548	136 933	12,8	93,3	93,7	6,3	10,03	0,32	12,11	31,8
3	3 515	430	100 868	28,7	69,4	97,3	2,7	6,14	0,51	11,95	128,8
	5 388	407	112 589	20,9	76,3	96,2	3,7	9,02	0,41	13,86	91,1
	10 364	487	139 637	13,5	86,90	94,2	6,8	15,7	0,36	15,22	50,3
4	10 364	409	139 637	13,5	77,6	94,0	6,0	23,6	0,38	15,49	79,7

*: 2,1 cm/s linear flow velocity; **: 2,73 cm/s linear flow velocity; other experiments conducted at a linear flow velocity approximately 1 cm/s

CF = concentration factor
CE = current efficiency
BV = brine volume
OP = output (yield)
WR = water recovery
EEC = electrical energy consumption

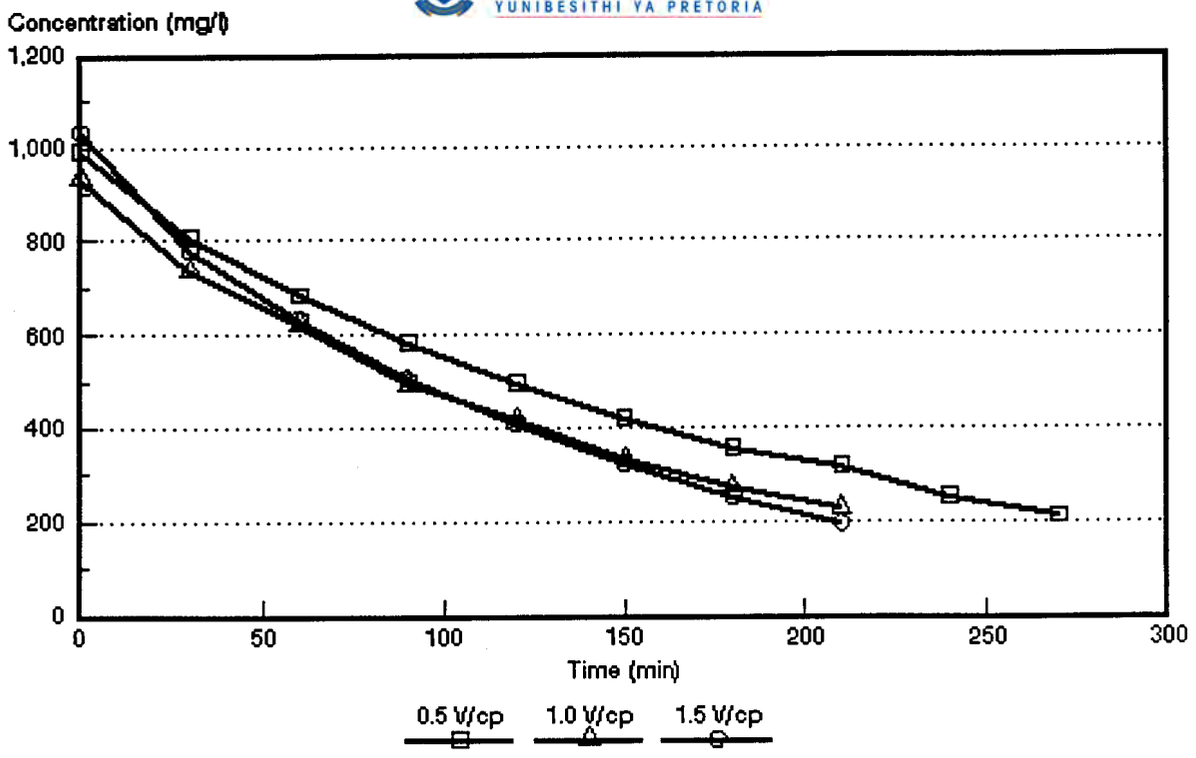

Figure 9.1: **Dialysate concentration as a function of time and cell pair voltage for an approximately 1 000 mg/ℓ sodium chloride feed solution.**

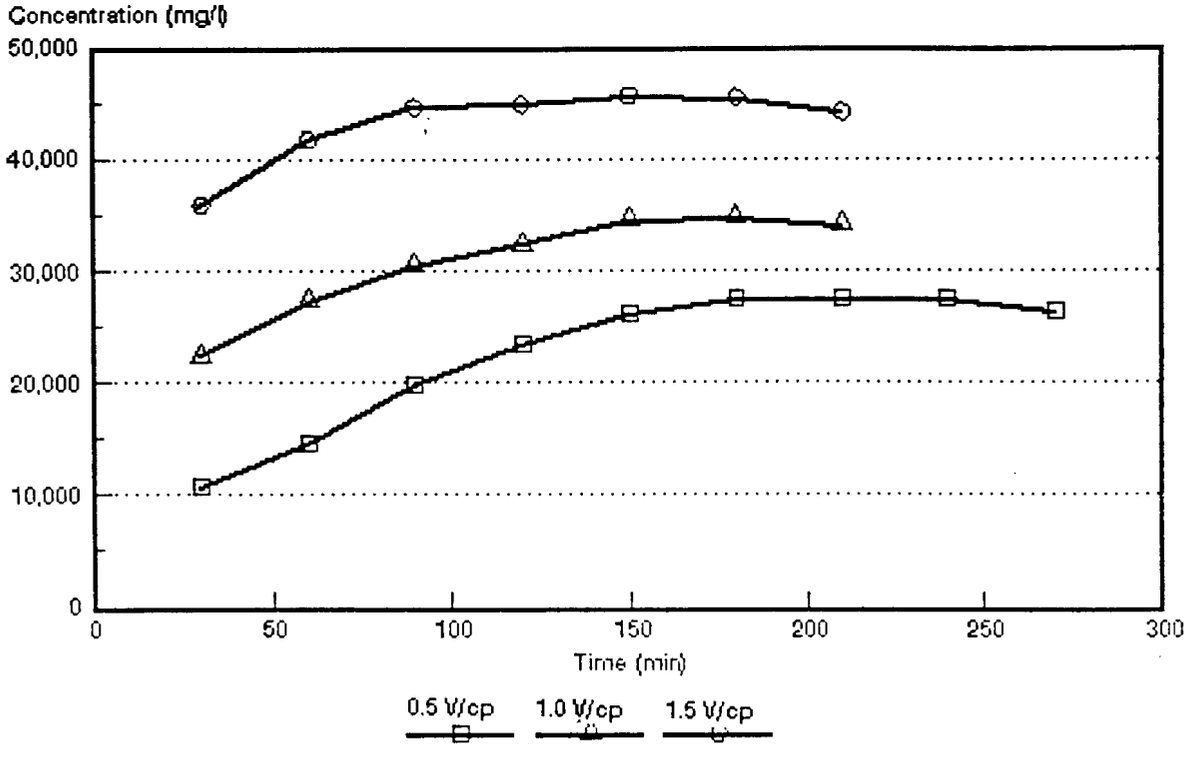

Figure 9.2: **Brine concentration as a function of time and cell pair voltage for an approximately 1 000 mg/ℓ sodium chloride feed solution.**

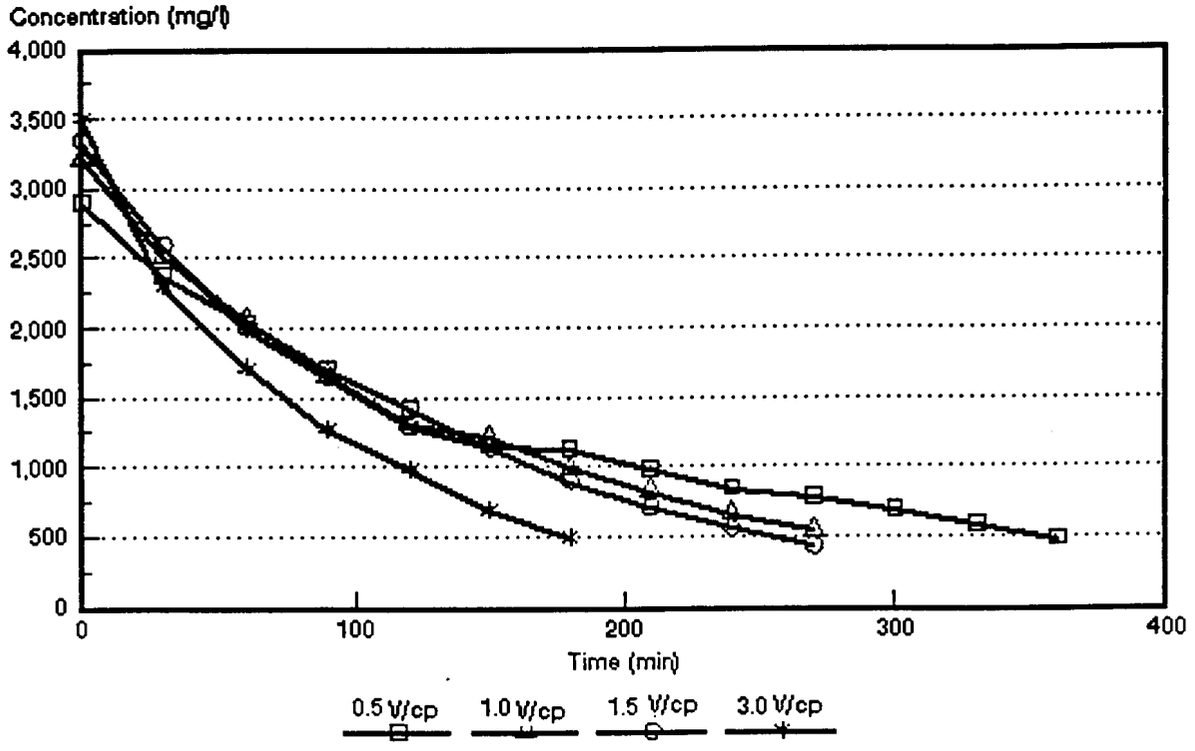

Figure 9.3: **Dialysate concentration as a function of time and cell pair voltage for an approximately 3 000 mg/ℓ sodium chloride feed solution.**

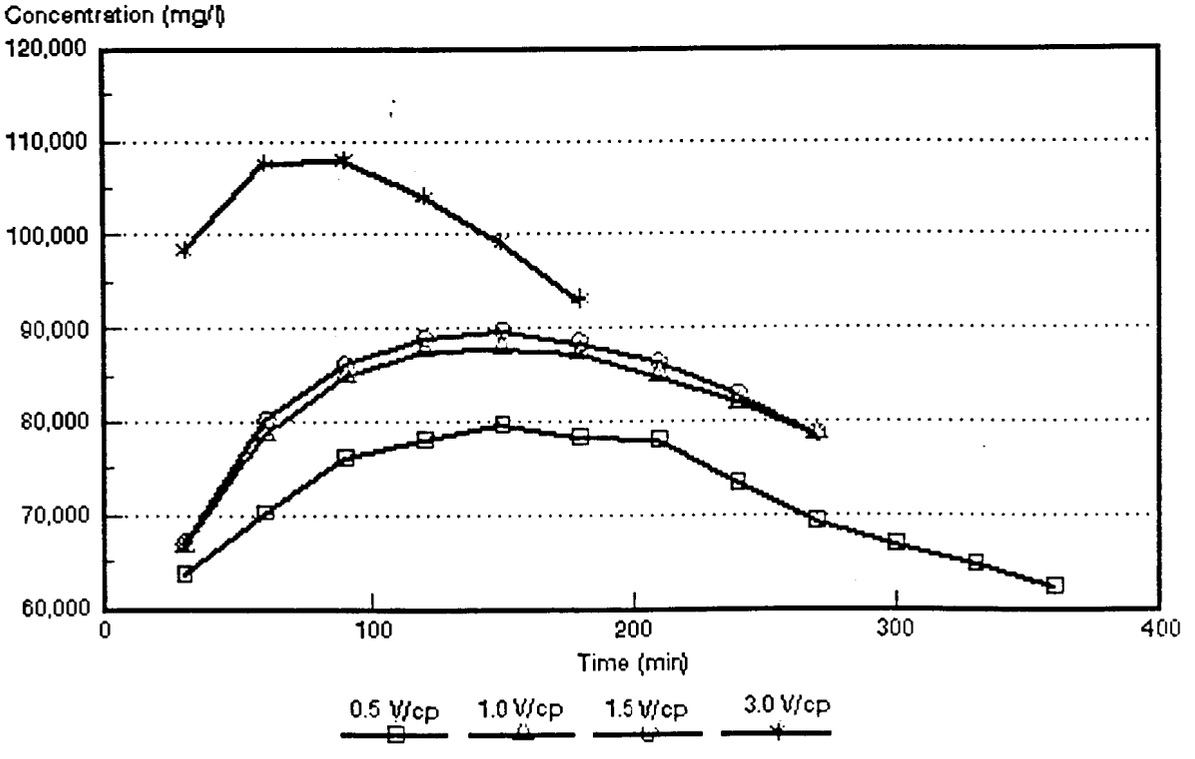

Figure 9.4: **Brine concentration as a function of time and cell pair voltage for an approximately 3 000 mg/ℓ sodium chloride feed solution.**

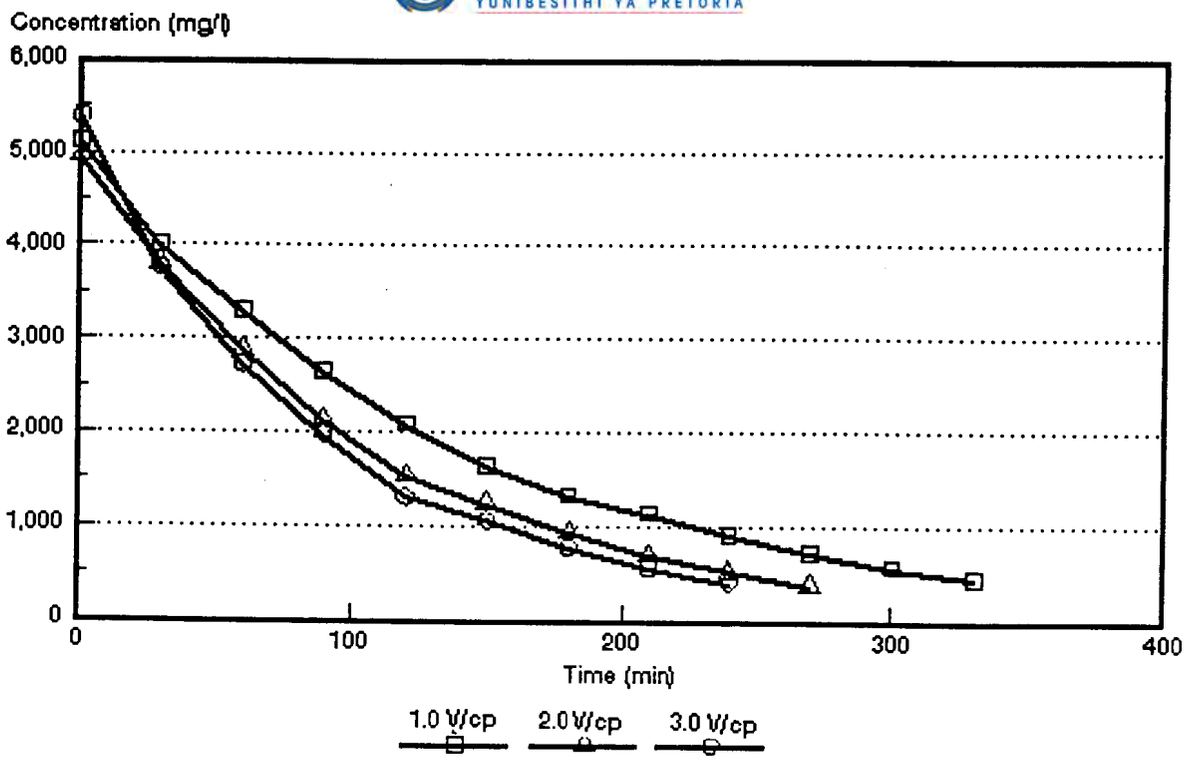

Figure 9.5: **Dialysate concentration as a function of time and cell pair voltage for an approximately 5 000 mg/ℓ sodium chloride feed solution.**

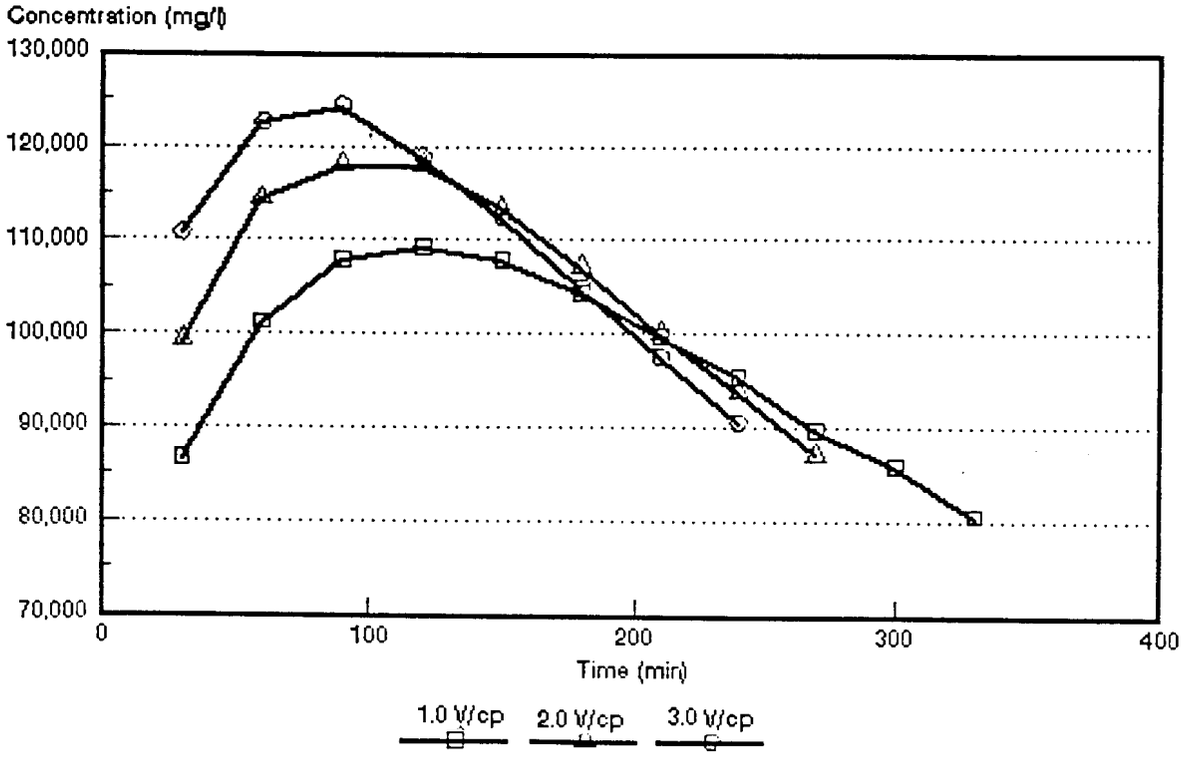

Figure 9.6: **Brine concentration as a function of time and cell pair voltage for an approximately 5 000 mg/ℓ sodium chloride feed solution.**

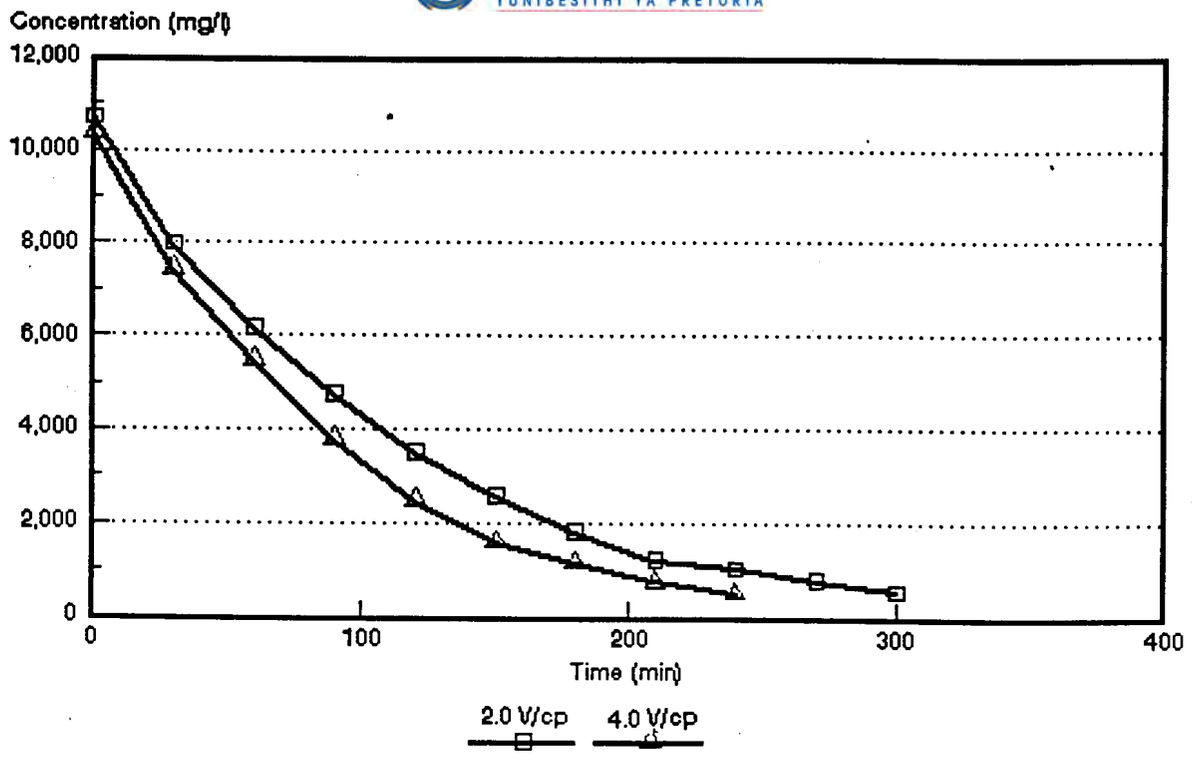

Figure 9.7: **Dialysate concentration as a function of time and cell pair voltage for an approximately 10 000 mg/ℓ sodium chloride feed solution.**

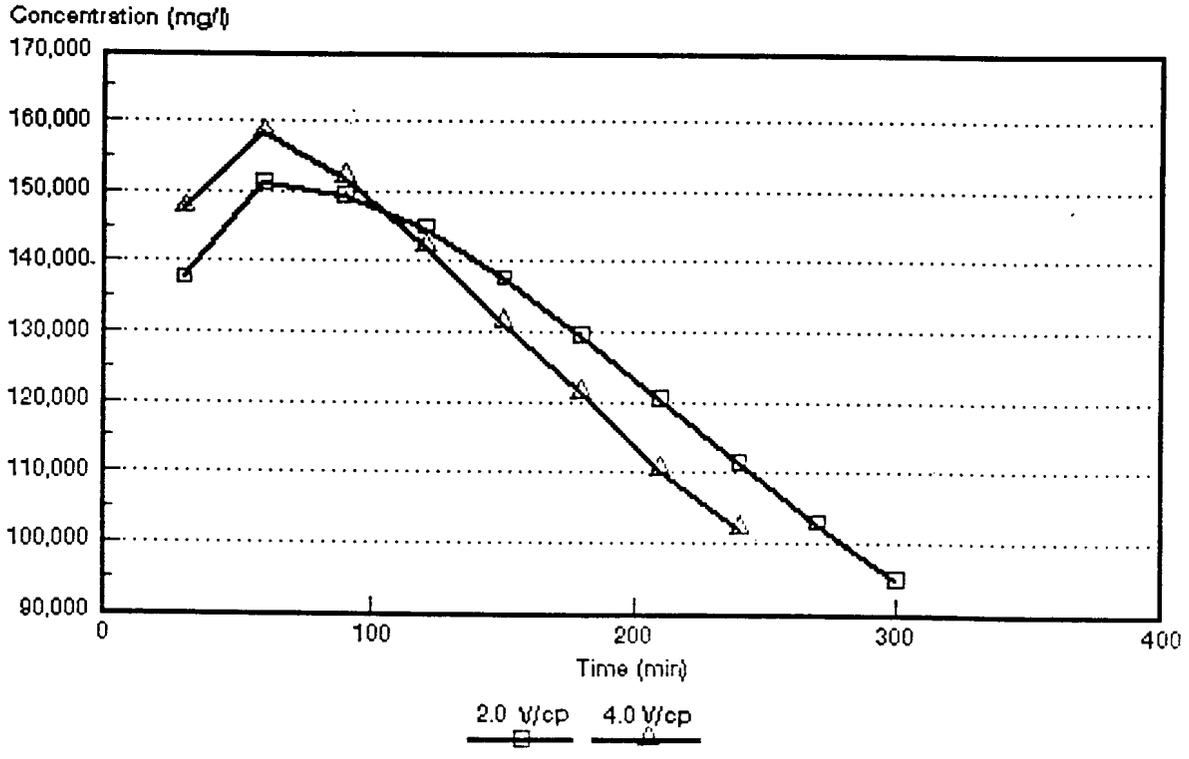

Figure 9.8: **Brine concentration as a function of time and cell pair voltage for an approximately 10 000 mg/ℓ sodium chloride feed solution.**

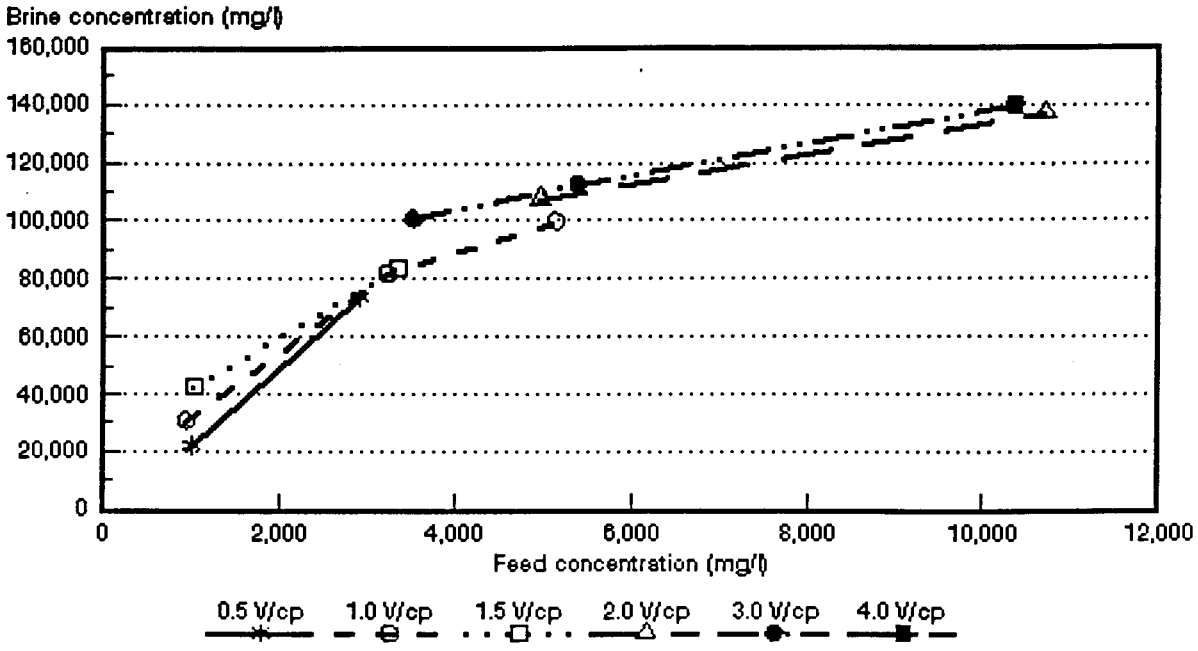

Figure 9.9: **Brine concentration as a function of sodium chloride feed water concentration and cell pair voltage.**

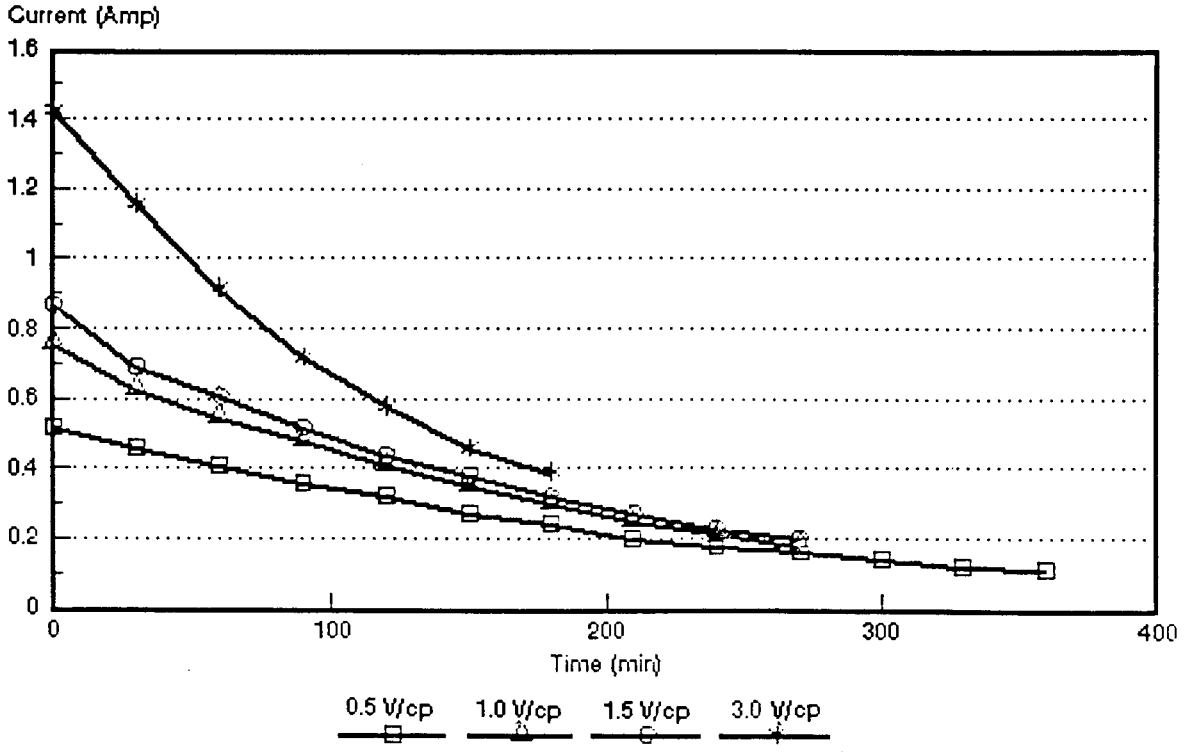

Figure 9.10: **Electrical current as a function of time and cell pair voltage during desalination of an approximately 3 000 mg/ℓ sodium chloride solution.**

range from 1 000 to 5 000 mg/ℓ (0,5 to 1,5 V/cp). Brine volume increased with increasing feed water concentration (Table 9.1) and a brine volume of 6,8% was obtained at a feed water concentration of approximately 10 000 mg/ℓ (3 V/cp). Water recoveries of approximately 96% were obtained in the feed water concentration range from 1 000 to 5 000 mg/ℓ. The lowest water recovery that was obtained was 93,7% (at approximately 10 000 mg/ℓ). Therefore, high water recoveries and low brine volumes could be obtained with EOP-ED.

9.1.3 Current efficiency

Current efficiency increased with increasing feed water concentration, especially at the higher cell pair voltages (Table 9.1 and Figure 9.11). This could be ascribed to an increasing flow of water through the membranes with increasing feed water concentration. Current efficiencies of 75,2 and 93,6% were obtained in the feed water and cell pair voltage ranges of 1 000 to 5 000 mg/ℓ and 0,5 to 1,5 V/cp, respectively. (Table 9.1). Current efficiencies of 69,4 to 86,9% were obtained in the feed water and cell pair voltage ranges of 3 000 to 10 000 mg/ℓ and 2 to 4 V/cp, respectively. Current efficiency further decreased with increasing cell pair voltage. This could be ascribed to increasing polarization that was taking place at the higher cell pair voltages.

9.1.4 Electrical energy consumption

Electrical energy consumption obtained during EOP-ED was low. Electrical energy consumption of less than 2,5 kWh/m^3 product water was obtained in the cell pair voltage and feed water concentration ranges of 0,5 to 1,5 V/cp (1 000 to 3 000 mg/ℓ)(Table 9.1), respectively. Electrical energy consumption further increased with increasing cell pair voltage and increasing feed water concentration (Fig. 9.12). Electrical energy consumption was 10 and 23,6 kWh/m^3 product water at 2 and 4 volt per cell pair, respectively (approximately 10 000 mg/ℓ feed). (Note: electrical energy consumption was only determined for ion transport).

9.1.5 Product water yield

Product water yield was low (Table 9.1). Product water yield varied between 0,28 and 0,67 m^3/m^2·d in the cell pair voltage and feed water concentration ranges studied. Water yield decreased as a function of feed water concentration and cell pair voltage (Table 9.1). A linear flow velocity of approximately 1 cm/s was used for most of the

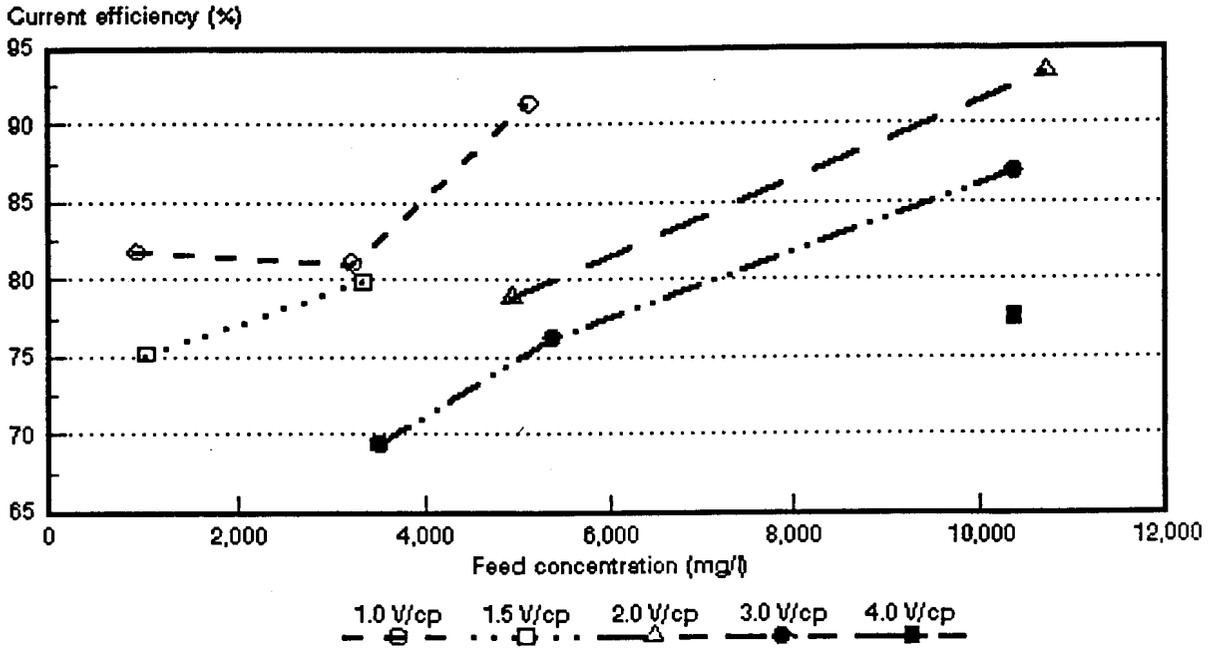

Figure 9.11: **Current efficiency as a function of sodium chloride feed concentration and cell pair voltage.**

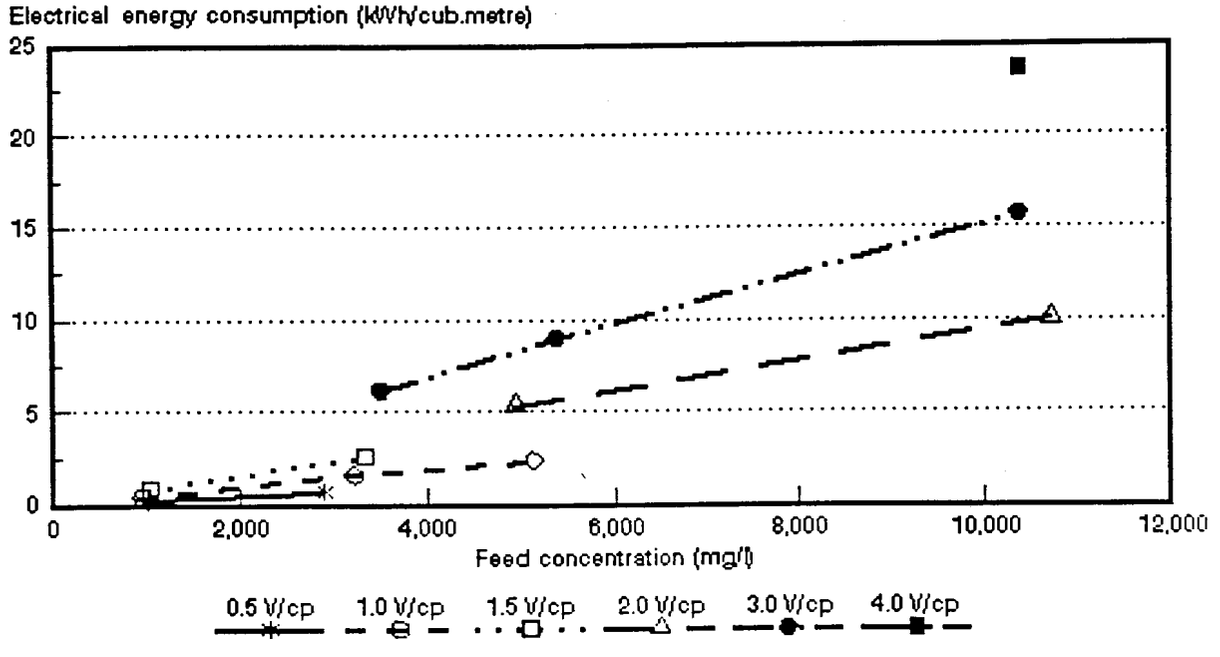

Figure 9.12: **Electrical consumption as a function of sodium chloride feed concentration and cell pair voltage.**

runs. However, linear flow velocity was increased to 2,1 cm/s and 2,7 cm/s at 3 000 mg/ℓ feed water concentration (1,5 V/cp)(Table 9.1). Product water yield was significantly increased when the linear flow velocity was increased.

9.1.6 Effective cell pair thickness and cell pair resistance

An example of cell pair resistance (R_{cp}) as a function of the specific resistance of the dialysate and cell pair voltage is shown in Figure 9.13. (Approximately 3 000 mg/ℓ feed). The lines through the linear region and extrapolation to the y-axis gives the cell pair resistance. The slope of the linear region gives the effective cell pair thickness, d_{eff}. The lines, however, deviate from linearity towards the end of the runs when the current is low and polarization is less. The effective cell pair thickness, d_{eff}, increased with increasing cell pair voltage and increasing feed water concentration. (Table 9.1). Cell pair resistance, R_{cp}, decreased with increasing feed water concentration and increased with increasing cell pair voltage (Table 9.1). The cell pair resistance increased slower than the specific resistance of the dialysate towards the end of the run because polarization is less. The effective thickness of the cell pair decreased significantly when the linear flow velocity was increased (Table 9.1).

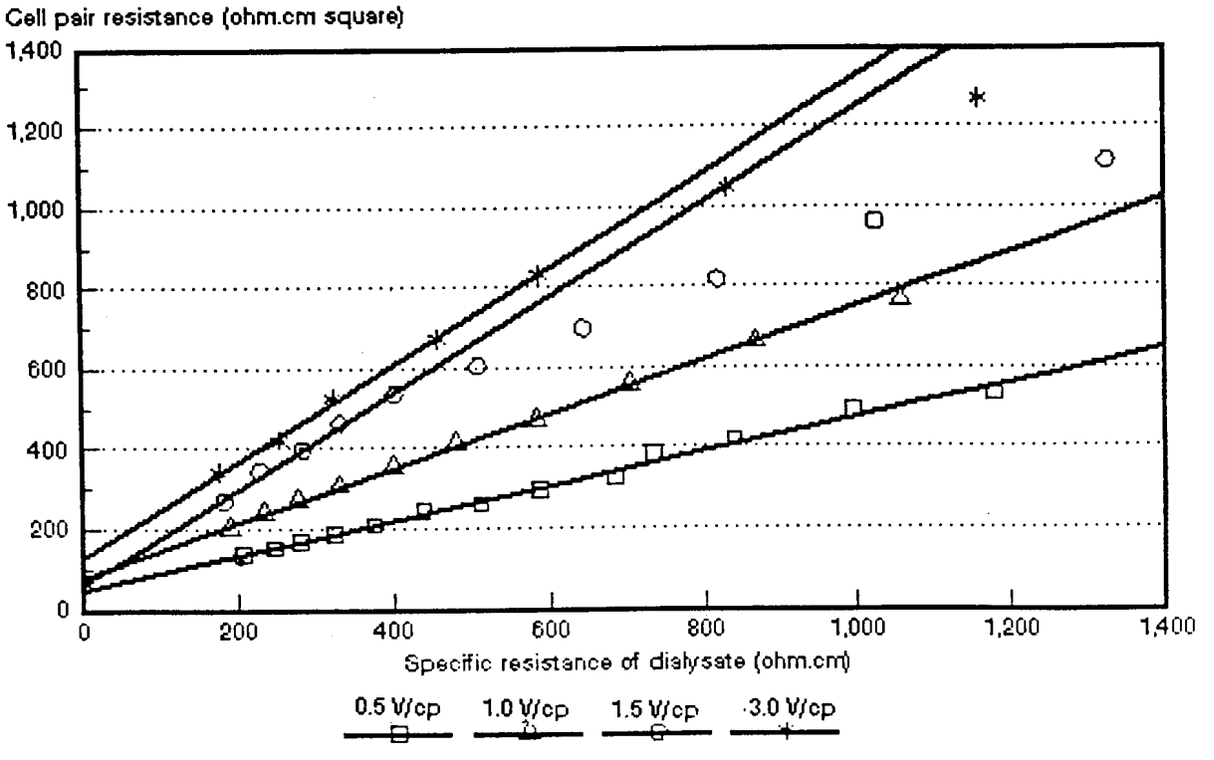

Figure 9.13: Cell pair resistance as a function of the specific resistance of the dialysate at different cell pair voltages (approximately 3 000 mg/ℓ sodium chloride feed).

9.2 Concentration/Desalination of Hydrochloric Acid Solutions with *Selemion* AAV and CHV Membranes

The concentration/desalination results of different hydrochloric acid feed water concentrations at different cell pair voltages are summarized in Table 9.2.

9.2.1 Acid brine and dialysate concentration

Dialysate and acid brine concentration as a function of time and cell pair voltage for different initial acid feed concentrations are shown in Figures 9.14 to 9.19. Acid brine concentration as a function of hydrochloric acid feed concentration and cell pair voltage is shown in Figure 9.20. Electric current as a function of time during concentration/desalination of an approximately 3 000 mg/ℓ hydrochloric acid feed solution is shown in Figure 9.21.

Faster and better acid removal was obtained at the higher cell pair voltages (Figs. 9.14, 9,16 and 9,18). Not much difference was experienced in the highest acid brine concentrations that could be obtained at the different cell pair voltages (Figs. 9.15, 9,17 and 9,19). Acid brine concentrations of 3,6 to 8,7% were obtained in the acid feed concentration range from approximately 1 000 to 5 000 mg/ℓ and cell pair voltage range from 0,5 to 4,0 volt per cell pair. Acid brine concentration further increased with increasing feed water concentration and increasing cell pair voltage (Fig. 9.20). Acid product water concentrations of less than 500 mg/ℓ could be obtained in the acid feed concentration and cell pair voltage range studied (Table 9.2).
Concentration factors were low. Concentration factors decreased as a function of acid feed concentration (Table 9.2).

9.2.2 Acid brine volume and water recovery

Low brine volumes and high water recoveries were obtained. Brine volume varied between 2,4 and 7,8% of the treated water volume in the acid feed concentration range of 1 000 to 5 000 mg/ℓ (0,5 to 4,0 V/cp)(Table 9.2). Brine volume also increased with increasing acid feed concentration and the highest acid brine concentration was obtained at an acid feed concentration of 5 000 mg/ℓ (1 V/cp). Water recovery was high. Water recovery of approximately 97% was obtained at an acid feed concentration of approximately 1 000 mg/ℓ (0,5 to 1 V/cp). The lowest water recovery obtained was 92,2% at an acid feed concentration of approximately 5 000 mg/ℓ (1,0

Table 9.2: **Concentration/desalination results of hydrochloric acid solutions at different feed concentrations and cell pair voltages using Selemion AAV and CHV membranes.**

Vcp	cf mg/ℓ	cp mg/ℓ	c_b mg/ℓ	CF	CE %	WR %	BV %	EEC kWh/m³	OP $m^3/m^2 \cdot d$	d_{eff} mm	Rcp ohm·cm²
0,5	1 130	197	36 460	32,3	37,8	97,1	2,9	0,182	0,33	5,1	15,1
0,5*	2 989	452	56 513	18,9	46,3	93,6	6,4	2,18	0,64	5,0	
1,0	1 021	175	36 460	35,7	29,2	97,6	2,4	2,14	0,39	7,90	58,4
1,0	3 281	452	67 451	20,6	35,6	94,6	5,4	5,90	0,36	13,80	1,9
1,0*	2 989	379	61 982	20,7	35,7	94,0	6,0	5,5	0,64	8,1	-1,6
1,0	5 032	510	85 681	17,0	32,0	92,2	7,8	10,5	0,31	13,50	
1,5	1 167	175	38 283	32,8	34,3	97,5	2,5	3,2	0,41	11,97	112,1
2,0	3 318	419	69 274	20,9	32,7	94,3	5,7	13,2	0,38	25,9	4,8
2,0*	3 099	510	43 752	14,12	38,6	92,5	7,5	10,83	0,70	21,4	-1,2
2,0	5 213	496	85 681	16,4	31,6	92,3	7,7	22,1	0,33	25,6	
3,0	3 354	467	72 920	21,7	33,9	94,6	5,4	18,99	0,43	37,3	3,5
3,0*	3 537	496	69 274	19,6	33,80	93,75	6,25	21,33	0,80	25,9	1,2
3,0	5 287	481	87 504	16,6	32,2	92,5	7,5	33,17	0,35	35,9	
4,0	3 208	423	72 920	22,7	33,3	94,9	5,1	24,76	0,46	46,8	13,2
4,0	4 958	467	85 681	17,2	31,3	92,8	7,2	42,58	0,40	44,9	3,9

* Linear flow velocity ≈ 5 cm/s. Other experiments conducted at a linear flow velocity of 1 cm/s.

CF = concentration factor
CE = current efficiency
BV = brine volume
OP = output (yield)
WR = water recovery
EEC = electrical energy consumption

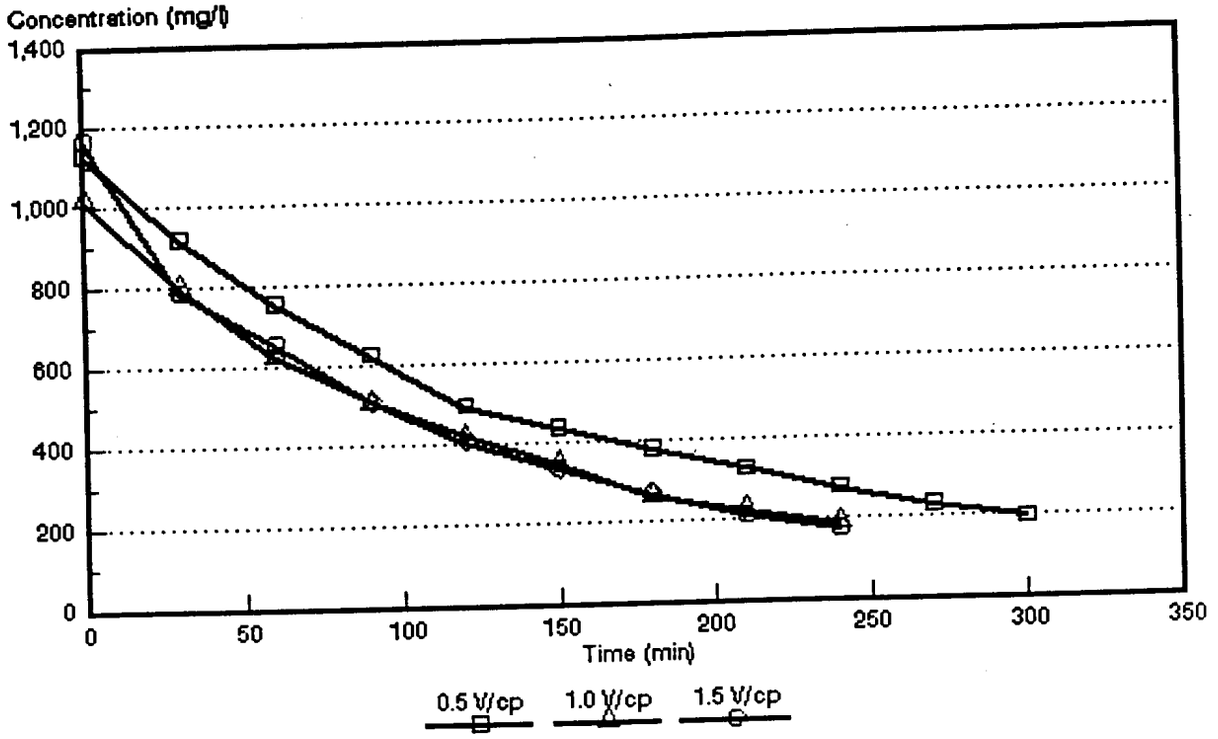

Figure 9.14: **Dialysate concentration as a function of time and cell pair voltage for approximately 1 000 mg/ℓ hydrochloric acid solutions.**

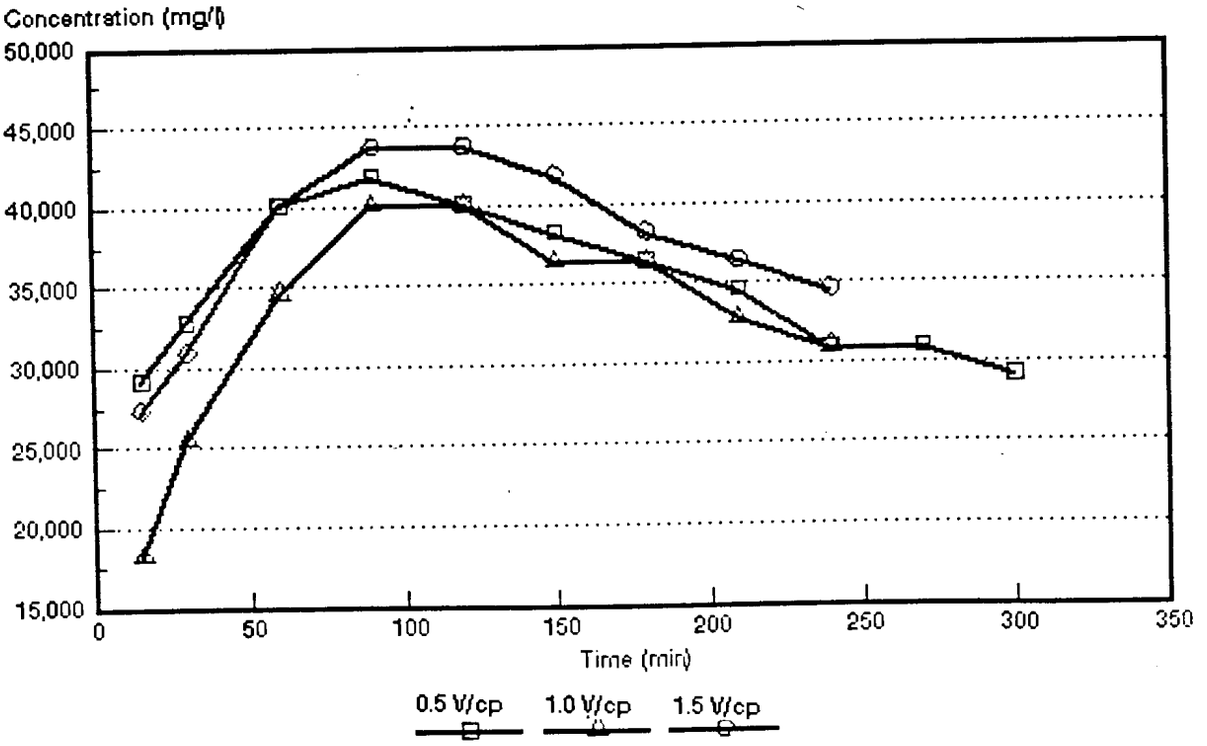

Figure 9.15: **Brine concentration as a function of time and cell pair voltage for approximately 1 000 mg/ℓ hydrochloric acid solutions.**

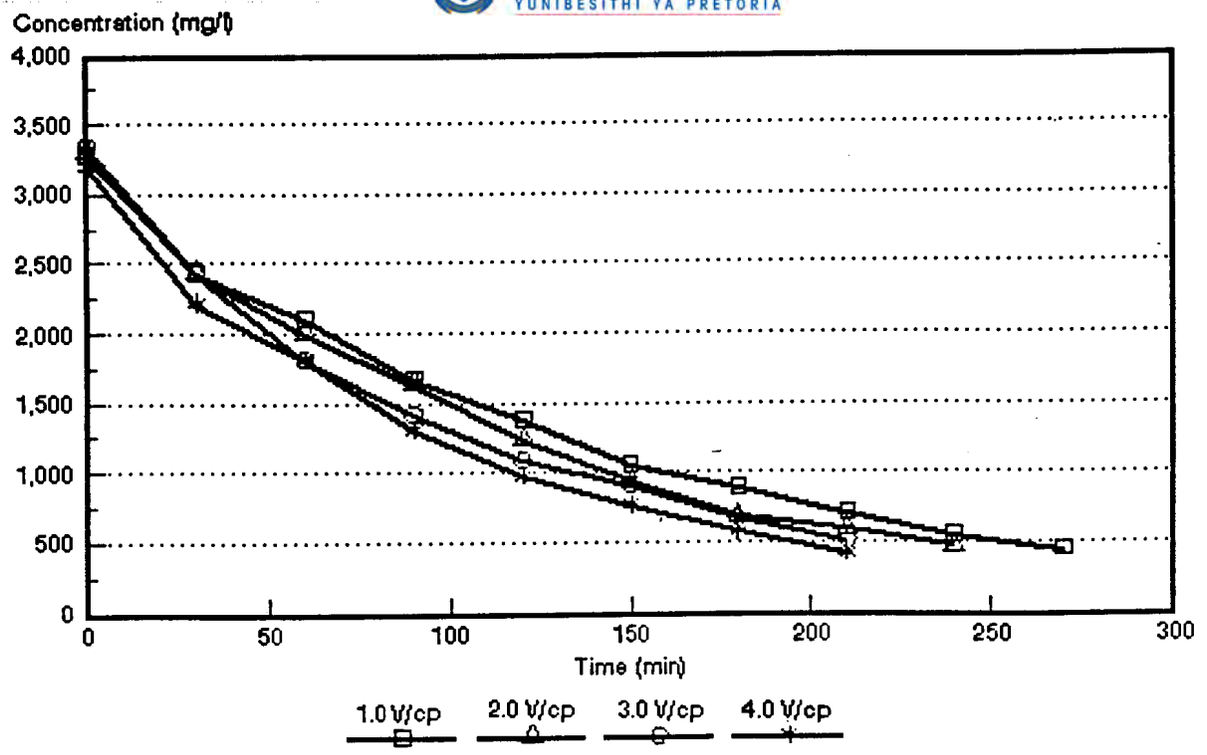

Figure 9.16: **Dialysate concentration as a function of time and cell pair voltage for approximately 3 000 mg/ℓ hydrochloric acid solutions.**

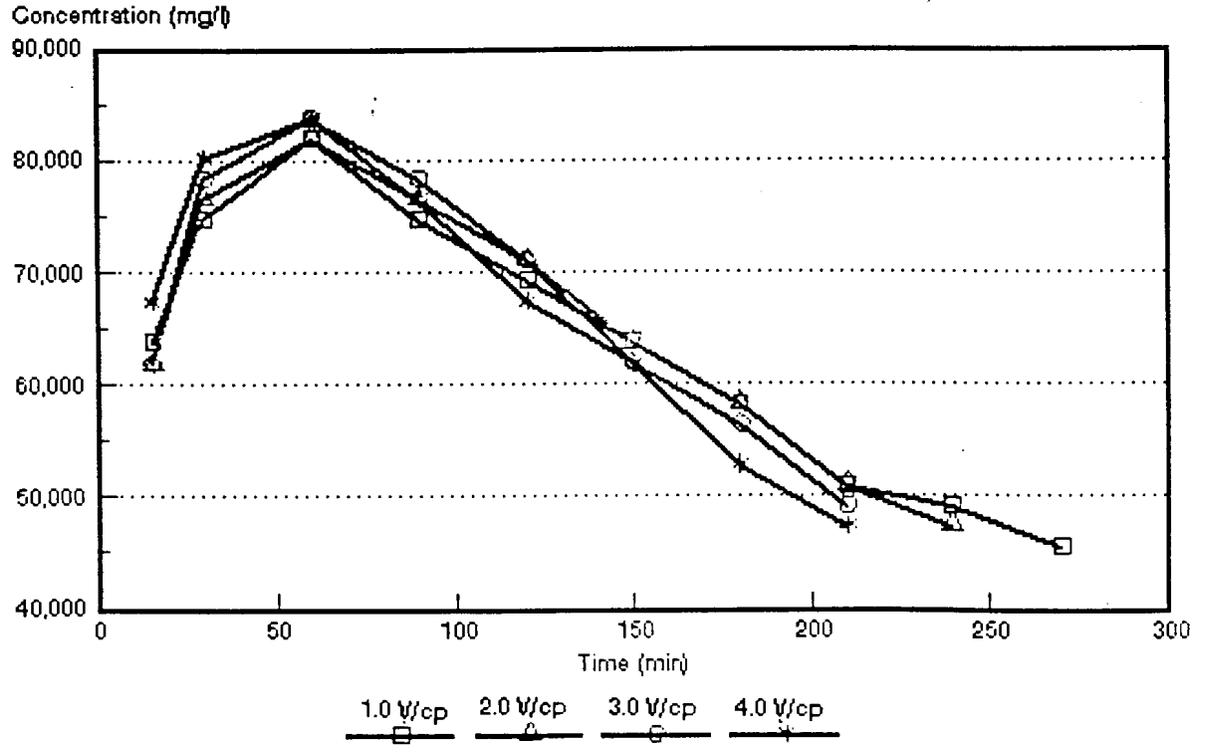

Figure 9.17: **Brine concentration as a function of time and cell pair voltage for approximately 3 000 mg/ℓ hydrochloric acid solutions.**

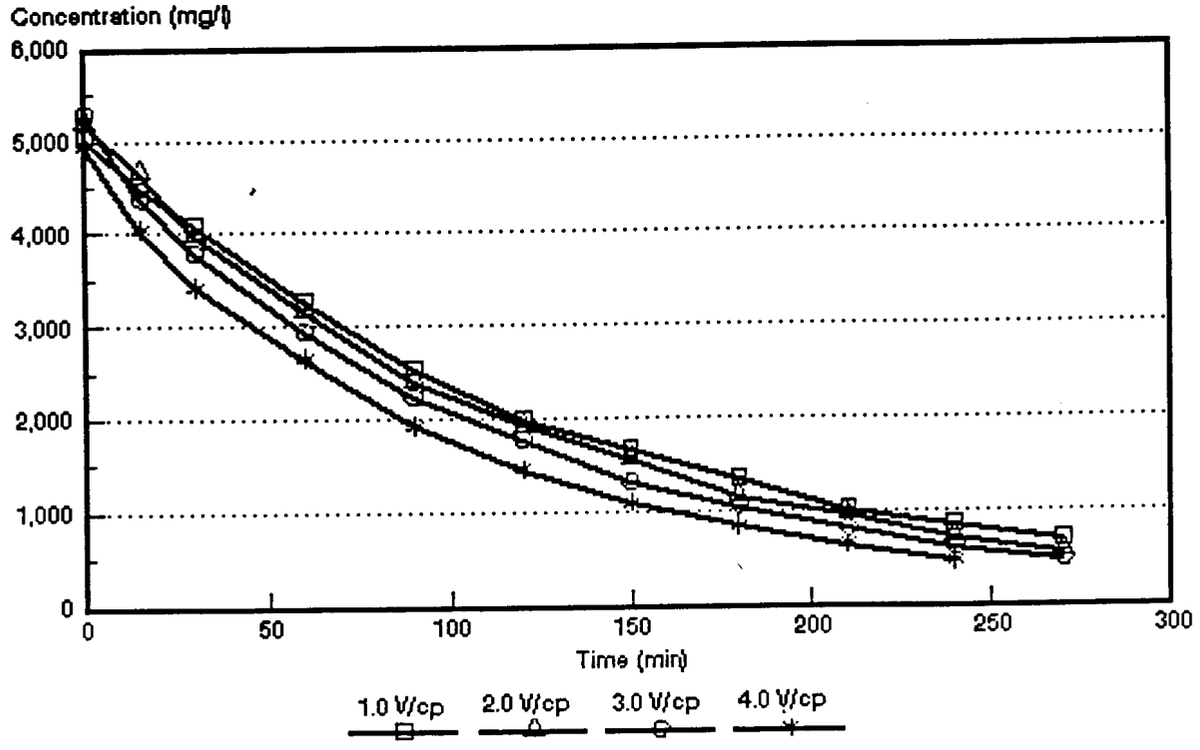

Figure 9.18: **Dialysate concentration as a function of time and cell pair voltage for approximately 5 000 mg/ℓ hydrochloric acid solutions.**

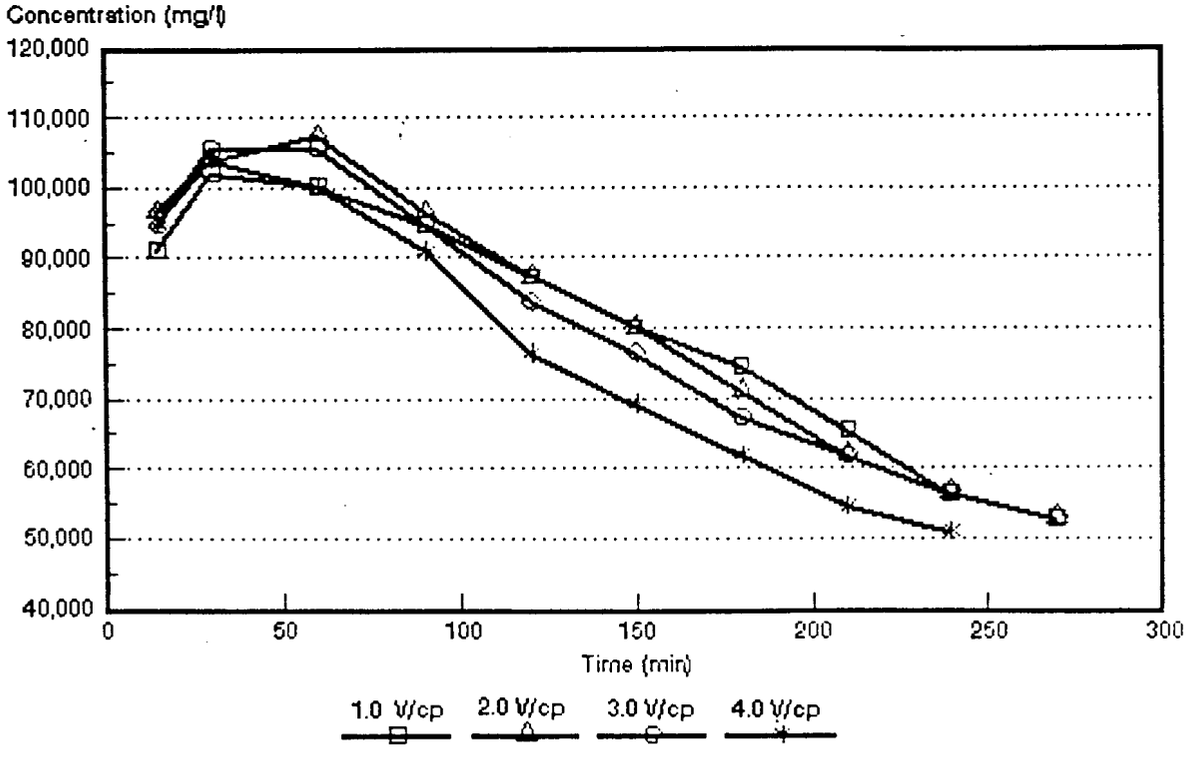

Figure 9.19: **Brine concentration as a function of time and cell pair voltage for approximately 5 000 mg/ℓ hydrochloric acid solutions.**

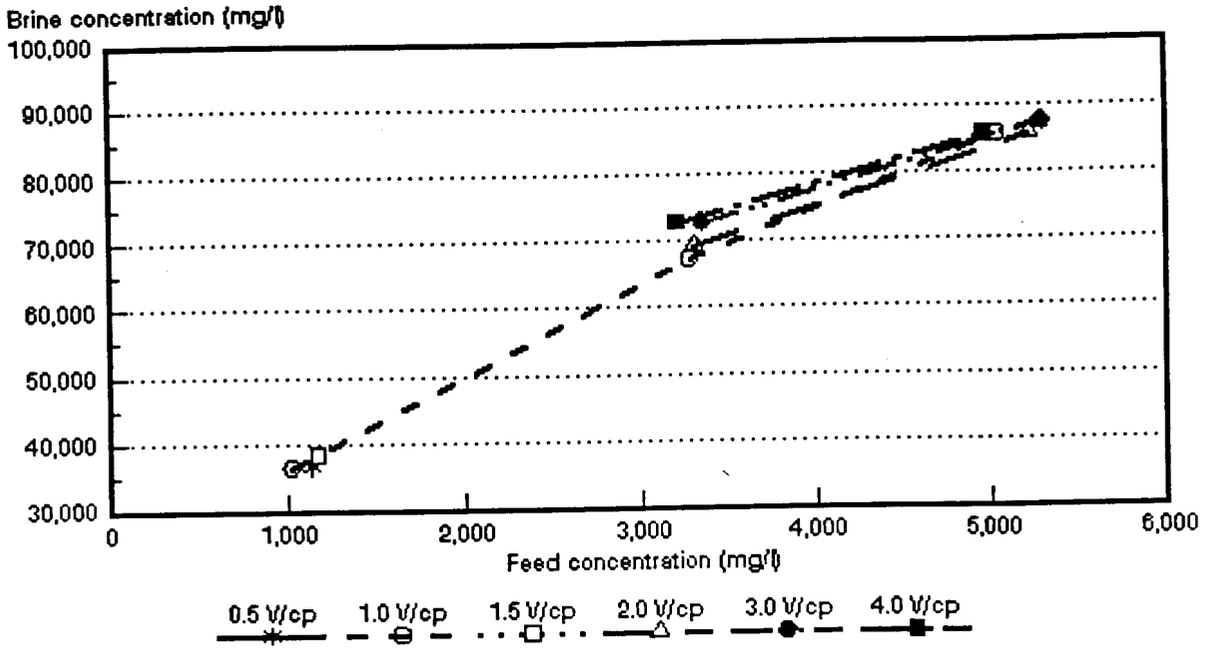

Figure 9.20: **Brine concentration as as a function of hydrochloric acid feed concentration and cell pair voltage.**

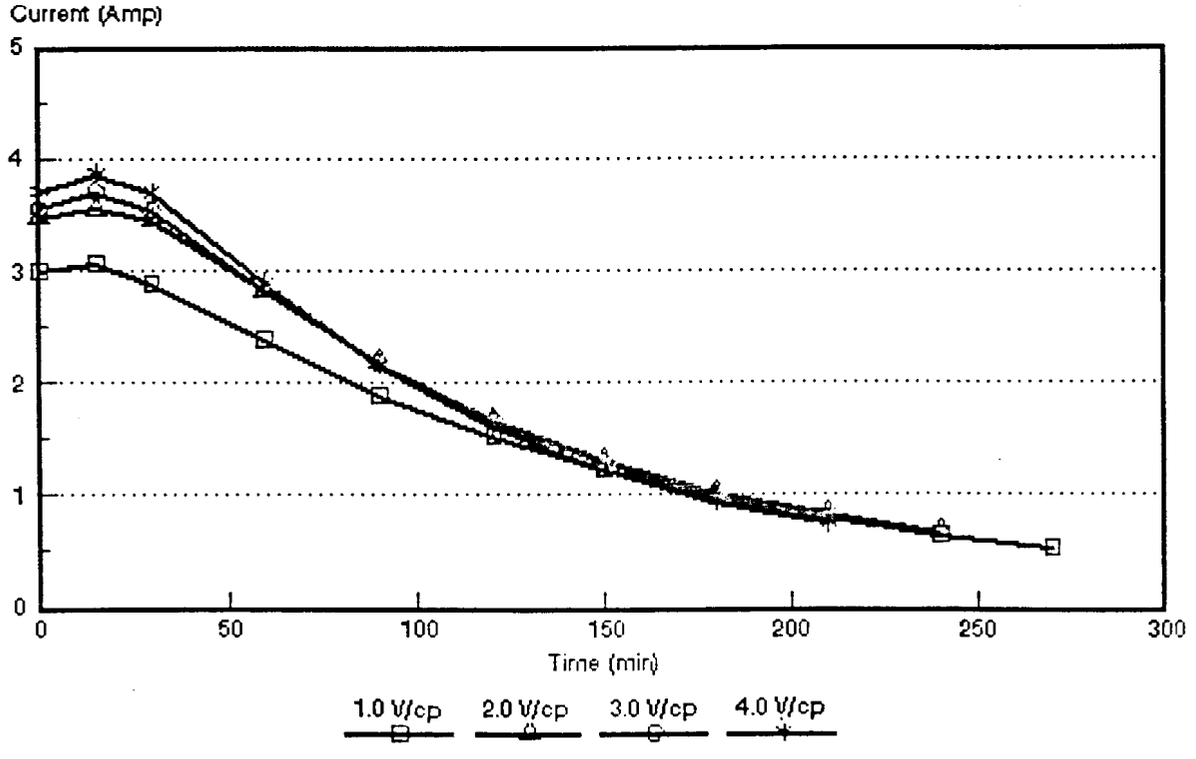

Figure 9.21: **Electric current as a function of time and cell pair voltage during concentration/desalination of approximately 3 000 mg/ℓ hydrochloric acid solutions.**

V/cp). Therefore, high water recoveries and low acid brine volumes could be obtained with EOP-ED of acidic solutions.

9.2.3 Current efficiency

Current efficiencies were low (Table 9.2). Current efficiency varied between 46,3 and 29,2% in the acid feed concentration and cell pair voltage ranges studied. Current efficiency did not change with increasing cell pair voltage and decreased with increasing feed water concentration especially at the higher acid feed concentrations (Fig. 9.22). This is contrary to what has been experienced during EOP-ED of sodium chloride solutions and can be ascribed to less water that permeates through the membranes at higher feed concentration. The low current efficiencies that were obtained with the acid solutions could be ascribed to the inability of the anion membranes to resist the passage of hydrogen ions. However, the permselectivity of the *Selemion* AAV membranes for hydrogen ions is much better than that of other membranes normally used for ED of saline solutions.

9.2.4 Electrical energy consumption

Electrical energy consumption increased with increasing cell pair voltage and increasing acid feed concentration (Table 9.2 and Fig. 9.23). Low electrical energy consumption was obtained at low cell pair voltages and low acid feed concentrations. Electrical energy consumptions of 0,2 to 3,2 kWh/m^3 product were obtained in the acid feed and cell pair voltage range of approximately 1 000 mg/ℓ and 0,5 to 1,5 V/cp, respectively. However, electrical energy consumption increased rapidly with increasing feed concentration and cell pair voltage. The electrical energy consumption at 2,0; 3,0 and 4,0 V/cp of an approximately 3 000 mg/ℓ hydrochloric acid solution was determined at 13,2; 18,9 and 24,8 kWh/m^3 product water, respectively.

9.2.5 Product water yield

Product water yield (output) increased with increasing cell pair voltage and decreased with increasing acid feed concentration (Table 9.2). Output also increased significantly with increasing linear flow velocity through the stack. Output was determined at 0,38 m^3/m^2·d at a linear flow velocity of 1 cm/s (2,0 V/cp). At a linear flow velocity of 5 cm/s, output was determined at 0,7 m^3/m^2·d (Table 9.2). Therefore, it would be advantageous to operate an EOP-ED stack at the highest possible linear flow velocity.

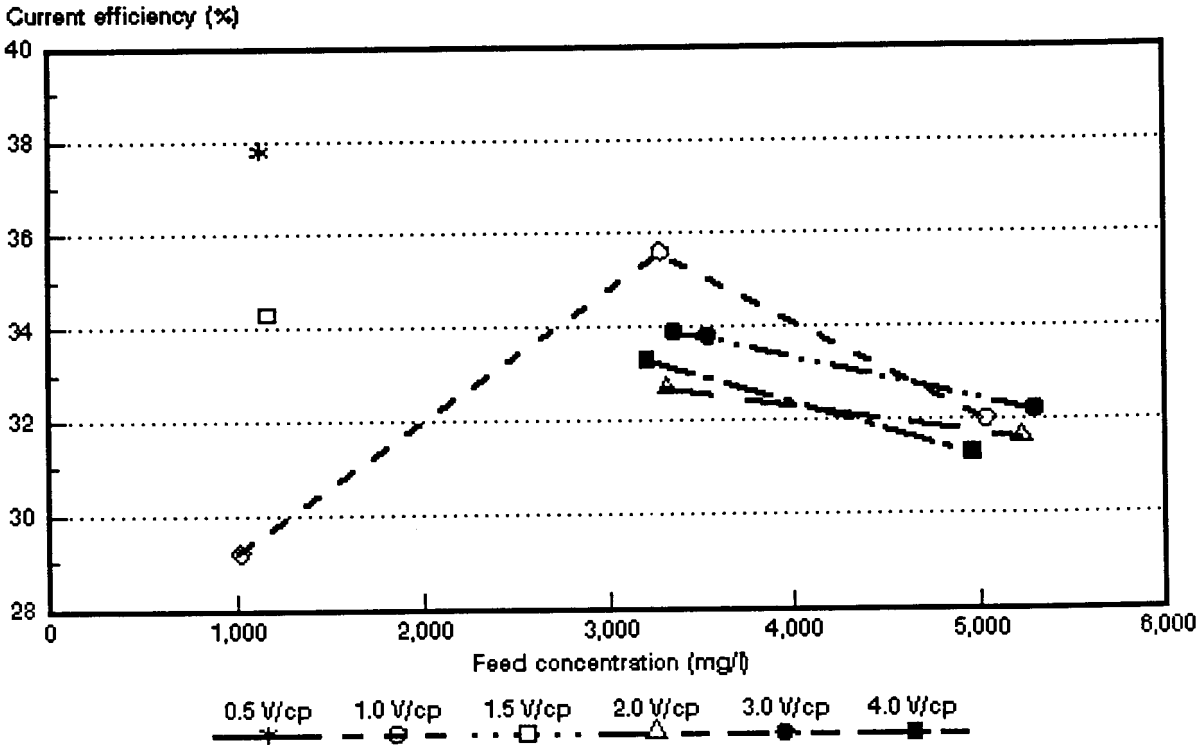

Figure 9.22: **Current efficiency as a function of hydrochlric acid feed concentration and cell pair voltage.**

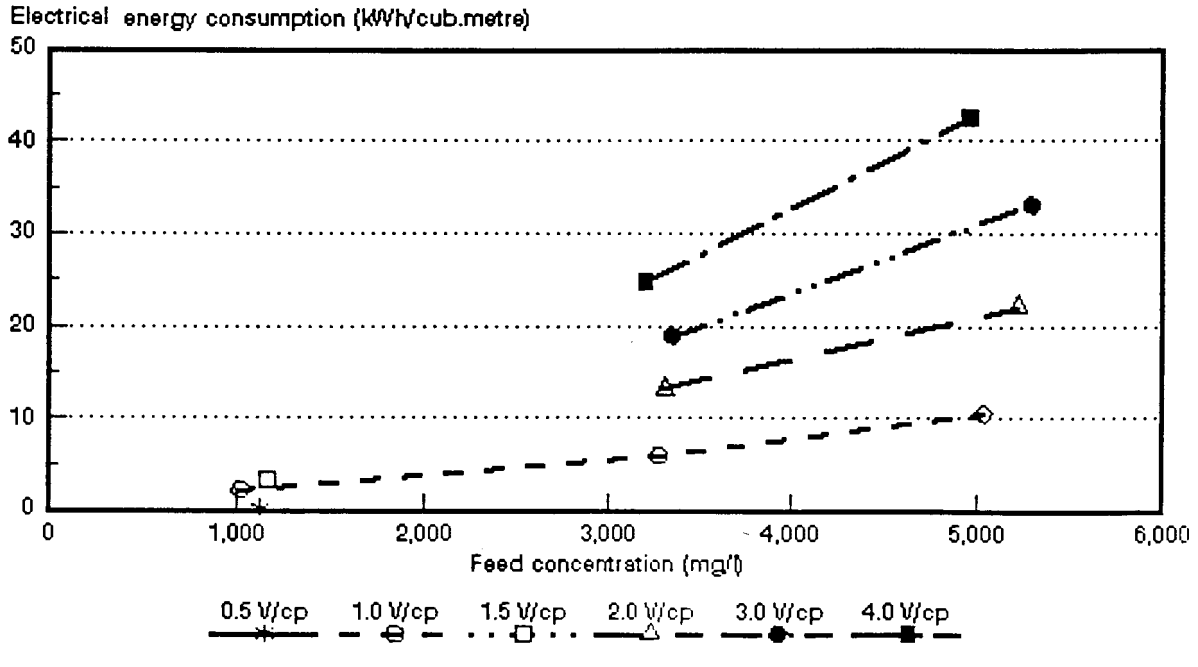

Figure 9.23: **Electrical energy consumption as a function of hydrochloric acid feed concentration and cell pair voltage.**

9.2.6 Effective cell pair thickness and cell pair resistance

An example of cell pair resistance (R_{cp}) as a function of the specific resistance of the dialysate and cell pair voltage is shown in Figure 9.24 for an approximately 5 000 mg/ℓ hydrochloric acid feed solution. Straight lines were obtained over the cell pair voltage range studied. The slope of the lines increased with increasing cell pair voltage as was experienced with sodium chloride solutions. However, the slopes of the lines were much steeper in the case of the acid especially at the higher cell pair voltages.

The effective cell pair thickness, d_{eff}, was determined at 13,5; 25,6; 35,9 and 44,9 mm at 1; 2; 3 and 4 V/cp, respectively (5 000 mg/ℓ feed) (Table 9.2). Effective cell pair thickness decreased significantly with increasing linear flow velocity. The effective cell pair thickness decreased from 13,8 mm to 8,1 mm at 1 V/cp (3 000 mg/ℓ feed).

Cell pair resistance, R_{cp}, decreased with increasing feed concentration and decreasing cell pair voltage. The negative cell pair resistances reported in Table 9.2 could be ascribed to experimental error due to the very low resistance of the cell pair.

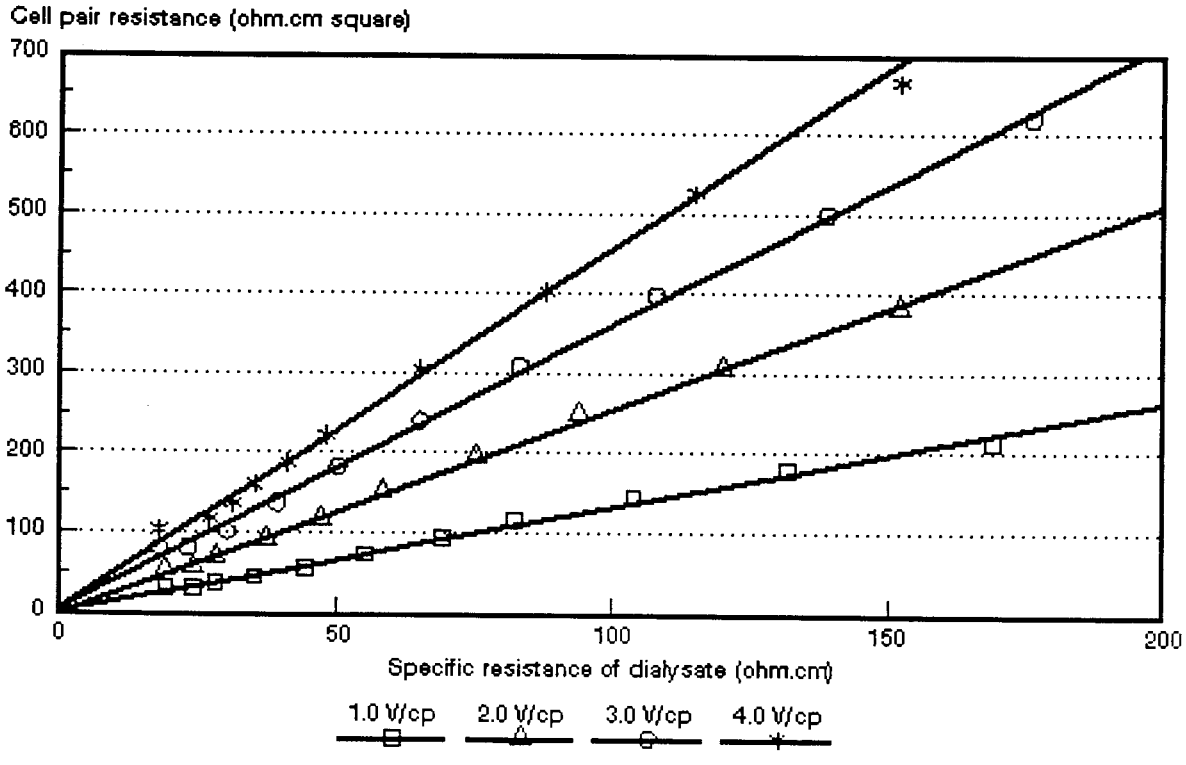

Figure 9.24: Cell pair resistance as a function of specific resistance of the dialysate and cell pair voltage for approximately 5 000 mg/ℓ hydrochloric acid solutions.

9.3 Concentration/Desalination of Caustic Soda Solutions with *Selemion* AMV and CMV Membranes

The concentration/desalination results of different caustic soda feed water concentrations at different cell pair voltages are summarized in Table 9.3.

9.3.1 Brine and dialysate concentration

Dialysate and brine concentrations as a function of time and cell pair voltage for different initial feed water concentrations are shown in Figs. 9.25 to 9.30. Caustic soda brine concentration as a function of feed concentration and cell pair voltage is shown in Figure 9.31. A typical example of electric current as a function of time and cell pair voltage for an approximately 5 000 mg/ℓ caustic soda feed solution is shown in Figure 9.32.

Desalination/concentration rate increased with increasing cell pair voltage (Figs. 9.25 to 9.30 and Fig. 9.32). Brine concentration increased as a function of feed concentration and cell pair voltage (Table 9.3 and Fig. 9.31). Caustic soda brine concentrations of 2,8 to 9,8% were obtained in the feed and cell pair voltage ranges of approximately 1 000 to 10 000 mg/ℓ and 0,5 to 3,0 V/cp, respectively.

Product water with a concentration of less than 400 mg/ℓ caustic soda could be produced (Table 9.3) from caustic soda feed waters in the feed and cell pair voltage ranges of 1 000 to 10 000 mg/ℓ and 0,5 to 3,0 V/cp, respectively. It was possible to produce a product water with a concentration of less than 100 mg/ℓ caustic soda.

Concentration factors increased with increasing cell pair voltage and decreased with increasing feed concentration as was experienced with sodium chloride and hydrochloric acid solutions.

9.3.2 Brine volume and water recovery

Low brine volumes and high water recoveries were again obtained (Table 9.3). Brine volume varied between 2,3 and 7,3% in the caustic soda feed water and cell pair voltage ranges of 1 000 to 5 000 mg/ℓ and 0,5 to 3 V/cp, respectively. Brine volume further increased with increasing caustic soda feed water concentration in the feed concentration range from 1000 to 10 000 mg/ℓ. The highest brine volume of 11,7%

Table 9.3: Concentration/desalination results of caustic soda solutions at different feed concentrations and cell pair voltages using Selemion AMV and CMV membranes.

Vcp	c_f mg/ℓ	c_p mg/ℓ	c_b mg/ℓ	CF	CE %	WR %	BV %	EEC kWh/m³	OP m³/m²·d	d_{eff} mm	Rcp ohm·cm²
0,5	1 008	168	30 000	29,8	75,1	97,7	2,3	0,77	0,42	6,03	56,1
1,0	1 056	120	28 000	26,5	68,96	97,55	2,45	0,91	0,44	11,6	54,8
	2 920	400	60 000	20,6	77,96	96,8	3,2	2,18	0,47		
	5 480	224	64 000	11,7	77,80	92,7	7,3	4,54	0,33		
	10 640	400	90 000	8,5	73,3	88,3	11,7	9,40	0,33	12,64	0,15
1,5	1 104	96	30 000	27,2	71,98	97,6	2,4	1,41	0,51	11,99	146,8
2,0	3 400	400	80 000	23,5	81,2	96,9	3,1	4,97	0,73		
	4 960	85	76 000	15,3	78,1	93,75	6,25	8,38	0,43		
	10 880	320	98 000	9,0	73,1	90,0	10,0	19,42	0,56	13,59	7,1
3,0	3 200	384	84 000	26,3	79,2	97,0	3,0	7,18	1,27		
	5 560	256	86 000	15,5	78,36	94,6	5,4	13,64	0,92		

Linear flow velocity 1 cm/s.

CF = concentration factor
CE = current efficiency
BV = brine volume
OP = output (yield)
WR = water recovery
EEC = electrical energy consumption

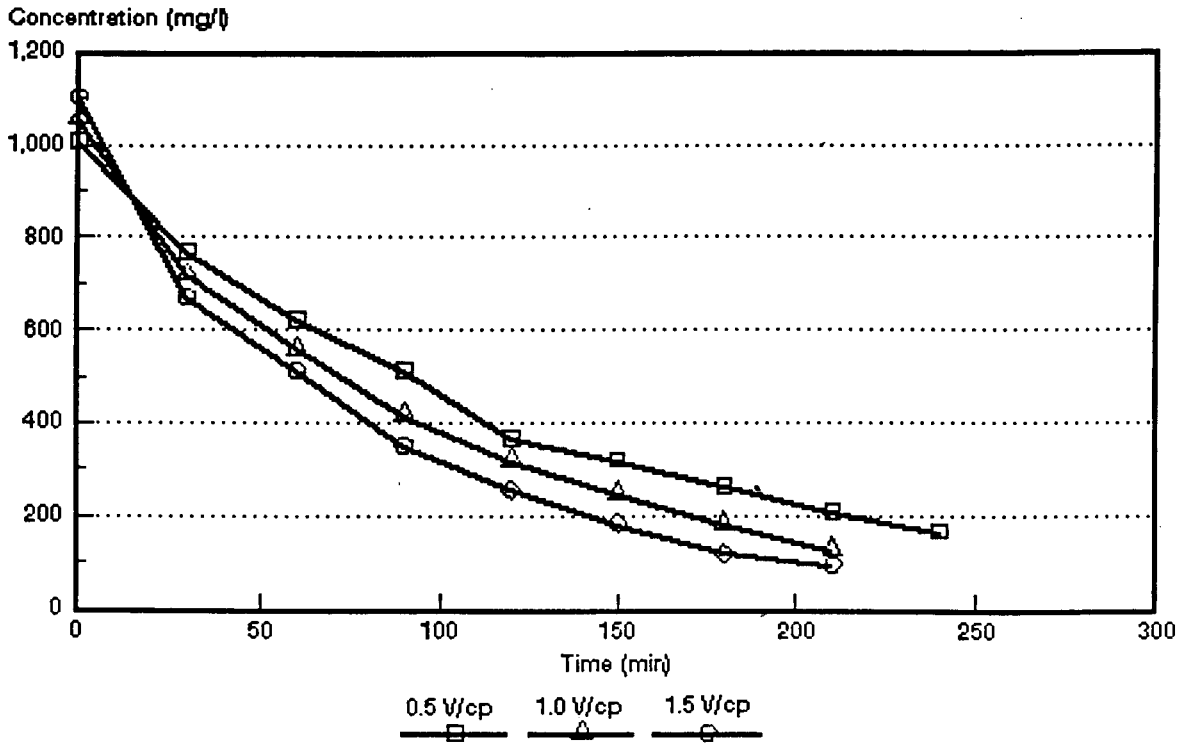

Figure 9.25: **Dialysate concentration as a function of time and cell pair voltage for an approximately 1 000 mg/ℓ caustic soda feed solution.**

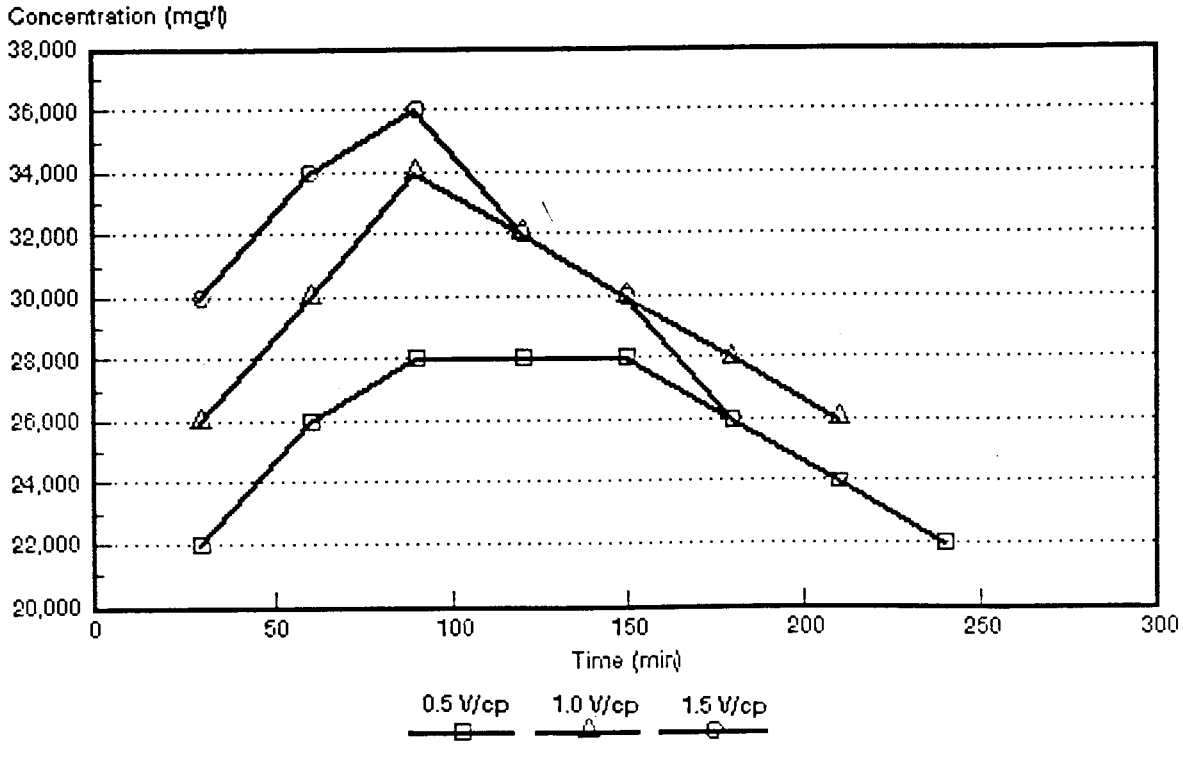

Figure 9.26: **Brine concentration as a function of time and cell pair voltage for an approximately 1 000 mg/ℓ caustic soda feed solution.**

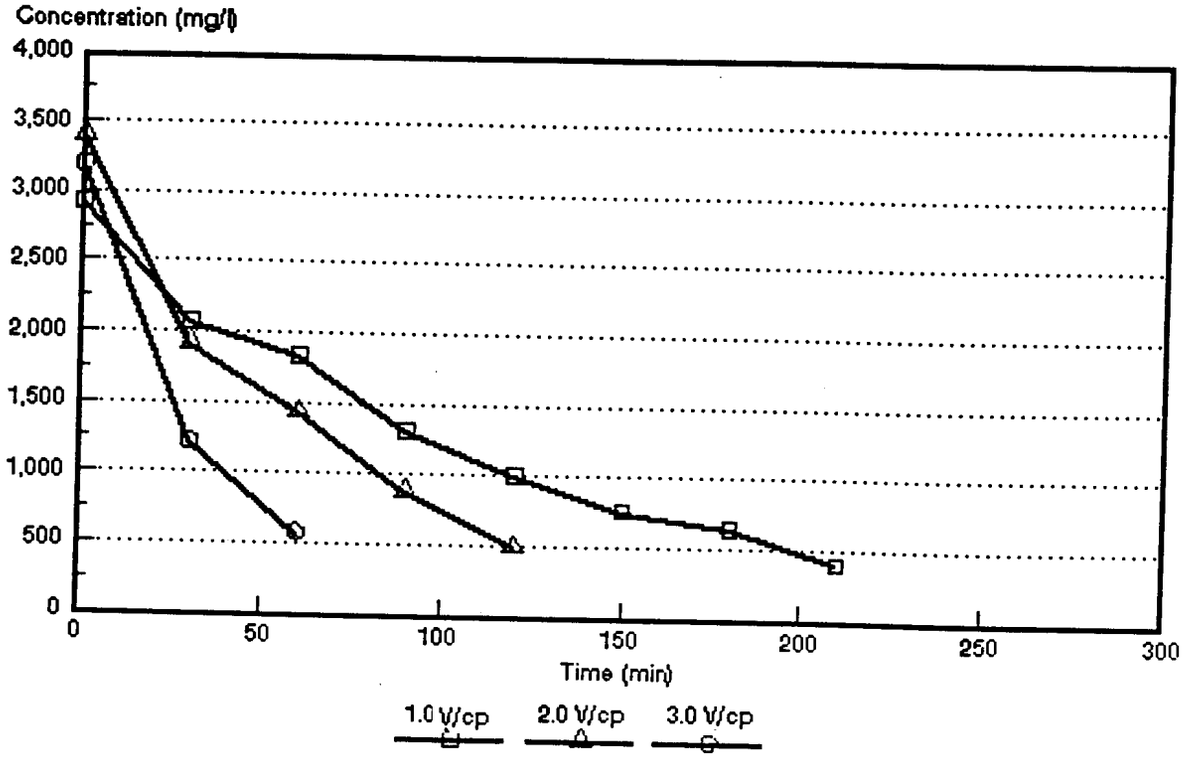

Figure 9.27: **Dialysate concentration as a function of time and cell pair voltage for an approximately 3 000 mg/ℓ caustic soda feed solution.**

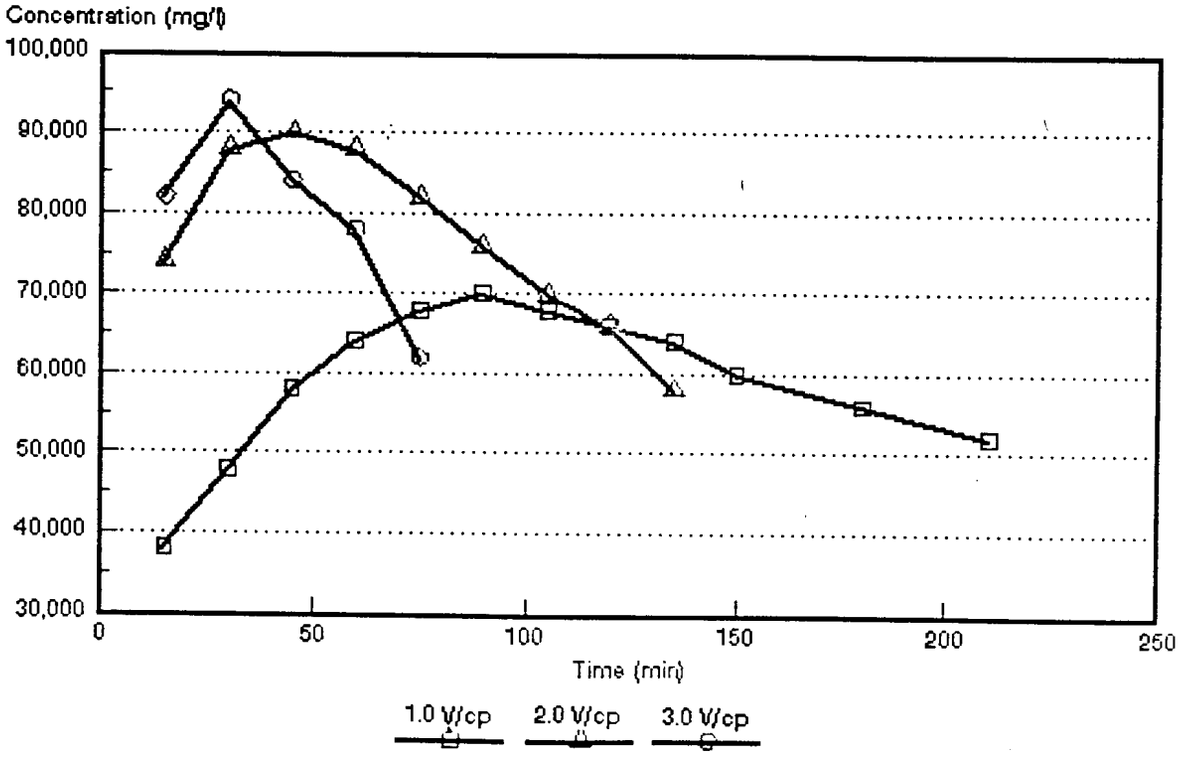

Figure 9.28: **Brine concentration as a function of time and cell pair voltage for an approximately 3 000 mg/ℓ caustic soda feed solution.**

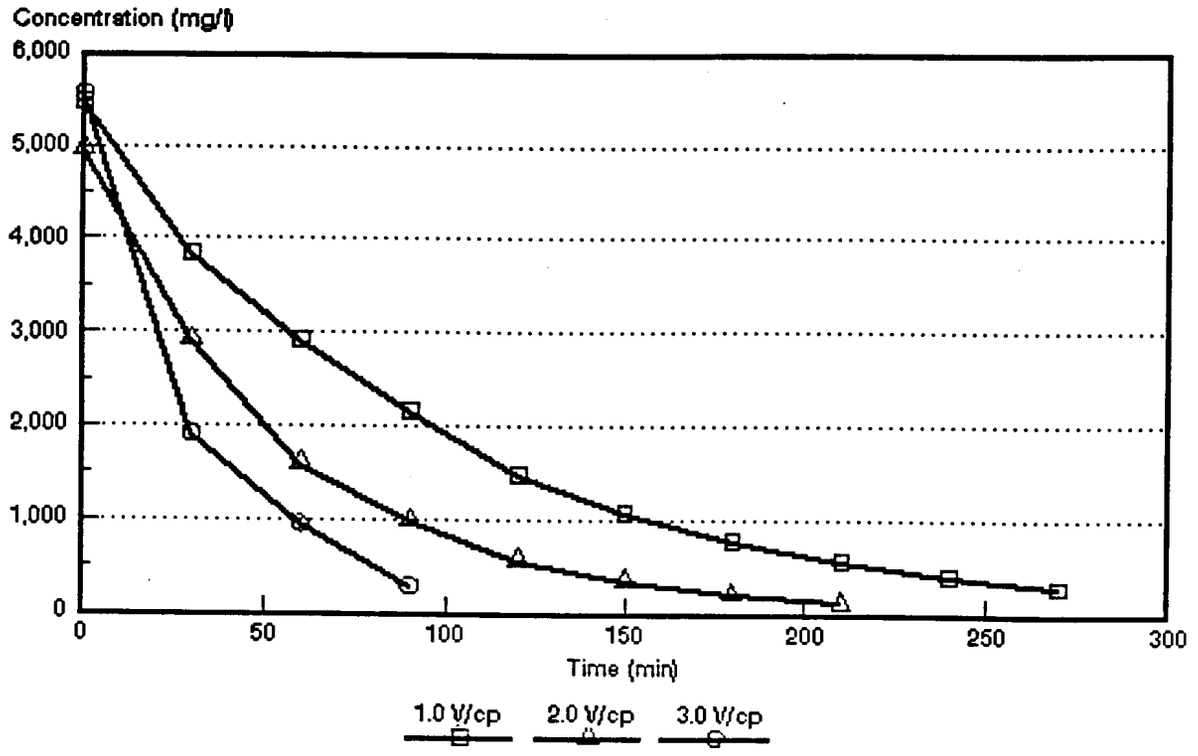

Figure 9.29: **Dialysate concentration as a function of time and cell pair voltage for an approximately 5 000 mg/ℓ caustic soda feed solution.**

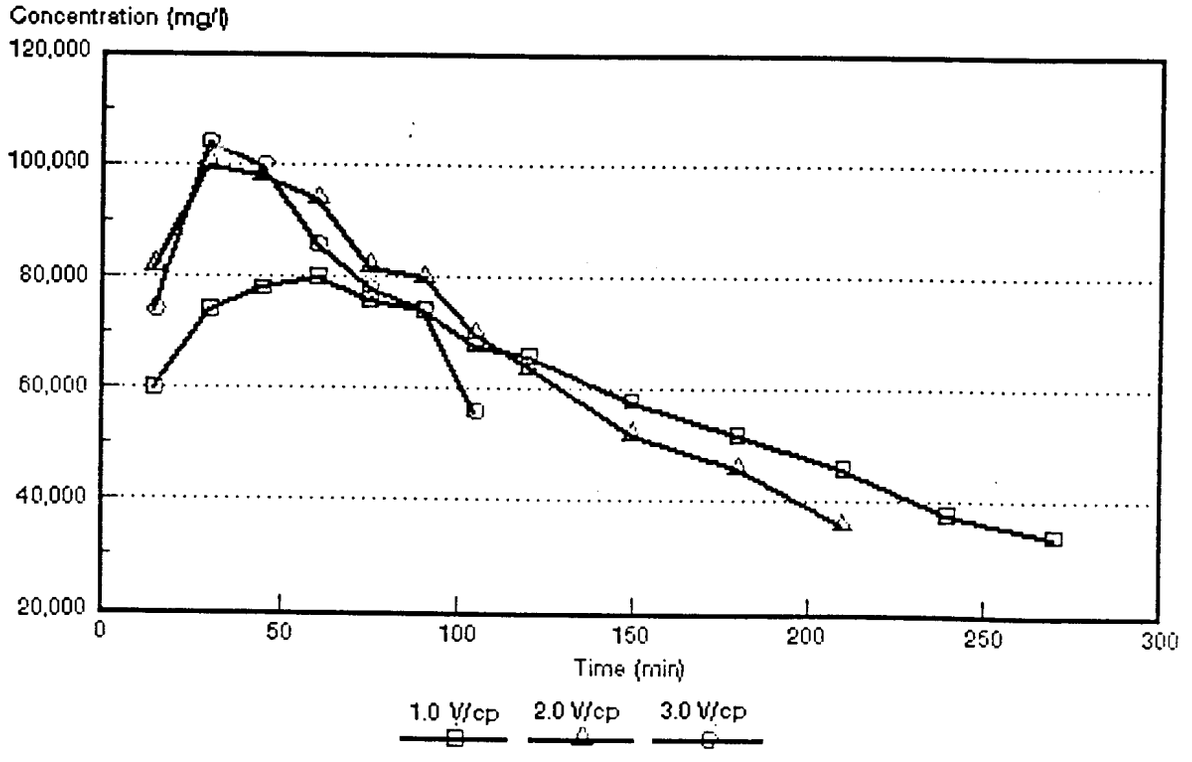

Figure 9.30: **Brine concentration as a function of time and cell pair voltage for an approximately 5 000 mg/ℓ caustic soda feed solution.**

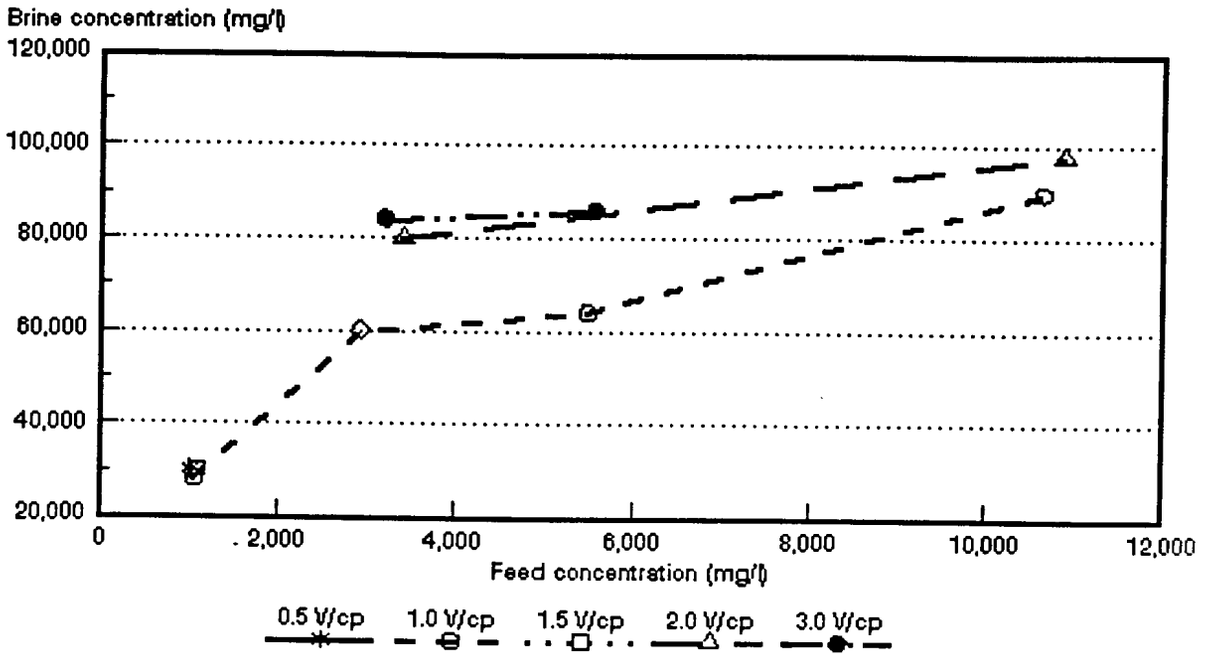

Figure 9.31: **Brine concentration as a function of sodium hydroxide feed concentration and cell pair voltage.**

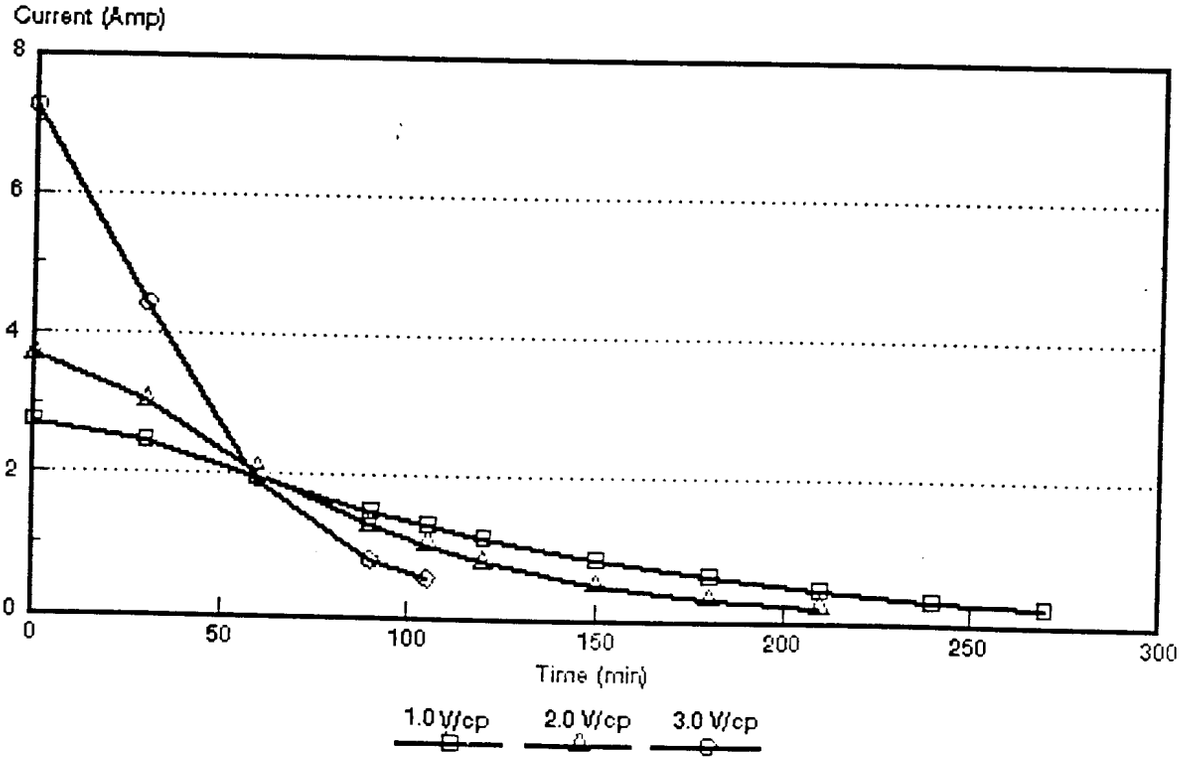

Figure 9.32: **Current as a function of time and cell pair voltage for an approximately 5 000 mg/ℓ caustic soda solution.**

was obtained at a caustic soda feed water concentration of approximately 10 000 mg/ℓ (1,0 V/cp). Water recoveries were high. Water recoveries of 93 to 97,5% were obtained in the caustic soda feed water concentration range from 1 000 to 5 000 mg/ℓ.

9.3.3 Current efficiency

Current efficiency increased with increasing caustic soda feed water concentration at 1,0 V/cp (Table 9.3 and Fig. 9.33). However, current efficiency slightly decreased with increasing caustic soda feed water concentration at the other cell pair voltages. Current efficiency did not decrease significantly with increasing cell pair voltage.

Current efficiencies of 73,3 to 77,9% were obtained in the caustic soda feed water and cell pair voltage ranges of 1 000 to 10 000 mg/ℓ and 0,5 to 1,5 V/cp, respectively. Current efficiencies of 73,1 to 81,2% were obtained in the caustic soda feed water and cell pair voltage ranges of 3 000 to 10 000 mg/ℓ and 2,0 to 3,0 V/cp, respectively.

9.3.4 Electrical energy consumption

Electrical energy consumption increased with increasing caustic soda feed water concentration and increasing cell pair voltage (Table 9.3 and Fig. 9.34). Electrical energy consumption was low at low cell pair voltages (0,5 to 1,5) and low feed concentrations (1 000 to 3 000 mg/ℓ). Electrical energy consumption varied between 0,4 and 2,2 kWh/m^3 product water in this range. However, electrical energy consumption became higher at higher cell pair voltages and caustic soda feed water concentrations. An electrical energy consumption of 19,4 kWh/m^3 product water was obtained at a cell pair voltage of 2,0 and a caustic soda feed water concentration of approximately 11 000 mg/ℓ.

9.3.5 Product water yield

Product water yield increased with increasing cell pair voltage and decreased with increasing feed concentration (Table 9.3).

9.3.6 Effective cell pair thickness and cell pair resistance

An example of cell pair resistance (R_{cp}) as a function of the specific resistance of the dialysate and cell pair voltage is shown in Figure 9.35 (approximately 1 000 mg/ℓ

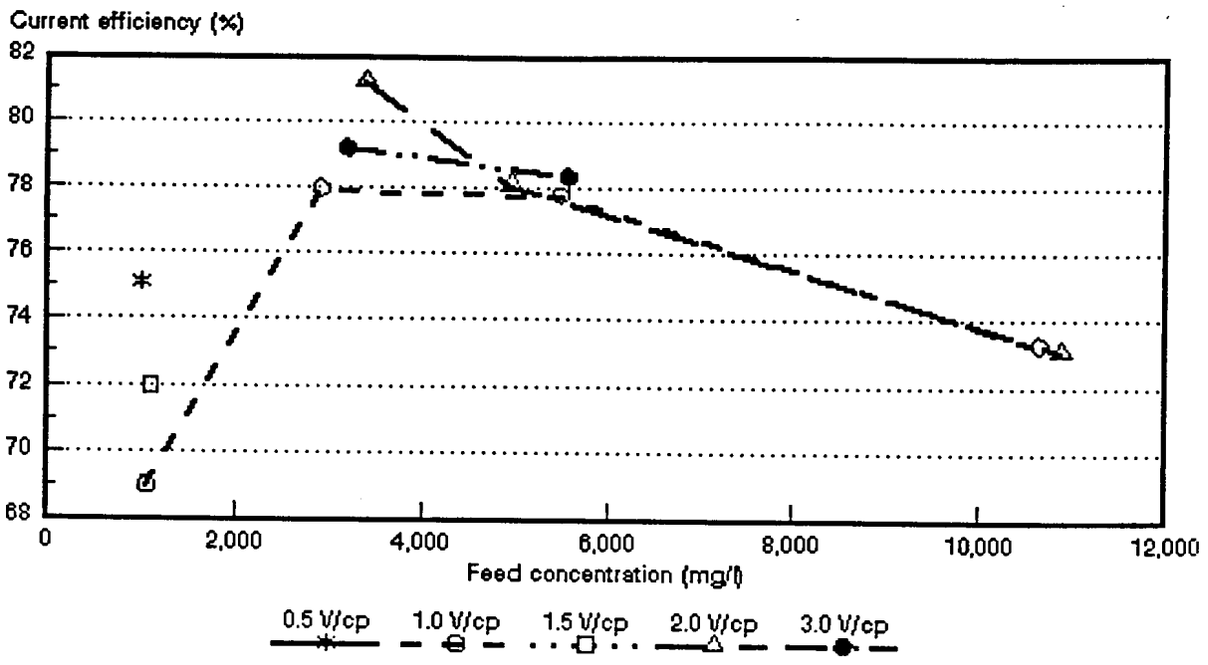

Figure 9.33: **Current efficiency as a function of sodium hydroxide feed concentration and cell pair voltage.**

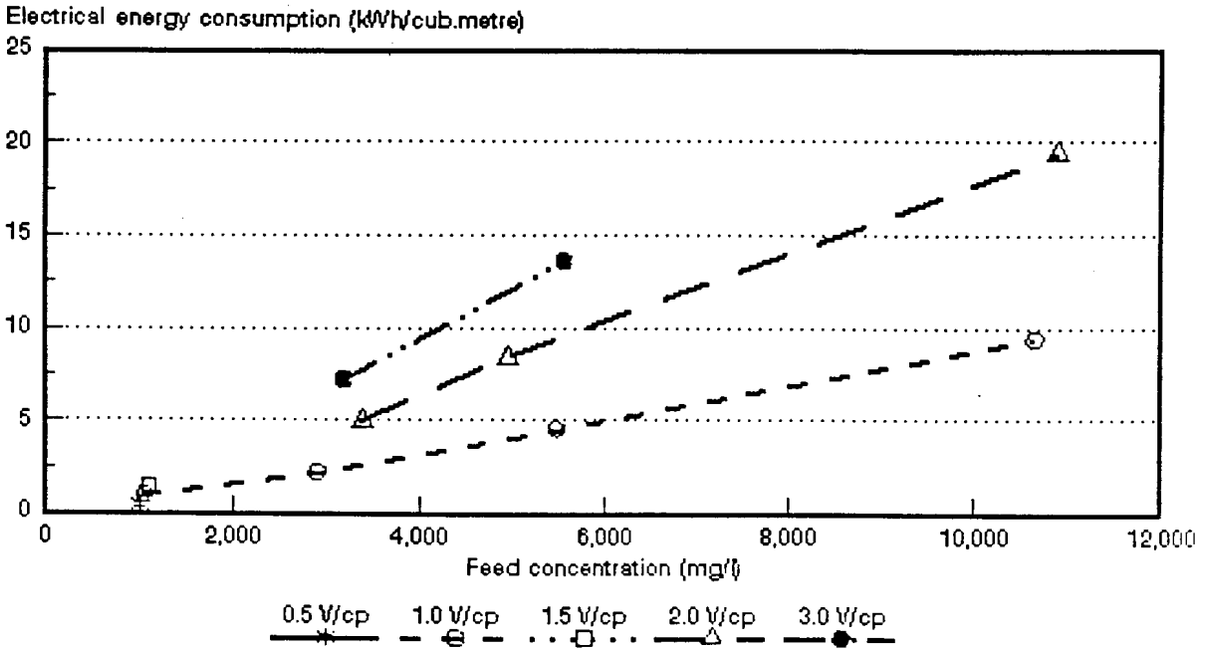

Figure 9.34: **Electrical energy consumption as a function of sodium hydroxide feed concentration and cell pair voltage.**

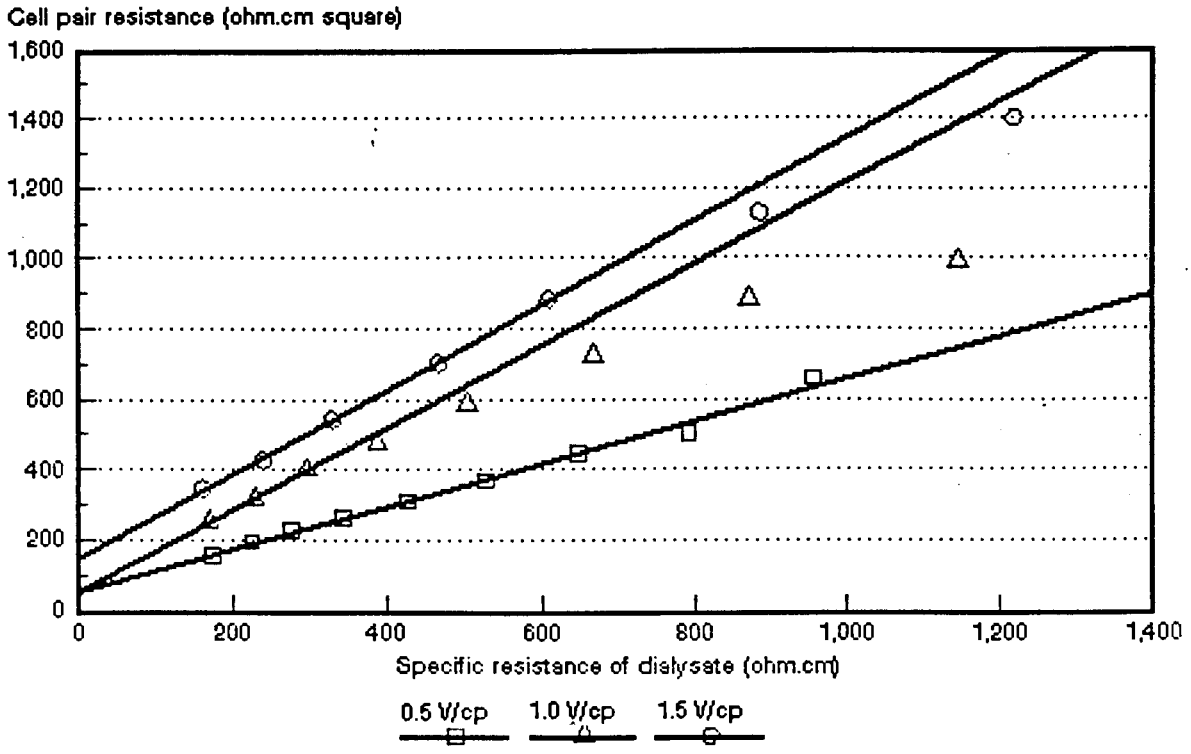

Figure 9.35: Cell pair resistance as a function of specific resistance of the dialysate and cell pair voltage for approximately 1 000 mg/ℓ caustic soda solution.

caustic soda feed). Polarization increased with increasing cell pair voltage in the cell pair voltage range from 0,5 to 1,0 V/cp. The effective cell pair thickness, d_{eff}, was determined at 6,03 mm at 0,5 V/cp (1 000 mg/ℓ feed). Cell pair thickness was 11,6 at 1,0 V/cp (1 000 mg/ℓ feed) and 11,99 at 1,5 V/cp (1 000 mg/ℓ feed). This showed that polarization was approximately the same at 1,0 and 1,5 V/cp.

Cell pair resistance decreased with increasing feed concentration (Table 9.3). A cell pair resistance of only 0,15 ohm·cm^2 was obtained at 10 000 mg/ℓ caustic soda feed concentration (1,0 V/cp).

10. CONCENTRATION/DESALINATION OF SALT SOLUTIONS AND INDUSTRIAL EFFLUENTS WITH SCED

10.1 Concentration of salt solutions

A summary of the concentration/desalination results of the different salt solutions is shown in Tables 10.1 to 10.5.

10.1.1 Desalination rate, product and brine concentration

Examples of the desalination/concentration of sodium chloride, ammonium nitrate and sodium sulphate solutions as a function of time at constant cell pair voltage are shown in Figures 10.1 to 10.3. The effect of increasing cell pair voltage on desalination/concentration of an approximately 1 000 mg/ℓ sodium sulphate solution is shown in Figure 10.4.

Desalination rate decreased with decreasing feed concentration (Figs. 10.1 to 10.3) and decreasing cell pair voltage (Figure 10.4). However, approximately the same initial desalination rate was obtained at 1,18 and 1,76 V/cp (Figure 10.4). The optimum cell pair voltage for desalination regarding polarization and electrical energy consumption should be determined for each feed concentration, because this information is required to operate an ED stack under optimum conditions. This, however, was not the main purpose of this investigation. The main purpose of this investigation was to evaluate the performance of the SCED unit for concentration/desalination of saline solutions at cell pair voltages normally applied in ED.

All the different salt solutions could be easily desalinated from approximately 10 000 mg/ℓ to 300 mg/ℓ and less (Figs. 10.1 to 10.3 and Tables 10.1 to 10.5). Product concentrations of less than 100 mg/ℓ could be obtained with ease in some cases. Therefore, SCED appears to be effective for the production of low TDS water.

Brine concentration increased with increasing feed concentration and increasing cell pair voltage (Tables 10.1 to 10.5 and Figure 10.5). Sodium chloride, ammonium nitrate, sodium sulphate, sodium nitrate and calcium chloride brine concentrations of 2,2 to 16,1%; 4,9 to 15%; 7,8 to 16,3%; 6,0 to 12,5% and 3,8 to 7,5% could be obtained, in the feed concentration and cell pair voltage range of 0,1 to 1% and 0,59 to 1,76 V/cp, respectively. Therefore, relatively high brine concentrations could be obtained

Table 10.1: Concentration/Desalination Results of Sodium Chloride Solutions at different cell pair voltages.

Vcp	Cf mg/l	Cp mg/l	Cb mg/l	CF	CE %	WR %	BV %	EEC kWh/m³	OP m³/m².d	d_{eff} mm	Rcp ohm·cm²
0,59	1010	282	22 450	22,20	72,20	96,00	4,00	0,34	1,22	0,95	38,8
1,18	950	35	31 000	35,40	66,70	96,30	3,70	0,77	1,53	1,01	39,2
	1 900	40	53 500	28,10	73,70	96,50	3,50	1,41	1,36	0,91	35,1
	3 400	125	72 000	21,20	56,40	96,40	3,60	3,26	1,36	0,97	21,3
	5 400	65	82 000	15,20	78,60	94,80	5,20	3,86	1,20	0,88	18,2
	10 200	195	161 000	15,80	67,90	93,50	6,50	8,04	1,19	0,87	14,4
1,76	985	25	37 000	37,70	63,90	96,70	3,30	1,25	1,75	1,09	46,5
	1 700	25	53 500	31,10	67,80	96,40	3,60	2,07	1,53	1,08	32,9
	2 700	48	72 000	27,40	55,20	96,50	3,50	3,74	1,75	1,05	26,7
	4 850	25	82 000	17,40	69,60	94,60	5,40	5,82	1,20	0,90	21,8
	9 400	120	161 000	18,10	71,90	94,00	6,00	11,10	1,49	0,95	15,1

Vcp = cell pair voltage
Cf = feed concentration
Cp = product concentration
Cb = brine concentration
CF = concentration factor
CE = current efficiency
WR = water recovery
BV = brine volume
EEC = electrical energy consumption
OP = output
d_{eff} = thickness of dialysate
Rcp = cell pair resistance

Table 10.2: Concentration/Desalination Results of Ammonia Nitrate Solutions at different cell pair voltages

Vcp	Cf mg/l	Cp mg/l	Cb mg/l	CF	CE %	WR %	BV %	EEC kWh/m³	OP m³/m².d	deff mm	Rcp ohm·cm²
0.59	580	240	58 000	100,00	29,70	99,30	0,70	0,23	1,58	0,97	25,6
	1 010	230	80 000	79,60	43,50	98,90	1,10	0,35	1,26	0,97	24,6
1.18	435	50	49 000	112,60	28 70	99,30	0,70	0,54	1,58	0,67	68,2
	1 100	55	87 500	79,60	51,80	98,80	1,20	0,80	1,39	0,84	38,6
	1 800	90	82 500	45,80	45,80	98,30	1,70	1,50	1,39	0,80	38,2
	3 100	125	117 630	30,70	48,20	98,00	2,00	2,45	1,38	0,75	20,2
	4 950	190	100 000	20,20	47,20	97,20	2,80	4,09	1,37	0,79	14,5
	9 100	320	146 000	16,00	49,40	95,30	4,70	7,37	1,21	0,85	14,7
1.76	420	42	64 500	153,50	22,40	99,00	1,00	1,00	1,58	0,85	45,3
	1 300	60	78 000	60,00	36,30	98,70	1,30	2,05	1,57	1,14	35,6
	1 800	35	120 000	66,70	41,70	98,50	1,50	2,54	1,39	0,87	28,8
	2 800	35	150 000	53,60	47,20	98,10	1,90	3,55	1,24	1,02	19,0
	4 525	45	136 500	30,20	47,20	97,30	2,70	6,78	1,24	1,06	12,8
	9 800	70	130 000	13,30	46,50	94,70	5,30	13,09	1,20	0,87	11,2

Table 10.3: Concentration/Desalination Results of Sodium Sulphate Solutions at different cell pair voltages.

Vcp	Cf mg/ℓ	Cp mg/ℓ	Cb mg/ℓ	CF	CE %	WR %	BV %	EEC kWh/m³	OP m³/m².d	d_{eff} mm	Rcp ohm·cm²
0.59	1 110	165	78 500	70,70	79,30	98,90	1,10	0,27	1,40	0,84	65,6
1.18	1 100	50	81 000	73,60	71,90	98,70	1,30	0,66	1,57	0,99	57,2
	2 100	70	120 000	57,10	71,70	98,50	1,50	1,28	1,39	0,99	47,7
	3 400	95	132 000	38,80	76,20	98,10	1,90	1,97	1,25	0,75	37,2
	5 350	445	133 000	24,80	62,30	97,50	2,50	3,59	1,24	1,02	32,3
	9 700	1 500	156 000	16,08	63,20	96,50	3,50	6,01	1,23	0,89	28,6
1.76	1 050	30	89 000	84,80	52,70	98,30	1,70	1,31	1,56	1,11	59,0
	1 900	35	123 000	64,60	63,40	98,50	1,50	1,99	1,39	1,25	42,8
	3 000	77	136 000	45,50	76,20	98,20	1,80	3,20	1,25	1,14	45,6
	4 950	65	134 000	27,10	62,30	97,50	2,50	4,75	1,24	1,25	29,9
	9 525	180	163 000	17,11	63,20	96,10	3,90	13,85	1,23	1,17	23,2

Table 10.4: Concentration/Desalination Results of Sodium Nitrate Solutions at different cell pair voltages

Vcp	Cf mg/ℓ	Cp mg/ℓ	Cb mg/ℓ	CF	CE %	WR %	BV %	EEC kWh/m³	OP m³/m².d	deff mm	Rcp ohm·cm²
0,59	1 100	465	65 000	59,30	41,50	98,90	1,10	0,28	1,57	1,01	28,8
1.18	1 000	90	63 500	63,3	47,0	98,6	1,40	0,73	1,57	0,99	32,1
	1 950	100	71 000	36,5	65,0,	98,4	1,60	1,07	1,39	1,01	30,4
	2 800	100	82 000	29,3	63,2	98,1	1,90	1,61	1,38	0,83	29,7
	5 000	140	102 000	20,5	56,67	97,3	2,70	3,29	1,24	0,86	19,3
	10 100	530	123 000	12,2	53,1	96,0	4,00	6,98	1,22	1,02	10,2
1.76	1 000	70	60 500	60,30	40,70	98,50	1,50	1,30	1,57	1,16	33,6
	2 100	60	69 500	33,10	51,30	98,20	1,80	2,25	1,39	1,12	28,3
	2 800	50	81 000	29,00	53.80	98,00	2,00	2,90	1,38	1,06	25,3
	5 200	90	117 000	22,50	55,00	97,10	3,90	5,34	1,23	1,27	17,0
	9 800	150	125 000	12,80	51,80	95,60	4,40	10,85	1,21	1,27	10,7

Table 10.5: Concentration/Desalination Results of Calcium Chloride Solutions at different cell pair voltages.

Vcp	Cf mg/ℓ	Cp mg/ℓ	Cb mg/ℓ	CF	CE %	WR %	BV %	EEC kWh/m³	OP m³/m².d	deff mm	Rcp ohm·cm²
0,59	1 100	310	42 000	38,20	47,80	98,70	1,30	0,48	1,57	0,93	40,3
1.18	970	50	41 200	42,50	45,70	98,50	1,50	1,17	1,56	1,05	36,4
	2 100	110	51 000	24,30	49,70	97,80	2,20	2,34	1,38	1,15	27,5
	2 950	160	57 000	19,30	46,30	97,20	2,80	3,53	1,37	1,19	19,9
	5 000	230	75 000	14,00	45,70	95,80	4,20	6,21	1,22	1,19	15,4
	10 300	940	75 000	7,30	44,30	92,70	7,30	13,06	1,18	1,12	9,6
1.76	840	20	38 500	45,80	36,50	98,50	1,50	1,94	1,56	1,18	34,7
	2 000	35	45 500	22,80	48,10	97,80	2,20	3,57	1,38	1,32	28,2
	3 000	85	54 500	18,20	43,40	97,00	3,00	5,91	1,37	1,37	22,9
	5 050	65	73 000	14,50	43,20	95,60	4,40	10,31	1,22	1,31	14,0

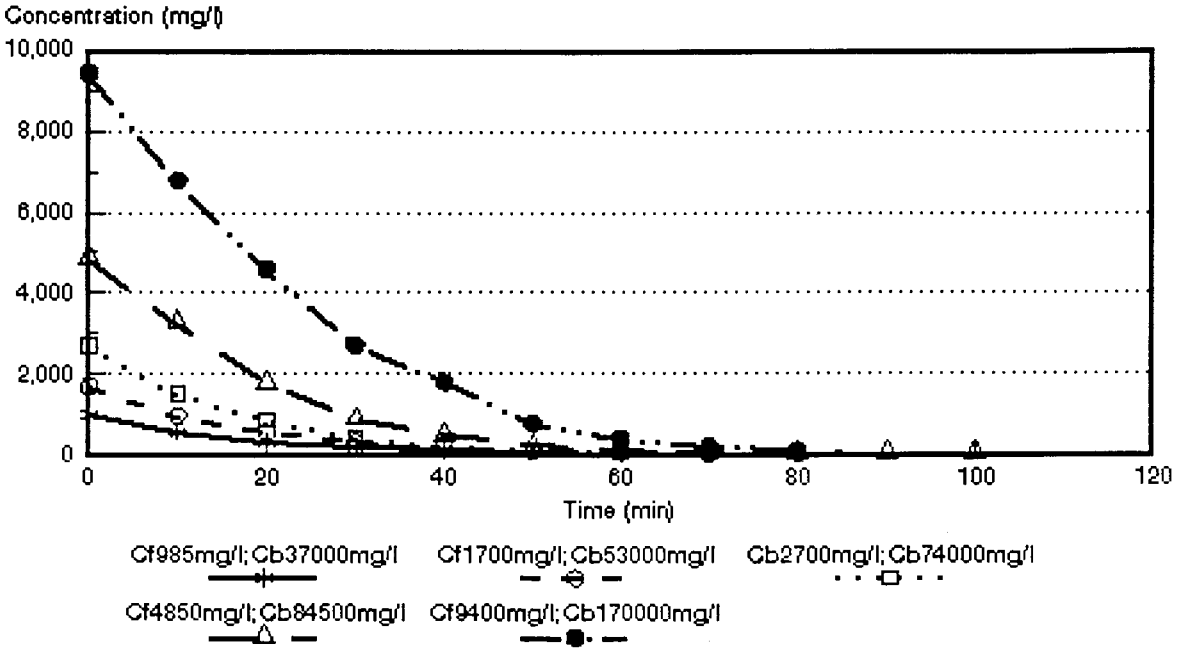

Figure 10.1: Concentration/desalination of different sodium chloride feed concentrations at 1,76 V/cp.

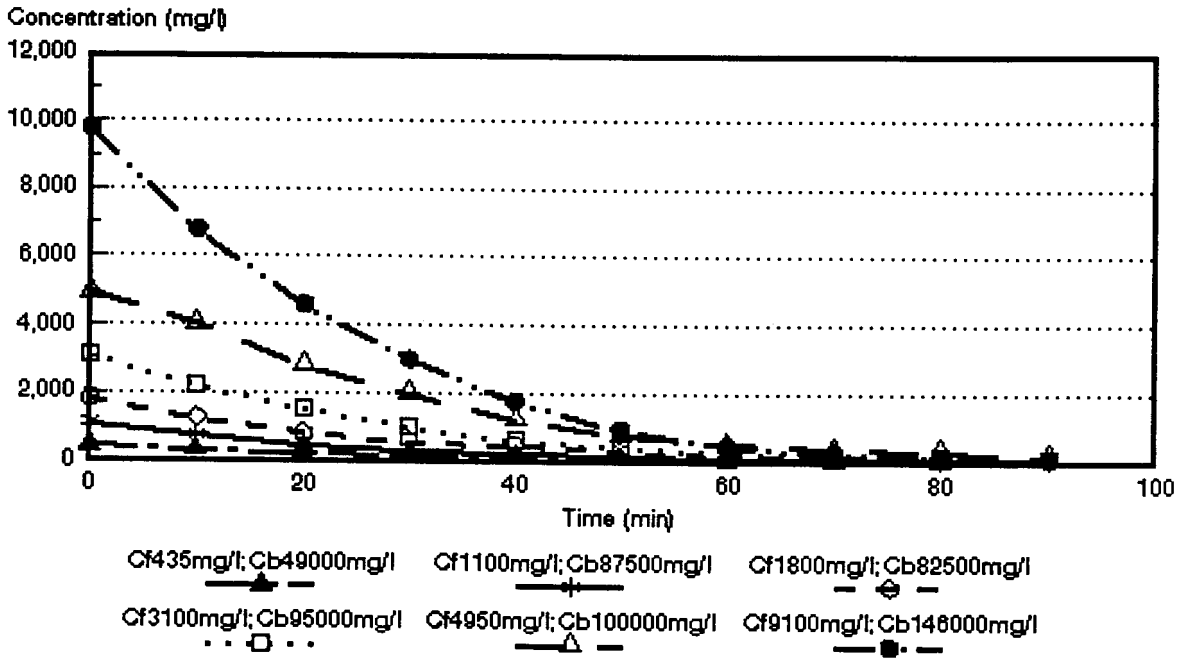

Figure 10.2: Desalination/concentration of different ammonium nitrate feed concentrations at 1,18 V/cp.

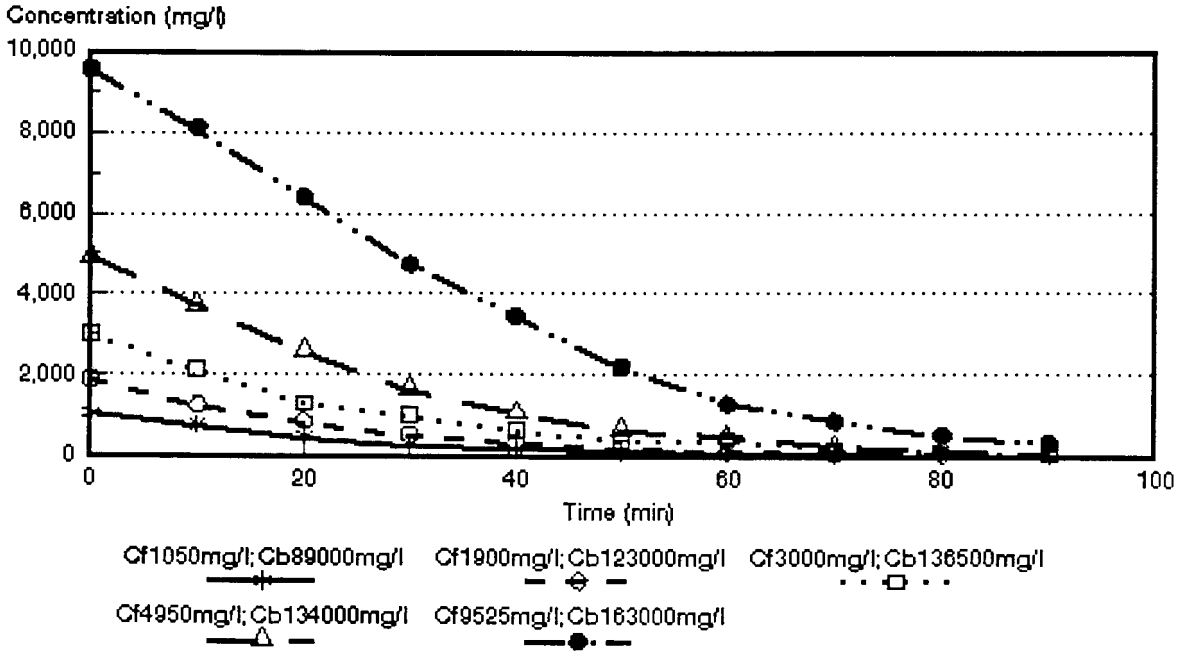

Figure 10.3: Desalination/concentration of different sodium sulphate feed concentrations at 1,76 V/cp.

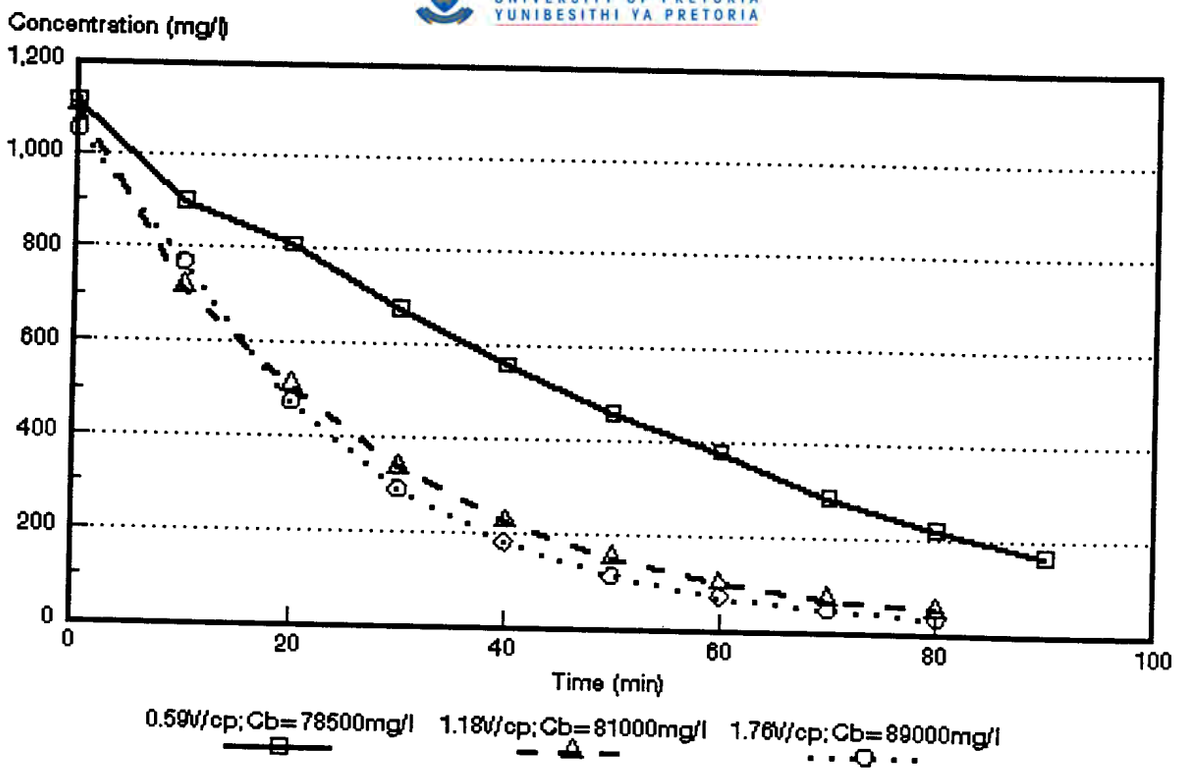

Figure 10.4: **Desalination/concentration of sodium sulphate solutions at different cell pair voltages.**

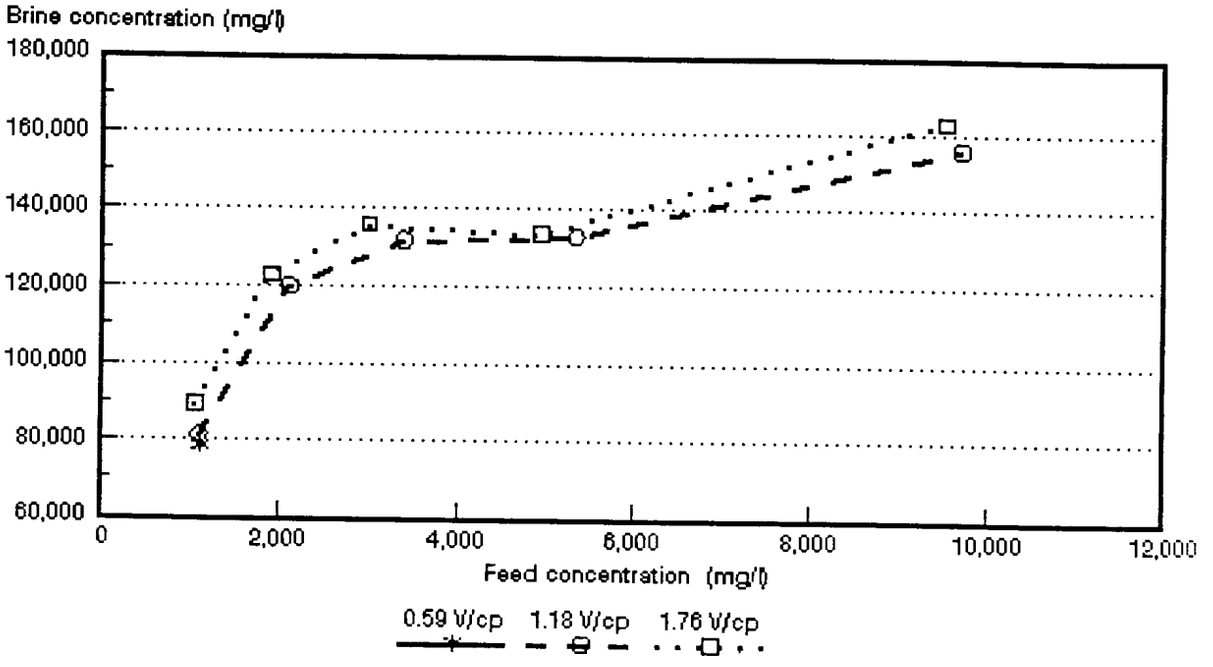

Figure 10.5: **Brine concentration as a function of sodium sulphate feed concentration and cell pair voltage.**

which would make the SCED technique suitable for concentration/desalination of industrial effluents. It is interesting to note that relatively low brine concentrations have been obtained with calcium chloride solutions (Table 10.5) in comparison with the other ions. However, the low current efficiency obtained with calcium chloride solutions explained the low brine concentrations that were obtained.

Concentration factors (brine/feed) decreased with increasing feed concentration (Tables 10.1 to 10.5). Therefore, there is a limit to the brine concentration that can be achieved. The brine concentration that can be obtained depends *inter alia* on the permselectivity of the ion-exchange membranes, feed concentration and current density used[6, 115]. Ion-exchange membranes tend to loose their permselectivity at high concentration due to backdiffusion of salt with the result that there is a limit to the brine concentration that can be achieved.

10.1.2 Current efficiency

Current efficiency increased with increasing feed concentration and decreasing cell pair voltage (Tables 10.1 to 10.5 and Figure 10.6). Current efficiency, however, decreased slightly at higher feed concentrations due to the lower permselectivity of the ion-exchange membranes at high feed concentration. Increasing current efficiency with increasing feed concentration may be ascribed to a higher flow of electro-osmotic water through the membranes at increasing feed concentration.

Current efficiencies of 55 to 74%; 30 to 52%; 53 to 79%; 42 to 65% and 37 to 50% were obtained with sodium chloride, ammonium nitrate, sodium sulphate, sodium nitrate and calcium chloride solutions, respectively, in the concentration and cell pair voltage ranges studied. Relatively low current efficiencies were obtained with ammonium nitrate and calcium chloride solutions. This shows that the ion-exchange membranes used do not have a very high permselectivity for ammonium nitrate and calcium chloride solutions.

10.1.3 Water recovery and brine volume

High water recovery and low brine volume were obtained at low to moderately high feed (1 000 to 3 000 mg/ℓ) concentrations (Tables 10.1 to 10.5). Brine volumes between 3 and 4%; 1 and 2%; 1 and 2%; 1 and 2% and 1 and 3% were obtained with sodium chloride, ammonium nitrate, sodium sulphate, sodium nitrate and calcium

chloride solutions, respectively. Higher brine volumes (3 to 7%), however, were obtained at higher feed concentrations (5 000 to 10 000 mg/ℓ). Therefore, very low brine volumes could be obtained with SCED. This low brine volume that is produced with SCED can reduce brine disposal cost significantly especially where brine is to be trucked away for disposal.

Excellent water recoveries were obtained. Water recoveries of approximately 96% were obtained in the feed concentration range of 1 000 to 3 000 mg/ℓ and of approximately 94% in the feed concentration range from 5 000 to 10 000 mg/ℓ. These high water recoveries and low brine volumes are significantly better than water recoveries of approximately 80% which is normally obtained with conventional electrodialysis.

10.1.4 Electrical energy consumption

Electrical energy consumption increased with increasing feed concentration and cell pair voltage (Figure 10.7 and Tables 10.1 to 10.5). Very low electrical energy consumptions (0,27 to 0,48 kWh/m^3 product water) were obtained at a cell pair voltage of 0,59 in the 1 000 mg/ℓ feed concentration range. Electrical energy consumptions of 0,66 to 5,91 kWh/m^3 were obtained in the feed concentration range of 1 000 to 3 000 mg/ℓ (1,18 to 1,76 V/cp range). Higher electrical energy consumption (3,29 to 13,06 kWh/m^3) was encountered in the feed concentration range from 5 000 to 10 000 mg/ℓ.

Electrical energy consumption was determined for ion transport only. The voltage drop across the electrode compartments was not taken into consideration because it is usually insignificant in a large membrane stack containing many membrane pairs (300 membrane pairs or more)[7]. The electrical energy consumption obtained during SCED usage would give a good indication of the operational cost that could be expected with SCED applications.

10.1.5 Product water yield

Product water yield (output) increased with increasing cell pair voltage and decreased with increasing feed concentration (Tables 10.1 to 10.5). Product water yield is a very important engineering design parameter because the membrane area required for a certain flow rate can be calculated from this figure.

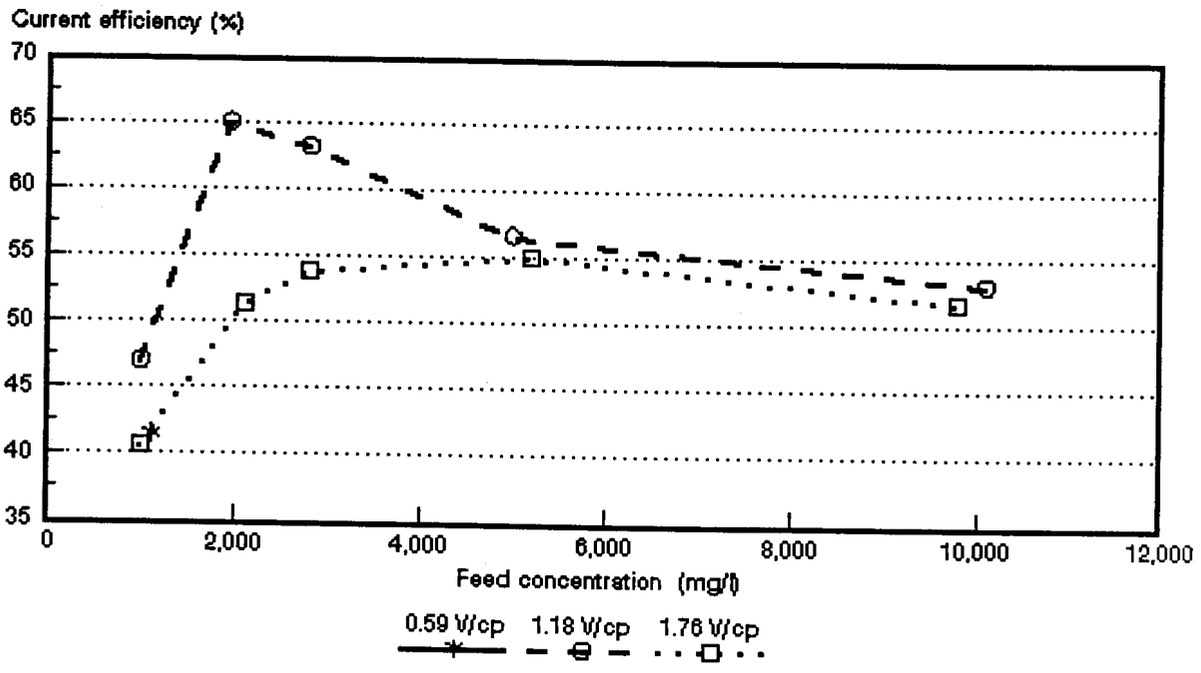

Figure 10.6: **Current efficiency as a function of sodium nitrate feed concentration and cell pair voltage.**

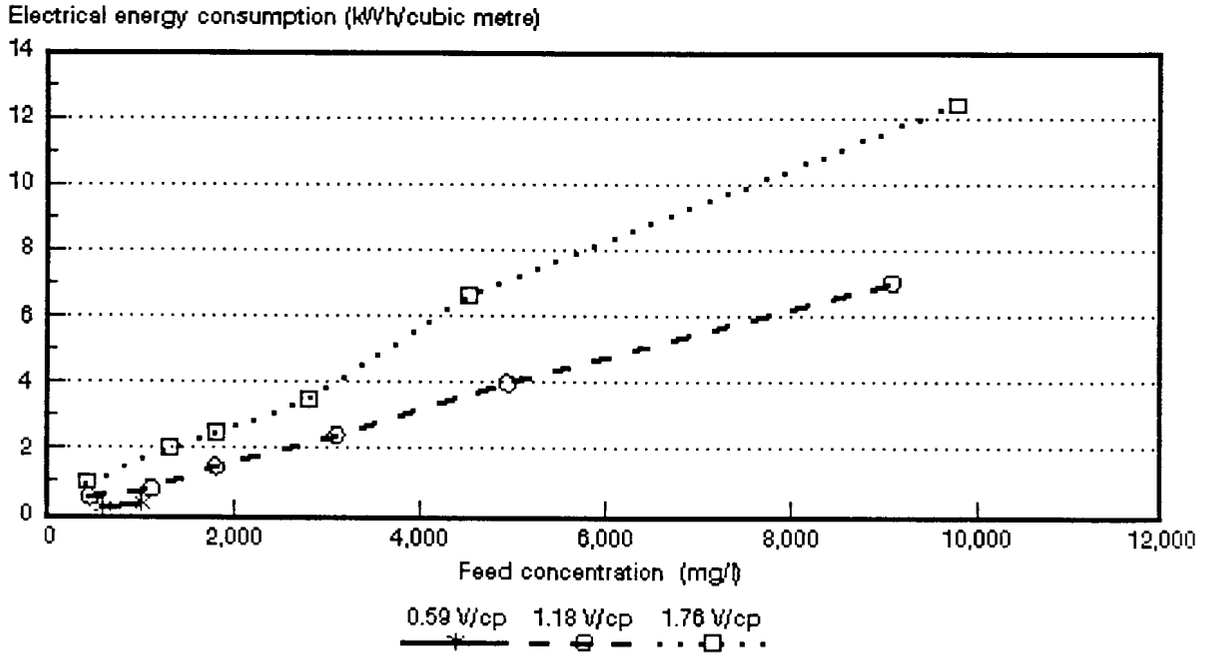

Figure 10.7: **Electrical energy consumption as a function of ammonium nitrate feed concentration and cell pair voltage.**

10.1.6 Cell pair resistance (R_{cp}) and effective thickness (d_{eff}) of the dialysate compartment

Cell pair resistance as a function of the specific resistance of the dialysate for sodium sulphate solutions at different cell pair voltages is shown in Figure 10.8. Similar graphs were obtained for the other salt solutions. The lines consist of a linear region followed by a curved region[116]. The line starts to curve when the specific resistance of the dialysate becomes very high. Linear regression through the linear region of the lines gives d_{eff} (slope) and the cell pair resistance (R_{cp}) (y-intercept). The lines show that polarization and hence effective thickness of the dialysate compartment depends on cell pair voltage. The effective thickness of the dialysate compartment increased from 0,84 (at 0,59 V/cp), 0,99 mm (at 1,18 V/cp) to 1,11 mm (at 1,76 V/cp). Membrane resistance (R_{cp}) for the sum of the anion- and cation-exchange membranes was determined at 65,6 - (0,59 V/cp), 57,2 - (1,18 V/cp) and 59,0 ohm·cm^2 (at 1,76 V/cp). It was further found that R_{cp} decreased with increasing feed concentration (Tables 10.1 to 10.5). The cell pair resistance at 1,18 V/cp and an initial ammonium nitrate feed concentration of 9 100 mg/ℓ was determined at only 14,7 ohm·cm^2 (Table 10.2).

The model $R_{cp} = R_m + \rho d_{eff}$ is applicable not only to sodium chloride solutions but also to ammonium nitrate, sodium sulphate, sodium nitrate and calcium chloride solutions. However, care must be taken to use the linear portion of the curve (R_{cp} vs specific resistance) in the determination of R_{cp} and d_{eff}. This is also a method that can be used for the determination of cell pair resistance. Cell pair resistance, however, depends on the initial feed concentration. Therefore, feed concentration must be specified when cell pair resistance is given.

10.2 Concentration/Desalination of Industrial Effluents

10.2.1 Treatment of runoff from a fertilizer factory terrain with SCED

Runoff from an ammonium nitrate fertilizer factory terrain is presently stored in evaporation ponds. This runoff contains, amongst other ions, ammonium, nitrate and phosphate ions which have the potential to pollute the environment. Water and chemicals can also be recovered from the effluent for reuse. Sealed-cell ED was therefore investigated for treatment of this effluent[116].

The concentration/desalination results of the relatively dilute runoff are shown in Table 10.6.

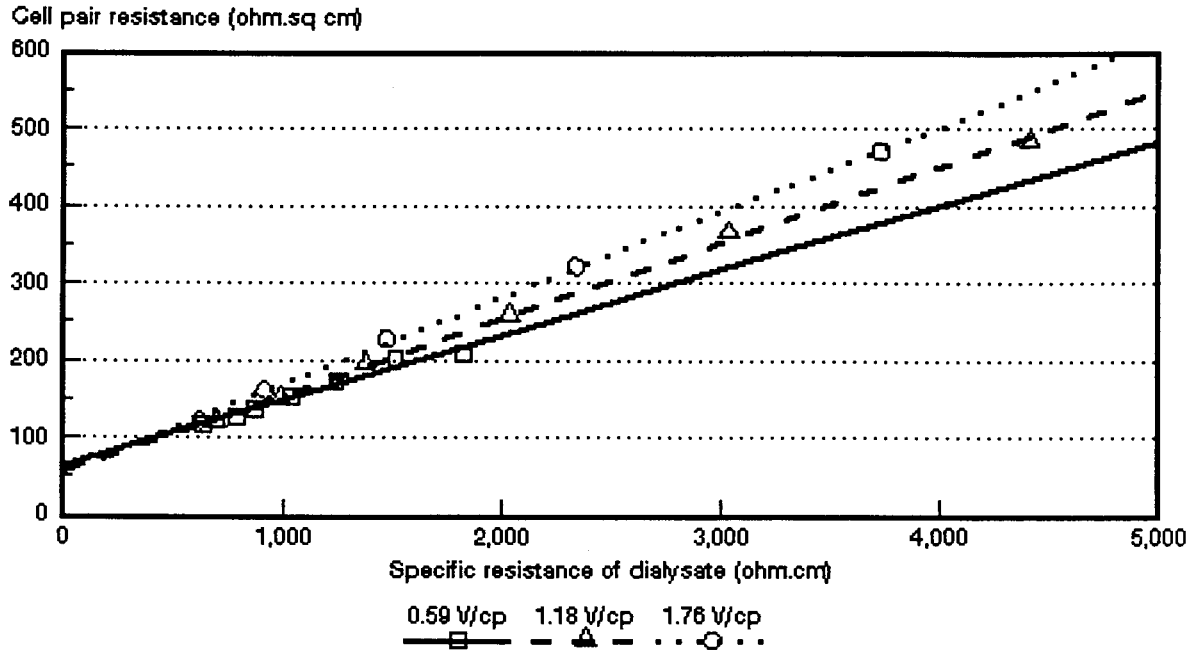

Figure 10.8: **Cell pair resistance as a function of specific resistance of dialysate at different cell pair voltages for approximately 1 000 mg/ℓ Na_2SO_4 feed solutions.**

Table 10.6: **Concentration/desalination results of fertilizer run-off at different cell pair voltages**

V_{cp}	C_f mS/m	C_p mS/m	C_b mS/m	% Conductivity Removal	CE %	WR %	BV %	EEC kWh/m³	OP m³/m²·d
1,18	545	29,8	10 724	94,5	56,9	97,2	2,8	2,7	1,03
0,88	556	48,9	10 312	91,2	63,3	97,2	2,8	2,0	0,77
0,59	520	53,3	8 830	89,7	-	96,9	3,1	1,24	0,54

Excellent salinity removals were obtained at the three cell pair voltages investigated. Salinity removal of 94,5% was obtained at a cell pair voltage of 1,18. Salinity removal decreased to only 89,7% at 0,59 V/cp.

Feed water conductivity was reduced from 545 mS/m to 29,8 mS/m at an electrical energy consumption of 2,7 kWh/m³ (1,18 V/cp). Brine volume comprised only 2,8% of the initial feed volume. Effluent volume could therefore be reduced significantly.

The chemical composition of feed, product and brine is shown in Table 10.7.

Table 10.7: Chemical composition of feed, product and brine

Constituent	Feed mg/ℓ	Product mg/ℓ	Brine mg/ℓ	% Removal
Sodium	111	25	3 758	77,50
Potassium	34	5	1 035	85,30
Calcium	93	24	3 404	74,20
Magnesium	64	8	2 121	87,50
Ammonium	621	30	16 638	95,20
Nitrate	1 936	73	63 783	96,30
Silica	7,70	4,60	54,40	40,30
Sulphate	299	48	8 469	83,90
Ortho-phosphate (P)	73,80	20,80	1 143	71,80
Chloride	187	14	5 371	92,50
Alkalinity ($CaCO_3$)	22	3	24	86,40
COD	219	19	587	91,30
Manganese	0,409	<0,025	18,90	42,90
Iron	<0,025	<0,025	0,91	
Fluoride	1,66	0,35	3,70	78,90
TDS (calculated)	3 602	296	108 114	91,80
pH	5,7	4,3	4,4	

TDS was reduced from 3 602 mg/ℓ to 296 mg/ℓ (1,18 V/cp) with ease. Therefore, a very good quality product water could be produced which might be reused at the factory. Very good ammonium (95,2%) and nitrate (96,3%) removals were obtained. Ammonium and nitrate were reduced from 621 and 1 936 mg/ℓ in the feed to 30 and 73 mg/ℓ in the product, respectively.

The brine had a TDS of 10,8%. Brine volume comprised only about 3% of the initial feed volume. Therefore, brine volume could be reduced significantly which means that smaller evaporation ponds would be required, or that the present ponds could last much longer. Ammonium and nitrate values may also be recovered from the brine for reuse. Potential pollution problems will therefore be reduced significantly.

The ion-exchange membranes used in the SCED unit performed well for treatment of the fertilizer runoff. However, membrane fouling or scaling in the long term may affect the process adversely. Therefore, membrane fouling and cleaning studies over an extended time period will be necessary to determine the effectiveness of SCED for this application.

10.2.2 Treatment of a concentrated Ammonium Nitrate Type effluent with SCED

The treatment of a more concentrated ammonium nitrate type effluent from a fertilizer manufacturing plant was also investigated with SCED. The pH of the effluent was approximately 11 and the effluent was neutralized with sulphuric acid prior to SCED treatment[116]. Concentration/desalination of the ammonium sulphate effluent was conducted in stages because of the high concentration of the effluent (13 230 mS/m or 123 700 mg/ℓ TDS). The product water after the first desalination stage was used as feed for the next concentration/desalination stage. The concentration/desalination results are shown in Table 10.8.

Table 10.8: Concentration/desalination results of ammonium sulphate effluent

Vcp	Cf mS/m	Cp mS/m	Cb mS/m	% Conductivity Removal	CE %	WR %	BV %	EEC kWh/m³	OP m³/m²·d
0,53	13 230	8 452	26 313	36,1	43,1	84,7	15,3	23,3	0,448
0,53	8 751	2 437	18 952	72,2	-	78,8	21,2	28,9	0,318
1,18	2 424	6,2	17 416	99,8	46,9	91,6	8,4	17,9	0,282

Feed (13 230 mS/m) was first desalinated to 8 452 mS/m. Desalination rate was low due to the low cell pair voltage (0,53 V/cp) that could be applied as a result of excessive current that was drawn by the high conductivity of the feed solution[116]. It was only at the third desalination stage that a higher cell pair voltage could be applied.

The chemical composition of the feed, product and brine after the third desalination/concentration stage is shown in Table 10.9.

Table 10.9: Chemical composition of feed, product and brine (3rd stage desalination)

Constituent	Feed mg/ℓ	Product mg/ℓ	Brine mg/ℓ	% Removal
Sodium	268	12	2 787	95,52
Potassium	3	1	17	66,67
Calcium	7	1	60	85,71
Magnesium	1	4	13	
Kjeldahl-N	3 340	17	38 199	99,49
Ammonium	4 179	10	48 214	99,76
Nitrate	2 215	17	25 473	99,23
Silica	9,50	3,90	40,10	58,95
Sulphate	9 762	10	113 184	99,90
Total phosphate (P)	3,20	0,20	28,20	93,75
Chloride	103	28	1 167	72,82
COD	41	19	163	53,66
TDS (Calculated)	16 557	88	191 208	99,47
pH	3,6	4,9	2,9	

Very good ion removals were obtained. TDS was reduced from 16 557 mg/ℓ to 88 mg/ℓ, a 99,5% removal. Ammonium and nitrate removals were both approximately 99%. Brine with a TDS of 19,1% was obtained. Brine volume comprised 8,4% of the initial feed volume. Electrical energy consumption was determined at 17,9 kWh/m^3 in this case. This energy consumption is high. However, an excellent quality product water was obtained which could be reused. This demonstrates that SCED may be effective for the treatment of relatively high TDS waters although the electrical energy consumption is high.

10.2.3 Treatment of an effluent saturated with Calcium Sulphate with SCED

Hydrochloric acid is used for extraction of calcium from activated carbon which is used for gold extraction by a gold recovery company. At times the effluent contains high concentrations of calcium (3 800 mg/ℓ), chloride (7 000 mg/ℓ) and sulphate (600 mg/ℓ). Sealed-cell ED was attempted for treatment of this high concentration calcium

sulphate effluent (TDS 23 000 mg/ℓ) for chloride recovery[116]. However, a white precipitate of calcium sulphate formed in the membrane bags shortly after the experiment was started. Therefore, calcium sulphate should be reduced to low levels to prevent calcium sulphate scaling during SCED treatment. This was done by treating another effluent sample (TDS 4 500 mg/ℓ) with barium carbonate. Sulphate was reduced from 339 mg/ℓ to 5 mg/ℓ.

The concentration/desalination results are summarized in Table 10.10.

Table 10.10: Concentration/desalination results of calcium chloride effluent

V_{cp}	C_f mS/m	C_p mS/m	C_b mS/m	% Conductivity Removal	CE %	WR %	BV %	EEC kWh/m³
1,18	1 182	362	13 548	69,4	32,5	97,0	3	6,4
1,18	383	51	9 609	86,7	28,8	97,7	2,3	3,1

Concentration/desalination was conducted in two stages. Conductivity was first reduced from 1 182 mS/m to 362 mS/m and then from 362 mS/m to 51 mS/m. Very low current efficiencies were obtained for the first (32,5%) and second (28,8%) desalination stages. Brine volume comprised approximately 3% (1st stage) and 2,3% (2nd stage) of the feed water volume and electrical energy consumption was determined at 6,4 and 3,1 kWh/m^3 for the first and second desalination stages, respectively.

The chemical composition of the feed, product and brine for the second desalination stage is shown in Table 10.11.

Table 10.11: Chemical composition of feed, product and brine (2nd stage desalination)

Constituent	Feed mg/ℓ	Product mg/ℓ	Brine mg/ℓ	% Removal
pH	8,1	8,1	6,7	
Conductivity (mS/m)	383	51	9 609	86,7
Sodium	191	77	4 862	59,7
Potassium	9	3	162	66,7
Calcium	278	10	17 045	96,4
Magnesium	5	4	7	20,0
Ammonium	27	7	447	274,1
Nitrate	4	2	241	50,0
Sulphate	3	4	3	-
Chloride	783	113	46 412	85,6
Alkalinity ($CaCO_3$)	139	65	338	53,2
TDS (calculated)	1 469	299	102 180	79,6

A very good quality product water was obtained after the second desalination stage. TDS was reduced from 1 469 mg/ℓ to 299 mg/ℓ at an electrical energy consumption of 3,1 kWh/m^3.

Chloride was effectively concentrated. The chloride concentration in the brine was 4,6%. This chloride may be converted into hydrochloric acid in an electrochemical cell. The recovered hydrochloric acid can then be used for removal of calcium from the spent activated carbon. This matter, however, warrants further investigation.

The high calcium concentration in the brine may cause scaling problems. However, no sign of scaling was detected during the laboratory tests. Membrane fouling and cleaning tests, however, should be conducted over an extended period of time to determine the practical feasibility of the process.

11. GENERAL DISCUSSION

11.1 Requirements for ED Membranes

The customary requirements for ED membranes are:

a) low electrical resistance[6] (< 20 ohm·cm^2);
b) high permselectivity[6] (> 0,9);
c) low electro-osmotic coefficient[7] (< 12 mol H_2O/Faraday);
d) good chemical and dimensional stability[114]; and
e) satisfactory polarization characteristics[7].

These requirements are also necessary for ED membranes for use in EOP. However, an additional requirement for EOP·ED is finite transport of water through the membranes. It has been shown that increasing flow of water through the membranes causes an increase in current efficiency.

It was shown by Narebska and Koter[18] that ion-water coupling became higher in more concentrated solutions (approximately 0,5 mol/ℓ). At higher concentrations (> 0,5 mol/ℓ), the amount of free water in the membrane, the water transport number and the osmotic flow decrease. Effects originating from the deswelling of the membrane at high external concentration, may result in the observed decrease of the electro-osmotic flow and the increased coupling between ions and the amount of water, crossing the membrane[18].

It has been found by Narebska *et al.*[31] that the resistance against flowing anions in a cation membrane is imposed by water; the lower the amount of water in the membrane, the higher the resistance. Consequently, increased ion-water coupling causes increased resistance to the penetration of co-ions into the membrane matrix. The result is an increase in current efficiency. It is therefore not necessary for ED membranes for use in EOP to have very high permselectivities, because permselectivity will be increased with increasing flow of water through the membranes. This was especially observed for the more porous heterogeneous membranes at high feed concentration (1 mol/ℓ). Consequently, membranes with a relatively low permselectivity (approximately 0,6) should be suitable for concentration of salt solutions with EOP·ED.

11.2 Permselectivity with Acids and Bases

An increasing amount of water flowed through the membranes with an increase in feed water concentration during EOP of salt solutions. However, a decrease in water flow was experienced with an increase in feed concentration during EOP of acid solutions. The anion membranes used for acid EOP had a very low permselectivity for chloride ions due to the very high mobility of the protons in the membrane[11]. Consequently, the protons which flowed in the opposite direction to the flow of water would inhibit water flow through the membranes. Therefore, very little water will pass through the anion membrane in the case of acid EOP.

The cation membranes used for acid EOP, on the other hand, had a very high permselectivity for protons (> 0,9). Back diffusion should be very low in this case because back diffusion would be inhibited by the opposite flow of protons[19]. Osmotic flow, however, can be high through the cation membrane[19].

The cation membranes had a lower current efficiency than the anion membranes during EOP of caustic soda solutions. This is due to the high mobility of the hydroxyl ion[30]. It was shown by Koter and Narebska[32] that hydroxide ions impeded cations, particularly at high external concentration, much more than chloride ions. This can be attributed to the higher partial friction between sodium and hydroxyl ions.

The resistance imposed by a membrane matrix on the permeating hydroxyl ions is much lower than that for chloride ions according to Narebska *et al.*[30]. Three factors contributing to this effect, viz: the friction imposed by the cation (f_{21}), water (f_{2w}); and the polymer matrix (f_{2m}) - influence the flow of hydroxyl and chloride ions to different degrees. Chloride ions are hindered mainly by water, especially at increasing sorption. The flow of hydroxyl ions in diluted solution is hindered by the matrix and at high concentration by the cation and then by water[30].

11.3 Brine Concentration, Electro-Osmotic and Osmotic Flows

Brine concentration increases with increasing feed water concentration and current density. This happens because the membranes become increasingly dewatered at high current density. Consequently, the electro-osmotic coefficient decreases.

The osmotic flow relative to the total flow through the membranes decreased with

increasing current density. Consequently, the relative amount of electro-osmotic flow through the membranes, increased as a function of current density. Osmotic flow, however, appears to contribute significantly to the total flow in EOP. The osmotic flow through the *Ionac* membranes at a current density of 20 mA/cm^2 (0,1 mol/ℓ feed) comprised 33,9% of the total flow through the membranes. Osmotic flow was reduced to 19,0% of the total flow at a current density of 50 mA/cm^2 (0,1 mol/ℓ feed). Osmotic flow through the *Selemion* AAV and CHV membranes contributed 64,1% to the total flow at a current density of 20 mA/cm^2 (0,1 mol/ℓ feed). Osmotic flow decreased to 20,9% at a current density of 100 mA/cm^2 (0,1 mol/ℓ feed). Osmotic flow through the *Selemion* AMP and CMV membranes contributed 61,4% to the total flow through the membranes at a current density of 20 mA/cm^2 (0,1 mol/ℓ feed). Osmotic contribution decreased to 25,7% at a current density of 100 mA/cm^2 (0,1 mol/ℓ).

Approximately 7 mol H_2O/Faraday permeated through the *Selemion* AAV and CHV membranes in the feed concentration range from 0,5 to 1,0 mol/ℓ. It is known that little water (< 1 mol/Faraday) can permeate acid blocking anion membranes[48]. Therefore, the water could have entered the membranes only through the cation membrane.

Osmotic flow increased with increasing feed water concentration. It was also observed that the osmotic flow decreased in some cases at the highest feed concentrations. This can be ascribed to stronger back diffusion at the highest feed water concentrations. It was also interesting to note that a decrease in osmotic flow had taken place with increasing feed water concentration in the case of the more hydrophobic *Ionac* and WTPS membranes. The osmotic flow also increased through the Israeli ABM and *Selemion* membranes with increasing feed concentration and higher current efficiencies were experienced.

11.4 Discrepancy between Transport Numbers Derived from Potential Measurements and Current Efficiency Actually Obtained

The correct relationships to be used when measuring membrane potential for the prediction of desalting in ED, are as follows:

$$[J/I]_{\Delta\mu_s;\ J_v = 0} = \Delta t/F$$

(see eqs. 3.2.23 and 3.2.24)

$$= -[\Delta\Psi/\Delta\mu_s]_{I = 0;\ J_v = 0}$$

The correct Onsager relationship for potential measured is at zero current and at zero volume flow, and for the transport number, at zero concentration gradient and zero volume flow[117]. In practical ED, measurements are conducted at zero pressure and in presence of concentration gradients and volume flows. These factors will influence the results considerably in all systems in which volume flow is important and where the concentration factor is high as is encountered in EOP. In the measurement of membrane potential, the volume flow is against the concentration potential and in general will decrease the potential. In ED water flow helps to increase current efficiency, but the concentration gradient acts against current efficiency.

In the case of sodium chloride solutions, the apparent transport number of the membrane pair ($\bar{\Delta}t$) was higher than current efficiency (ϵ_p) at low feed water concentrations (approximately 0,05 mol/ℓ). This was predicted with the following relationship:

$$\eta < \frac{\Delta\Psi_m^c + |\ \Delta\Psi_m^a\ |}{|\ 2\Delta\Psi_I\ |} \qquad \text{(see eq. 3.11.12)}$$

Equation (3.11.12) is valid if the influence of volume flow is negligible.

The apparent transport number ($\bar{\Delta}t$) decreased with increasing feed water concentration. Current efficiency, however, increased with increasing feed water concentration as a result of increasing water flow. Consequently, current efficiency became higher than the apparent transport number at higher feed water concentrations (0,5 to 1 mol/ℓ). Current efficiency, however, decreased at very high feed concentrations as a result of back diffusion. Similar results were obtained with EOP of caustic soda solutions.

Current efficiency was much lower than $\bar{\Delta}t$ during EOP of acid solutions. This can be ascribed to back diffusion of acid through the membranes during EOP which reduces current efficiency significantly.

Garza and Kedem[2] have found that the apparent transport number of a membrane

pair ($\bar{\Delta}t$) gave a good lower estimate of the actual Coulomb efficiency of the EOP process in the case of sodium chloride solutions (0,1 mol/ℓ feed) using *Selemion* AMV and CMV and polyethylene based membranes. However, it was found in this study that the apparent transport number of a membrane pair gave a higher estimate of the Coulomb efficiency of the EOP process in the 0,05 to 0,1 mol/ℓ feed concentration range. The apparent transport number of a membrane pair gave a lower estimation of the actual current efficiency in the feed water concentration range from approximately 0,5 to 1,0 mol/ℓ. However, the apparent transport number of a membrane pair gave a much too high estimation of current efficiency of the EOP process for hydrochloric acid concentration. The apparent transport number of the anion membrane, however, gave a much better estimation of current efficiency.

11.5 Current Efficiency and Energy Conversion in ED

The effects which diminish current efficiency in ED are the following[17]:

a) electric transport of co-ions;
b) diffusion of solute;
c) electro-osmotic flow; and
d) osmotic water flows.

The imperfect selectivity, $\bar{t}_2$, assumed to be one of the most important characteristics of a membrane can produce up to 8% (NaCl) and 35% (NaOH) of the current efficiency losses at $\tilde{m} = 2$[17]. Similar to $\bar{t}_2$, the effect of electro-osmotic flow of water ($\bar{t}_w$) increases with m. It plays a significant role in the system with sodium chloride where it diminishes current efficiency up to 30% according to Koter and Narebska[17]. However, it was found in this study that electro-osmotic flow of water increased current efficiency significantly in the 0,05 to 1,0 mol/ℓ feed concentration range.

Depending on the working conditions, i.e. on the concentration ratio m'/m" and current density, the decrease in current efficiency due to osmotic and diffusion flows can be larger than that caused by electric transport of co-ions and water. This effect is especially seen at the higher mean concentrations where the current efficiency can be reduced to zero[17].

Efficiency of energy conversion in ED consists of the following two terms, viz., η_{IE} (ion-current coupling) and η_{WE} (ion-water coupling) according to Narebska and Koter[18]. The first term expresses the storage of energy in producing a concentration difference

in the permeant. The second term corresponds to the transport of water, which acts opposite to the separation of the components. It causes a waste of energy by decreasing the concentration difference. This water flow has a negative effect on energy conversion in ED. However, electro-osmosis can also have a positive effect on ED by increasing current efficiency as has been demonstrated in this study.

11.6 Water Flow, Concentration Gradient and Permselectivity

Salt flux (S^c) through a cation-exchange membrane can be predicted with the following relationship:

$$S^c = \frac{J_1^c + J_2^c}{2} = c_s(1 - \sigma)J_v^c + \bar{P}\Delta C + \frac{\Delta t^c}{2} I/F \qquad \text{(see eq. 3.11.1)}$$

Salt flux (both cation and anion) through ion-exchange membranes depends on water flow (J_v) through the membranes, concentration gradient (ΔC) across the membrane and membrane permselectivity ($\bar{\Delta}t$). It was shown that increasing water flow through the membranes increased current efficiency. It was also shown that an increasing concentration gradient (ΔC) across the membranes decreased current efficiency. Current efficiency or salt flux was also low when the permselectivity of the membranes was low. The experimental data for salt, acid and base EOP can therefore be satisfactorily described by eq. (3.11.1).

Back diffusion through ion-exchange membranes in presence (at zero pressure) and absence of water flow can be predicted with the following relationship according to Kedem[15]:

$$\left[\frac{J_s}{X_s/C_s} \Big/ \frac{J_1 - J_2}{X_1}\right]_{\Delta p = 0} < \left[\frac{J_s}{X_s/C_s} \Big/ \frac{J_1 - J_2}{X_1}\right]_{J_v = 0} \qquad \text{(see eq. 3.3.45)}$$

Back diffusion of salt through a membrane is less when water flows from the opposite side (l.h.s. of eq. 3.3.45). However, back diffusion of salt is more in the absence of volume flow (r.h.s. of eq. 3.3.45). Therefore, current efficiency will be higher when salt diffusion is lower and this will occur when water flows through the membrane. This was illustrated especially during EOP of sodium chloride solutions.

A decreasing amount of water permeated the membranes during acid EOP with increasing acid feed water concentration. It was also found that back diffusion was

high during acid EOP. Therefore, the right hand side of equation (3.3.45) is applicable to the experimental data that have been observed with EOP of hydrochloric acid solutions.

11.7 Prediction of Brine Concentration

Maximum brine concentration, c_b^{max} was predicted with the following two relationships:

$$c_b^{max} = \frac{1}{2FB} \qquad \text{(see eq. 3.10.28)}$$

and

$$c_b^{max} = c_b(1 + J_{osm}/J_{elosm}) \qquad \text{(see eq. 3.10.31)}$$

Brine concentration (salt, acid or base) at high current density, c_b^{max}, appeared to attain a constant value, independent of current density and dependent on the feed water concentration. Maximum brine concentration was more dependent on feed concentration where the membranes deswelled more with increasing feed water concentration.

Maximum brine concentration could be predicted accurately with equations (3.10.28) and (3.10.31). Therefore, any one of these two methods can be used to predict c_b^{max}.

Brine concentration, c_b, was predicted from the water flow through the membranes and the apparent transport of the membrane pair ($\bar{\Delta}t$) with the following relationship:

$$c_b = \frac{I\bar{\Delta}t}{2FJ} \qquad \text{(see eq. 3.10.17)}$$

Brine concentration could be predicted more accurately in the case of sodium chloride and caustic soda solutions than in the case of hydrochloric acid solutions. This can be explained by back diffusion of acid that has been experienced during EOP of the hydrochloric acid solutions. However, a much better prediction of acid brine concentration should be obtained by using the apparent transport number of the anion membrane (Δt^a) in the above equation.

The permselectivity of the membranes ($\bar{\Delta}t$'s) decreased with increasing feed water concentration. Brine concentration, on the other hand, increased with increasing feed water concentration. Therefore, the ratio $c_{b\ calc}/c_{b\ exp}$ decreased with increasing feed

concentration. The accuracy of prediction of brine concentration will therefore depend on the feed concentration used for the determination of the apparent transport number.

11.8 Membranes for Sodium Chloride, Hydrochloric Acid and Caustic Soda Concentration

The *Selemion* and *Ionac* membranes performed satisfactorily for concentration of sodium chloride solutions. The *Raipore* membranes, however, did not perform well, due to the high water transport that was experienced with this membrane type. Consequently, lower concentrations and efficiencies were obtained. The *Ionics*, WTPS, WTPVC and WTPST membranes all gave good results in terms of brine concentration and current efficiency. However, serious polarization was experienced with the WTPS membranes and ways to improve the polarization characteristics of these membranes should be investigated.

The presently commercially available anion-exchange membranes are not stable for long periods when exposed to high pH values[114]. Consequently, the membranes that were evaluated for caustic soda concentration would have a relatively short life time when treating caustic soda effluents. Nevertheless, satisfactory results were obtained with the *Selemion* and *Ionac* membranes that were used for caustic soda concentration. Membrane life time studies, however, should be conducted to determine the effectiveness of these membranes for caustic soda concentration.

The newly developed Israeli ABM membranes compared favourably with the *Selemion* AAV membrane for acid concentration. The *Selemion* AAV membranes were specially designed for acid concentration. It was shown that the *Selemion* AAV membrane adsorbed a substantial amount of acid[48]. The low dissociation of sorbed acid in the membrane was shown to be a factor which was responsible for the decrease in proton leakage of this anion membrane.

A high degree of ion-coupling will be observed in the case of charged hydrophobic membranes when acid is absorbed by the membrane. It was shown that the flux of chloride ions from the anode to the cathode steadily increased as the amount of sorbed acid was increased[48]. This result showed that chloride ions are associated with the movement of positively charged species. This may be due to the formation of an aggregate form such as $(CH_4OCl)^+$ resulting from the solvation of a proton by a water and an hydrochloric acid molecule[48].This shows that ion association is taking

place inside the membrane.

11.9 Conventional EOP·ED Stack

It was demonstrated that a conventional ED stack can be used as an EOP·ED stack for concentration of sodium chloride, hydrochloric acid and caustic soda solutions using commercially available ion-exchange membranes. Relatively high brine concentrations and low brine volumes were obtained. Electrical energy consumption was also low at low cell pair voltages.

An advantage of using a conventional ED stack as an EOP·ED stack is that the membranes can be taken out of the stack for cleaning purposes if it should be required. It is not possible to open sealed-cell ED membranes for cleaning. A disadvantage of using a conventional ED stack as an EOP·ED stack is that the membrane utilization factor will be low (approximately 80%). However, it should be possible to improve the membrane utilization factor with improved gasket design and this matter needs further investigation.

11.10 Sealed-Cell Electrodialysis

The sealed-cell ED unit performed satisfactorily for concentration/desalination of salt solutions and industrial effluents. High brine concentrations and low brine volumes were obtained. Low electrical energy consumptions were also obtained at low feed concentrations. Electrical energy consumptions obtained with the conventional EOP·ED stack were comparable to the electrical energy consumptions obtained with the sealed-cell ED stack.

The effective thickness of the dialysate compartment, d_{eff}, was much lower in the case of the sealed-cell ED unit than in the case of the EOP·ED stack. This can be ascribed to the thinner dialysate compartments that have been used in the sealed-cell unit and to the higher linear flow velocities used.

The advantages and disadvantages of SCED are as follows: The capital cost of SCED equipment should be less than that of a conventional plate-and-frame ED stack, because of the simpler construction of the SCED stack. The membrane utilization factor in the membrane bags is approximately 95% compared to approximately 80% for membranes in conventional ED stacks. Higher current densities can be used in

SCED than in conventional sheet flow ED because higher linear flow velocities can be obtained with ease. The higher current densities will result in higher water production rates. Brine volumes produced by SCED are smaller than those obtained with conventional ED. Therefore, the brine disposal problem will be reduced.

More electrical energy per unit of product water produced, will be used in the SCED stack due to the higher current densities used. However, the increased cost for electrical energy should be off-set by a decrease in capital cost. Scale may form more readily in the membrane bags because the SCED stack does not have a built-in self cleaning device such as encountered in the EDR system[8]. It will be difficult to remove scale from the membrane bags once it has formed because the bags cannot be opened for cleaning. Therefore, scale forming chemicals should be removed by ion-exchange or nanofiltration prior to SCED treatment. This will affect the economics of the process adversely, especially if large flows are involved.

Scale-up of a laboratory size SCED unit (100 cm^2/cp) to a pilot or full-scale plant would be possible. It would be possible to manufacture large-scale membrane bags commercially and the bags would be robust. An advantage of the membranes that were used in the SCED stack was that they could be stored dry. This is usually not the case with ion-exchange membranes normally used in conventional ED. The successful application of SCED technology seems to depend on the need to apply this technology in preference to conventional ED for specific applications where high brine concentrations and small brine volumes are required.

12. SUMMARY AND CONCLUSIONS

Salts, acids and bases frequently occur in industrial effluents. These effluents usually have a large pollution potential. Often the effluents also contain valuable chemicals and water that can be recovered for reuse. Effluent disposal cost can be high, especially where effluents must be trucked away for safe disposal. However, it would be possible to reduce disposal cost significantly if effluent volume could be reduced to a significant extent.

Electro-osmotic pumping ED has the potential to be applied for industrial effluent treatment. Preliminary work has indicated that small brine volumes and high brine concentrations could be achieved with EOP·ED at attractive electrical energy consumptions. However, it was determined that the following needs still existed regarding the application of EOP·ED for industrial effluent treatment:

a) to consider and document the relevant EOP·ED and ED theory properly;
b) to study the EOP·ED characteristics (transport numbers, brine concentration, current efficiency, current density, electro-osmotic coefficient, etc.) of commercially available and other ion-exchange membranes in a single cell pair with the aim to identify membranes suitable for EOP·ED;
c) to develop a simple method and to evaluate existing models with which membrane performance for salt, acid and base EOP·ED, can be predicted; and
d) to evaluate the EOP·ED process for industrial effluent treatment.

The following conclusions can be drawn as a result of this investigation:

- A conventional ED stack which was converted into an EOP·ED stack performed satisfactorily for concentration/desalination of sodium chloride, hydrochloric and caustic soda solutions. Dialysate concentrations of less than 500 mg/ℓ could be obtained in the feed water and cell pair voltage ranges from 1 000 to 10 000 mg/ℓ and 0,5 to 4 V/cp, respectively. Brine concentrations of 2,1 to 14,0%; 3,6% to 8,7% and 2,3% to 7,3% were obtained for sodium chloride, hydrochloric acid and caustic soda solutions, respectively.

  Current efficiency increased with increasing feed water concentration during EOP·ED of sodium chloride and caustic soda solutions. This is in contrast to what is usually happening. Increasing feed water concentration causes increasing water flow through the membranes which inhibits co-ion invasion. Therefore, higher current efficiency is obtained. This supported the results that were obtained in a single cell pair. Current

efficiencies varied between 75,2 and 93,6%; 29,2 and 46,3% and 68,9 and 81,2% for sodium chloride (1 000 to 5 000 mg/ℓ feed; 0,5 to 1,5 V/cp); hydrochloric acid (1 000 to 5 000 mg/ℓ feed; 0,5 to 4,0 V/cp); and caustic soda solutions (1 000 to 10 000 mg/ℓ feed; 0,5 to 3 V/cp), respectively.

Low brine volumes and high water recoveries were obtained. Brine volume increased with increasing feed water concentration and decreased with increasing cell pair voltage. Brine volume varied between 1,5 and 4,0% for sodium chloride (1 000 to 5 000 mg/ℓ feed; 0,5 to 1,0 V/cp); between 2,4 and 7,8% for hydrochloric acid (1 000 to 5 000 mg/ℓ feed; 0,5 to 1,5 V/cp); and between 2,3 to 7,3% for caustic soda solutions (1 000 to 5 000 mg/ℓ feed; 0,5 to 1,5 V/cp).

Electrical energy consumption was low at low feed water concentrations and low cell pair voltages. Electrical energy consumption increased with increasing feed water concentration and increasing cell pair voltage. Electrical energy consumption of less than 2,5 kWh/m^3 product water was obtained for sodium chloride (0,5 to 1,5 V/cp; 1 000 to 3 000 mg/ℓ feed); between 0,2 and 3,2 kWh/m^3 product for hydrochloric acid (0,5 to 1,5 V/cp; approximately 1 000 mg/ℓ feed); and between 0,4 and 2,2 kWh/m^3 product for caustic soda solutions (0,5 to 1,5 V/cp; 1 000 to 3 000 mg/ℓ feed).

Water yield increased with increasing cell pair voltage and decreased with decreasing feed water concentration. Water yield was 0,38 m^3/m^2.d at a linear flow velocity of 1 cm/s through the stack when hydrochloric acid was concentrated (2 V/cp; 3 000 mg/ℓ feed). Water yield was increased to 0,7 m^3/m^2.d when linear flow velocity was increased to 5 cm/s. A higher linear flow velocity will also depress polarisation. Therefore, it would be advantageous to operate an EOP-ED stack at the highest possible linear flow velocity.

- Sealed-cell ED should be effective for concentration/desalination of relatively dilute (500 to 3 000 mg/ℓ TDS) non-scaling forming salt solutions. Product water with a TDS of less than 300 mg/ℓ could be produced in the feed water concentration range from 500 to 10 000 mg/ℓ TDS. Electrical energy consumption of 0,27 to 5,9 kWh/m^3 product was obtained (500 to 3 000 mg/ℓ feed range). Brine volume comprised approximately 2% of the initial feed water volume. Therefore, brine disposal costs should be significantly reduced with this technology.

Sealed-cell ED became less efficient in the 5 000 to 10 000 mg/ℓ TDS feed water

concentration range due to high electrical energy consumption (3,3 to 13,0 kWh/m^3 product). However, SCED may be applied in this TDS range depending on the value of the products that can be recovered.

Treatment of scale forming waters will affect the process adversely because scale will precipitate in the membrane bags which cannot be opened for cleaning. Membrane scaling may be removed by current reversal or with cleaning solutions. However, this matter needs further investigation. Scale-forming waters, however, should be avoided or treated with ion-exchange or nanofiltration prior to SCED.

It was demonstrated that a relatively dilute ammonium nitrate effluent (TDS 3 600 mg/ℓ) could be successfully treated in the laboratory with SCED. Brine volume comprised only 2,8% of the treated water volume. Electrical energy consumption was determined at 2,7 kWh/m^3 product. Both the brine and the treated water could be reused. Membrane fouling or scaling, however, may affect the process adversely and this matter needs further investigation.

It was difficult to concentrate/desalinate a concentrated ammonium sulphate effluent (approximately 13 200 mS/m or 123 700 mg/ℓ TDS) with SCED. Concentration/desalination was conducted in stages. Nevertheless, it was possible to desalinate the effluent to 6,2 mS/m (88 mg/ℓ TDS). However, electrical energy consumption was high (59 kWh/m^3 product). Brine volume comprised 45% of the treated volume. A very high brine concentration (approximately 26 300 mS/m or 332 000 mg/ℓ TDS) could be obtained after the first desalination stage. However, a more dilute (16 557 mg/ℓ TDS) ammonium sulphate effluent (3rd stage) could be more easily concentrated/desalinated to 88 and 191 208 mg/ℓ TDS product water and brine, respectively, at water recovery and electrical energy consumption of 91,6% and 17,9 kWh/m^3, respectively. Therefore, SCED could also be effectively applied for the desalination/concentration of relatively high TDS waters.

It was not possible to concentrate/desalinate an effluent saturated with calcium sulphate with SCED due to membrane scaling which took place. However, it was possible to concentrate/desalinate the effluent effectively after sulphate removal by chemical precipitation. It was possible to concentrate/desalinate the effluent from 1 182 mS/m (4 461 mg/ℓ TDS) to 51 mS/m (299 mg/ℓ TDS) at an electrical energy consumption of 9,5 kWh/m^3 product. Brine volume comprised 5,3% of the treated feed. The cost effectiveness of these procedures need to be evaluated.

The ion-exchange membranes used in the SCED stack performed very well for ammonium and nitrate removal. Ammonium and nitrate ions were removed from 4 179 and 2 215 mg/ℓ in one case to 10 - (99,8% removal) and 17 mg/ℓ (99,2% removal), respectively.

Capital cost of SCED equipment should be less than that of conventional ED due to the simpler design of the SCED stack. The membrane utilization factor of 95% is much higher than in conventional (approximately 80%) ED.

Sealed-cell ED has potential for treatment of relatively dilute (< 3 000 mg/ℓ TDS) non-scaling waters for water and chemical recovery for reuse. However, high TDS (up to 16 000 mg/ℓ) waters can also be treated depending on the value of the products that can be recovered.

Studies in a single cell pair have shown the following:

- Brine concentration increased with increasing current density and increasing feed water concentration. Brine concentration appeared to attain a constant value at high current density dependent on the electro-osmotic coefficients of the membranes.

- Current efficiencies were nearly constant in a wide range of current densities (0 to 70 mA/cm^2) and feed water concentrations (0,05 to 1,0 mol/ℓ) in the case of the *Selemion* and *Raipore* membranes used for sodium chloride concentration. The same phenomenon was observed for the *Selemion* membranes used for acid concentration. However, all the other membranes showed a slight decrease in current efficiency with increasing current density. This showed that the limiting current density was exceeded and that polarization was taking place. Significant polarization took place with the WTPS membranes at relatively low current density (> 20 mA/cm^2).

- Water flow through the membranes increased with increasing current density. Water flow through the membranes also increased with increasing feed water concentration, especially for the membranes that were used for salt and caustic soda concentration. This increasing water flow improved current efficiency and water flow can therefore also have a positive effect on ED. However, water flow decreased through the *Selemion* membranes that were used for acid concentration when feed water concentration was increased and no increase in current efficiency was observed. Current efficiency,

however, increased through the Israeli ABM membranes when water flow increased.

The electro-osmotic coefficients were determined to be a function of feed water concentration. The coefficients decreased with increasing feed water concentration until a constant value was obtained at high current density. The decrease in electro-osmotic coefficients with an increase in feed water concentration can be ascribed to deswelling of the membranes with increasing feed water concentration or to a reduction in membrane permselectivity when the feed water concentration is increased.

Osmotic flow in EOP decreases relative to the total flow with increasing current density while the electro-osmotic flow increases relative to the osmotic flow. Osmotic flow, however, contributes significantly to the total water flow in EOP. Osmotic flow through the *Selemion* AAV and CHV membranes contributed 64,1% of the total flow through the membranes at a current density of 20 mA/cm^2 (0,1 mol/ℓ feed). Osmotic flow was 20,9% of the total flow at a current density of 100 mA/cm^2 (0,1 mol/ℓ feed).

- Membrane permselectivity decreased with increasing brine and feed water concentration and increasing concentration gradient across the membranes.

- *Selemion* AMV and CMV and *Ionac* membranes performed satisfactorily for concentration of sodium chloride solutions. Salt brine concentrations of 19,3%; 25,1%; 27,2% and 29,8% were obtained at feed water concentrations of 0,05; 0,1; 0,5 and 1,0 mol/ℓ, respectively, with the *Selemion* AMV and CMV membranes. Current efficiency in this feed water concentration range varied from 62 to 91%. Performance of the *Ionics* and WTPS membranes were poorer while the poorest results were obtained with the WTPVC, WTPST and *Raipore* membranes.

Satisfactory results were obtained with the *Selemion* AAV and CHV and newly developed Israeli ABM-3 and ABM-2 membranes for hydrochloric acid concentration. Acid brine concentrations of 18,3%; 20,9%; 25,0% and 27,2% were obtained at 0,05; 0,1; 0,5 and 1,0 mol/ℓ feed water concentration, respectively, for the *Selemion* AAV and CHV membranes. Current efficiency varied between 35 and 42%. Higher current efficiencies, however, were obtained with the Israeli ABM-3 membranes. Current efficiency varied between 34 and 60% in the same feed water concentration range.

Selemion AMV and CMV, *Selemion* AMP and CMV and *Ionac* membranes performed well for caustic soda concentration. Caustic soda brine concentrations of 14,3%;

17,7%; 20,1% and 24,4% were obtained at high current density at 0,05; 0,1; 0,5 and 1,0 mol/ℓ feed water concentration, respectively, with the *Selemion* AMV and CMV membranes. Current efficiency varied from 47 to 76%.

Membrane current efficiency in EOP increased with increasing water flow through the membranes. This was especially observed for the more porous heterogeneous membranes at high feed water (1,0 mol/ℓ) concentration. It will therefore not be necessary for membranes to have very high (> 0,9) permselectivities for use in EOP-ED.

- It has been found that a simple potential measurement can be used effectively to predict membrane performance for salt, acid and base concentration with ED. The ratio between the apparent transport number ($\bar{\Delta}t$) and current efficiency (ϵ_p), however, depends on the feed concentration and current density used. Ratio's of $\bar{\Delta}t/\epsilon_p$ varied between 1,0 and 1,07 (0,1 mol/ℓ feed, *Selemion* AMV and CMV, salt concentration); 0,95 to 1,09 (0,5 mol/ℓ feed, *Ionac*); 1,02 and 1,05 (0,5 mol/ℓ feed, *Raipore*); 0,95 and 1,02 (0,5 mol/ℓ, *Ionics*). Consequently, it should be possible to predict current efficiency for concentration of sodium chloride solutions with an accuracy of approximately 10% and better from the apparent transport number of the membrane pair.

  Correlations obtained between the apparent transport number ($\bar{\Delta}t$) and current efficiency for membranes used for acid concentration, were unsatisfactory. The apparent transport number of the membrane pair ($\bar{\Delta}t$) was from 1,5 to 4 times higher than current efficiency in the feed acid concentration range from 0,05 to 1,0 mol/ℓ. Back diffusion of hydrochloric acid through the membranes caused the lower current efficiency. However, the apparent number of the anion membrane (Δt^a) gave a much better indication of membrane performance for acid concentration. Ratio's of $\Delta t^a/\epsilon_p$ of 1,1 to 1,2 (1,0 mol/ℓ, *Selemion* AAV); 0,97 to 0,84 (1,0 mol/ℓ, ABM-2); 0,92 to 0,97 (0,1 mol/ℓ, ABM-1) were obtained. Consequently, it should be possible to predict current efficiency for concentration of hydrochloric acid solutions with an accuracy of approximately 20% and better from the apparent transport number of the anion membrane.

  Correlations obtained between the apparent transport number ($\bar{\Delta}t$) and current efficiency of the membranes investigated for caustic soda concentration were satisfactory. Ratio's of $\bar{\Delta}t/\epsilon p$ of 1,0 to 1,1 (0,05 mol/ℓ, *Ionac*); 0,9 to 1,0 (0,1 mol/ℓ, *Ionac*); 0,9 (1,0 mol/ℓ, *Selemion* AMV and CMV); 1,1 to 1,2 (0,1 mol/ℓ, *Selemion* AMP

and CMV); 1,1 (0,5 mol/ℓ, *Selemion* AMP and CMV) were obtained. Therefore, it should be possible to predict current efficiency for concentration of caustic soda solutions with an accuracy of approximately 20% and better from the apparent transport number of the membrane pair. Good correlations were also obtained between the apparent transport number of the cation membrane (Δt^c) and current efficiency. Consequently, it should also be possible to predict current efficiency with an accuracy of approximately 20% and better from the apparent transport number of the cation membrane.

- The correct Onsager relationships to be used for potential measurement ($\Delta\Psi$) and for the transport number (JF/I) are at zero current and zero volume flow, and at zero concentration gradient and zero volume flow, respectively. In practical ED, measurements are conducted at zero pressure and in the presence of concentration gradients and volume flows. These factors will influence the results considerably in all systems in which volume flow is important and where the concentration factor is high as is encountered in EOP. In measurement of membrane potential, the volume flow is against the concentration potential and in general will decrease potential. In ED, water flow helps to increase current efficiency, but the concentration gradient is against current efficiency.

- Brine concentration can be predicted from apparent transport numbers ($\bar{\Delta t}$'s) and water flows through the membranes. The ratio c_{bcalc}/c_{bexp} decreased with increasing feed concentration.

- Maximum brine concentration, c_b^{max}, can be predicted from two simple models. A very good correlation was obtained by the two methods. Maximum brine concentration increased with increasing feed concentration and appeared to level off at high feed concentration (0,5 to 1,0 mol/ℓ).

- Models described the system satisfactorily for concentration of sodium chloride, hydrochloric acid and caustic soda solutions with commercially available membranes. Brine concentration approached a limiting value (plateau) at high current density dependent on the electro-osmotic coefficients of the membranes. A constant slope (electro-osmotic coefficient) was obtained when water flow was plotted against current density. Straight lines were obtained when cell pair resistance was plotted against the specific resistance of the dialysate. Current efficiency increased with increasing flow of water, decreased when back diffusion was high and transport numbers were low.

13. NOMENCLATURE

Sections 2.1 and 2.2

c_b^{max}	-	Maximum brine concentration (mol/ℓ)
ϵ_p, η_c	-	current efficiency (%)
J	-	volume flow through membranes (cm/h)
I_{eff}	-	effective current density (Coulomb efficiency x current density)
c_b	-	brine concentration (mol/ℓ)
β	-	electro-osmotic coefficient (ℓ/Faraday)
F	-	Faraday's constant (96 500 Coulomb/ge)
J_{osm}	-	osmotic water flow (cm/h)
J_{elosm}	-	electro-osmotic water flow (cm/h) ($J = J_{osm} + J_{elosm}$)
c_f	-	feed concentration (mg/ℓ)
c_p	-	product concentration (mg/ℓ)
d_{eff}	-	effective thickness of dialysate compartment (mm) (polarisation factor)
V_{cp}	-	cell pair voltage (volt)
R_{cp}	-	cell pair resistance ($\Omega \cdot cm^2$)
ρ	-	specific resistance of dialysate ($\Omega \cdot cm$)
a	-	anion membrane
c	-	cation membrane
$\Delta\Psi_m$	-	membrane potential (mV)
$\bar{\Delta}t$	-	apparent transport number of membrane pair

Section 2.3

r_{ik}	-	phenomenological resistance coefficient
f_{ik}	-	phenomenological friction coefficient
f_{21}	-	friction imposed by cation (1) on anion
f_{2w}	-	friction imposed by water (w) on anion (2)
f_{2m}	-	friction imposed by polymer matrix (m) on anion (2)
r_{ii}	-	straight resistance coefficients
m_{ext}	-	external concentration
2m	-	anion-polymer frictional force
2w	-	anion-water frictional force
$\bar{\Delta}t$	-	apparant transport number of membrane pair

Section 2.4

$\bar{a}_w$	-	water activity in interior of membrane
a_w	-	water activity outside membrane
Π	-	membrane internal osmotic pressure
R	-	gas constant
T	-	absolute temperature
v_w	-	partial molar volume of internal water component of membrane
n_o	-	equilibrium water content

Section 2.5

E	-	membrane potential
E_{max}	-	maximum membrane potential
$\bar{t}_+$	-	transport number
$\bar{t}_{+(app)}$	-	apparent transport number
a'	-	activity on one side of the membrane
a"	-	activity on the other side of the membrane
F	-	Faraday's constant
I	-	electric current
J_i	-	ion flux of species i
$\bar{t}_i$	-	transport number of species i inside the membrane

Sections 3.1.1 and 3.1.2

J_i	-	Flux density of i ($mol/cm^{-2}s^{-1}$)
c_i	-	concentration of i ($mol\ cm^{-3}$)
μ_i	-	electrochemical potential of i
x	-	distance from reference plane in membrane
R	-	gas constant
T	-	absolute temperature
γ_i	-	activity coefficient of i
V_i	-	partial molar volume of i
p	-	pressure
z_i	-	number of positive charges per ion (valency)
F	-	Faraday's number
ψ	-	electrical potential

D_i	-	diffusion coefficient of i
u_i	-	absolute mobility of i
v	-	velocity of local center of mass
L_{ik}	-	phenomenological conductance coefficient
X_k	-	force on k per mole
σ	-	rate of entropy production, reflection coefficient
ϕ	-	dissipation function
n	-	number of components
J_D	-	exchange flow
π_s	-	osmotic pressure
L_p	-	phenomenological coefficient
L_{pD}	-	phenomenological coefficient
L_D	-	phenomenological coefficient
J_v	-	total volume flux density (cm/s^{-1})
ω	-	solute permeability
R_{ik}	-	phenomenological resistance coefficient
A_{ik}	-	minor of L_{ik} in $\|L\|$
$\|L\|$	-	determinant of L_{ik}
μ_s	-	chemical potential of electrolyte
I	-	electric current density (amp/cm^2)
E	-	electromotive force

Section 3.1.3

c_i	-	concentration of i ($mol.cm^{-3}$)
F	-	Faraday's number
F_{ik}	-	frictional force of k on i per mol of i
f_{ik}	-	molar frictional coefficient of i with k
J_i	-	flux density of i ($mol.cm^{-2}s^{-1}$)
k	-	specific electrical conductance
v_i	-	mean velocity of i
X_i	-	force on i per mol

Section 3.2

J_1	-	flow of cation J_1
J_2	-	flow of anion J_2

$\Delta\tilde{\mu}_i$	-	difference in electrochemical potential
L_i	-	phenomenological coefficient
$\Delta\mu_s$	-	chemical potential
I	-	electric current
z_1	-	valance of cation
z_2	-	valance of anion
F	-	Faraday's constant
E	-	electromotive force
J_v	-	volume flow
Δt	-	apparent transport number
$\Delta\Psi$	-	potential difference across the membrane

Section 3.3

a	-	$a = X^*/X_t$
c_2^t	-	total concentration of salt in membrane
c_s'	-	salt concentration in the aqueous solution
$c_s'^{av}$	-	average concentration of salt in the two solutions adjacent to the membrane
c_1^*, c_2^*	-	concentration of the free counter- and co-ions in the membrane
c_s	-	concentration of associated salt in the membrane
E	-	electromotive force
F	-	Faraday's constant
f_{ij}	-	frictional coefficient
f_{12}	-	frictional coefficient between co- and counter-ions
I	-	electrical current
J_i	-	flow of species i
J_1, J_2	-	stoichiometric flows of counter-ions and co-ions, respectively
J_s	-	flow of salt
J_1^*, J_2^*	-	flow of free counter-ions and co-ions, respectively
k	-	distribution coefficient of salt between membrane and aqueous phases
K_d^s	-	dissociation constant of salt in the membrane
K_d^f	-	dissociation constant of fixed group in the membrane
L_p	-	filtration coefficient
m	-	$m = K_d^s/K_d^f$
Δp	-	pressure difference
P_E	-	electro-osmotic pressure measured at zero volume flow and the absence of salt gradients

q^2	-	degree of coupling
R_{11}^*,	-	straight resistance coefficients for transport of counter-ions, co-ions
R_{22}^*, R_s		and salt, respectively
R_{12}	-	coupling resistance coefficient between flows of ion 1 and 2
R	-	universal gas constant
T	-	absolute temperature
X_i	-	driving force for species i
X_1,	-	driving forces for transport of counter-ions, co-ions and salt,
X_2, X_s	-	respectively
X_t	-	total concentration of fixed groups in the membrane
X^*	-	concentration of dissociated fixed groups in the membrane
Xc_1	-	associated fixed groups in the membrane
z_i	-	valency of ion i
α	-	$\alpha = K_d^s \, kc_s'^2$
β	-	electro-osmotic permeability measured at zero pressure and salt gradient
t_1, t_2	-	transport number of counter-ions and co-ions, respectively
ψ', ψ	-	electric potential in aqueous and membrane phases
μ_i^0 $\mu_i^{0'}$	-	standard chemical potential of species i in membrane and aqueous solution, respectively
$\tilde{\mu}_1$, $\tilde{\mu}_2$	-	electrochemical potential of counter-ion 1 and of co-ion 2 in membrane, respectively
$\Delta\tilde{\mu}_i$	-	difference in electrochemical potential of species i
$\tilde{\mu}_1'$,$\tilde{\mu}_2'$	-	electrochemical potential of counter-ion 1 and of co-ion 2 in aqueous solution, respectively
μ_s	-	chemical potential of salt in membrane
$\Delta\tilde{\mu}_i$	-	difference in electrochemical potentials of species i
κ	-	membrane conductance measured in the absence of salt gradient and volume flow
κ'	-	membrane conductance measured in the absence of a pressure gradient
ω_s	-	salt permeability defined for $J_v = 0$
ω_s'	-	salt permeability defined for $\Delta p - \Delta\pi = 0$ and $I = 0$
ω_s''	-	salt permeability defined for $\Delta p = 0$ and $I = 0$
$\frac{\omega_s c_s'^{av}}{\kappa F^2}$	-	leak conductance (LC) ratio defined for $J_v = 0$
σ	-	reflection coefficient

Section 3.5

Δc°	-	concentration difference across membrane at time t = 0
$c^{\circ\prime}$	-	concentration at one side of the membrane at time t = 0
$c^{\circ\prime\prime}$	-	concentration at other side of memtrane at time t = 0
Δc^t	-	concentration difference across membrane after time t
J_1	-	total counter-ions
J_w	-	water flux
$\bar{t}_2$	-	co-ion transport number
$\bar{t}_w$	-	water transport number
$\bar{t}_1$	-	counter-ion transport number
$\bar{t}_1^r$	-	reduced transport number of counter-ions
$\tilde{m}$	-	mean molality
J_s, J_w^{os}	-	diffusion and osmotic fluxes
I	-	electric current
ω	-	-1 for cation-exchange membrane; +1 for anion-exchange membrane
$f(L_{ik}, \tilde{m})$	-	combination of the phenomelogical conductance coefficient L_{ik} and the mean mobility, $\tilde{m}$, of a solute
$\Delta\mu_s$	-	chemical potential difference of the solute
I	-	electric current
Δc_a^t, Δc_c^t	-	concentration changes of anolyte and catholyte after time Δt
$\bar{c}^\circ$	-	mean concentration of anolyte and catholyte at time t = 0, $\bar{c}^\circ = (c_a^\circ + c_k^\circ)/2$
η_E	-	efficiency of energy conversion
J_1^w	-	$J_1/v_1 - 0{,}018\,\tilde{m}\,J_w$
ΔE	-	difference of electrical potential measured with electrodes reversible to co-ions

Section 3.6

c_i	-	concentration of species i, $mol.m^{-3}$
E	-	potential difference. V
I	-	current density, $A{\cdot}m^2$
J_i	-	flux density of species i, $mol.m^{-2}.s^{-1}$
L_{ik}	-	conductance coefficients
m_{ext}	-	external molality of NaCl
q, q_{ik}	-	coupling coefficients
$\bar{t}_w$	-	transport number of water, mol per Faraday
X_i	-	thermodynamic force

x	-	force ratio
Z	-	square route of the straight conductance coefficients
η	-	efficiency of energy conversion
μ_i	-	chemical potential of species i, $J.mol^{-1}$
π	-	osmotic pressure, Pa
ϕ	-	dissipation function
1	-	sodium ions
s	-	solute
w	-	water

Section 3.7

J_w	-	osmotic flow of water
J_s	-	diffusion flow of solute
$\Delta\mu_s$, $\Delta\mu_w$	-	differences of chemical potential of solute and water, respectively
L_{ik}	-	phenomenological conductance coefficient
J'_w	-	flow of water against the flow of solute conjugated to the concentration part of the chemical potential difference of water, $\Delta\mu_w^c$
J_v	-	total volume flow conjugated to the difference of pressure in the compartments on the opposite side of the membrane, Δp
ϕ	-	dissipation function
η	-	efficiency of energy conversion
q	-	coupling coefficient
$\Delta\pi$	-	difference in osmotic pressure
σ	-	reflection coefficient

Section 3.8

Π	-	osmotic swelling pressure
$\bar{a}_w$	-	water activity in membrane
a_w	-	water activity outside membrane
R	-	gas constant
T	-	absolute temperature
$\bar{C}$	-	internal equilibrium electrolyte concentration
C	-	concentration mol/ℓ
v_w	-	partial molar volume of the internal water component

Section 3.9

E	-	total electromotic force of membrane cell
M	-	molecular mass of solvent
m	-	concentration
$\bar{t}_w$	-	water transport number
$\bar{t}_i$	-	transport number
R	-	gas constant
T	-	absolute temperature
F	-	Faraday
a	-	activity
$t_{+(app)}$	-	apparent transport number
t_+	-	true transport number
$\bar{X}$	-	fixed charge density (equivalent per unit volume of swollen membrane)
$\bar{s}$	-	equivalent of co-ions per equivalent of fixed group present in the membrane
u's	-	mobilities of ions
$\bar{k}'$	-	specific conductance of membrane
β	-	volume of water flowing per Coulomb
V	-	volume of water flowing per second (millilitre)
i	-	current in amperes
k_i	-	specific conductance of pore liquid
A	-	pore area
φ_w	-	volume fraction of water in the membrane
$\bar{X}_v$	-	equivalent of fixed groups per unit volume of interstitial water
ΔV_c	-	volume decrease at anode due to water transport
ΔV_o	-	observed volume change
$\bar{V}$	-	partial molar volume

Sections 3.10 and 3.11

a_i	-	activity of species i (mol/ℓ)
A_m	-	effective membrane area (cm^2)
c_i	-	concentration of species i (mol/ℓ)
F	-	Faraday's constant - 96 500 (amp.sec/mol)
F_i	-	driving force acting on species i
I	-	electric current density (amp/cm^2)
I_{eff}	-	effective current density (amp/cm^2)

j_i	-	flux of species i through a membrane (mol/(sec.cm^2))
J	-	volume flow through a membrane (cm/sec = cm^3/cm^2.sec)
L_p	-	filtration coefficient
P	-	solute permeability
Q	-	amount of feed solution entering a diluate channel per unit time
R	-	universal gas constant
s^c	-	salt flux (cation)
s^a	-	salt flux (anion)
t_i	-	transport number of ionic species i
$\bar{t}_i$	-	effective transport number of the ionic species i
Δt	-	difference between counter-ion and co-ion effective transport members
$\overline{\Delta t}$	-	effective transport number of a membrane pair
T	-	absolute temperature, °K
V_w	-	water flow through a membrane (cm/s)
V	-	volume of solution that enters a membrane bag per unit area
$\bar{V}$	-	molar volume of species i
Δx	-	membrane thickness
β_i	-	drag coefficients associated with the ionic species i
γ_i	-	activity coefficient of species i
δ	-	thickness of the unstirred layer next to a solid surface
ϵ_c	-	overall current efficiency
ϵ_p	-	Coulomb efficiency (current efficiency)
ϵ_w	-	efficiency associated with water transport through membranes
Λ	-	degree of demineralization
μ_i	-	chemical potential of ionic species i
$\tilde{\mu}_i$	-	electrochemical potential of ionic specie i
$\Delta\Psi_m$	-	electrical potentical difference between reversible electrodes, due to a difference of concentration at both sides of the membrane
π	-	osmotic pressure
σ	-	reflection coefficient
ω	-	salt permeability
η	-	current efficiency
a	-	anion-exchange membrane
c	-	cation-exchange membrane
F	-	Faraday's constant (Coulomb equiv^{-1})
I	-	current density, amp cm^{-2}
J	-	molar flux, mol cm^{-2} sec^{-1}

J_v	-	volume flux, $cm \cdot sec^{-1}$
L_p	-	hydraulic permeability $cm \cdot sec^{-1}$ per unit pressure
P	-	local solute permeability, $cm^2 \cdot sec^{-1}$
R	-	universal gas constant
R_{cp}	-	apparent resistance of cell pair ohm cm^2
R_m	-	resistance of membrane pair ohm cm^2
S	-	rate of salt removal, $mol/cm^2.s$
T	-	absolute temperature
V_{cp}	-	voltage per cell pair, volts
c_s	-	salt concentration, mol/cm^3
c_b, c_f,	-	concentration of brine, feed, product
c_p		respectively, mol/cm^3
d_{eff}	-	effective thickness of dialysate cell, mm
β	-	electro-osmotic coefficient, cm^3 Coulomb $^{-1}$
$\gamma \pm$	-	activity coefficient
μ_i	-	thermodynamic potential
μ_i	-	electrochemical potential
η η_c	-	efficiency, current efficiency
π	-	osmotic pressure
ρ	-	specific resistance of dialysate, ohm·cm
t	-	transport number
ψ	-	potential, volt
ω	-	Permeability coefficient

Section 3.12

t_1	-	transport number of cations in solution
t_2	-	transport number of anions in solution
$\bar{t}_1^c$	-	transport number of cations in CPM
$\bar{t}_2^c$	-	transport number of anions in CPM
$\bar{t}_1^a$	-	transport number of cations in APM
$\bar{t}_2^a$	-	transport number of anions in APM
T_{DC}	-	apparent diffusion transport number of anion near cation membrane
T_{DA}	-	apparent diffusion transport number of cation near anion membrane
N	-	number of membrane pairs
F	-	Faraday's constant
R	-	gas constant

T	-	absolute temperature
E_m	-	membrane potential
T_D	-	flux of salt from the diluate channel
d	-	desalting rate (equiv $cm^{-2}.s^{-1}$)
p^c	-	permselectivity of cation membrane
p^a	-	permselectivity of anion membrane
P	-	power required to drive cell pair
i	-	current density
V_{cp}	-	cell pair voltage
δ	-	thicknes of boundary layer
R_d	-	resistance 1 cm^2 cross section, d.
κ	-	conductivity $(ohm/cm)^{-1}$
C_d	-	concentration of diluate stream $(equiv/cm^3)$
C_c	-	brine concentration $(equiv/cm^3)$
C_c/C_d	-	C = non-dimentsional concentration ratio term
Λ	-	equivalent conductivity in cm^2/ohm equiv.
R_{BC}	-	boundary layer resistance at cation membrane
R_{BA}	-	boundary layer resistance at anion membrane
C_w	-	solute concentration at membrane/diluate interface
C_{w1}	-	bulk concentration of concentrated salt on one side of membrane
C_{w2}	-	bulk concentration of dilute salt solution on other side of membrane
C_{wbc}	-	concentration-polarized membrane/boundary layer concentration at brine side of cation membrane
C_{wdc}	-	concentration-polarization membrane/boundary layer concentration at diluate side of anion membrane
Ud	-	flow rate
λ	-	cell to boundary layer thickness ratio
D	-	diffusion coefficient (cm^2/s)
R	-	gas constnt
β	-	$\frac{F^2D}{\Lambda t_2 RT}$

14. LITERATURE

1. Garza, G. (1973): Electrodialysis by Electro-Osmotic Pumping and Ion Separation with Charged Membranes. Thesis submitted to the Weizmann Institute of Science, Rehovot, Israel.

2. Garza, G., and Kedem, O. (1976): Electro-Osmotic Pumping in Unit-Cells. 5th International Symposium on Fresh Water from the Sea, 13, 79-87.

3. Kedem, O., Tanny, G. and Maoz, G. (1978): A simple Electrodialysis Stack. *Desalination*, 24, 313-319.

4. Kedem, O., and Cohen, J. (1983): EDS-Sealed-Cell Electrodialysis. *Desalination*, 46, 291-299.

5. Kedem, O., and Bar-On, Z. (1986): Electro-Osmotic Pumping in a Sealed-Cell ED Stack. AIChE Symposium Series, Industrial Membrane Processes, 248, 82, 19-27.

6. Nishiwaki, T. (1972): Concentration of Electrolytes prior to Evaporation with an Electromembrane Process, **In**: R.E. Lacey and S. Loeb (Ed.), Industrial Processing with Membranes, Wiley-Inter-Science, New York.

7. Wilson, J.R. (1960): Demineralization by Electrodialysis, London, Butterworth Scientific Publications.

8. U.S.A.I.D. Desalination Manual (1980). CH & M, International Corporation, 7201 NW, 11th Place, Gainesville, Florida, USA, 32601.

9. Meares, P., Thain, J.F., and Dawson, D.G. (1972): Transport Across Ion-Exchange Resin Membranes: The Frictional Model of Transport, **In**: Eisenmann, G. (Ed), Membranes, A Series of Advances, Volume 1, Macroscopic Systems and Models, Marcel Dekker, Inc. New York.

10. Teorell, T. (1953): Transport Processes and Electrical Phenomena in Ionic Membranes. *Progr. Biophys. Biophys. Chem.*, 3, 305.

11. Helfferich, F. (1962): *Ion-Exchange,* McGraw-Hill, New York, 344.

12. Staverman, A.J. (1952): Non-Equilibrium Thermodynamics of Membrane Processes. *Trans. Faraday soc.*, 48, 176.

13. Catchalsky, A., and Curren, P.F. (1965): Non-Equilibrium Thermodynamics **in** Biophysics, Harvard University Press, Cambridge Mass.

14. Kedem, O., and Katchalsky, A. (1963): Permeability of Composite Membranes. *Trans. Faraday Soc.*, 59, 1918, 1931, 1941.

15. Kedem, O. (1983): A Simple Procedure for Estimating Ion Coupling from Conventional Transport Coefficients. *Journal of Membrane Science*, 14, 249-262.

16. Johnstone, B.L. (1987): Lecture on Basic Principles of Electrodialysis.

17. Koter, S., and Narebska, A. (1989/90): Current Efficiency and Transport Phenomena in Systems with Charged Membranes. *Separation Science and Technology*, 24, (15), 1337-1354.

18. Narebska, A., and Koter, S. (1987): Irreversible Thermodynamics of Transport Across Charged Membranes. Part III - Efficiency of Energy Conversion in Separation Processes with Nafion 120 Membrane from Phenomenological Transport Coefficients. *Journal of Membrane Science*, 30, 141 - 152.

19. Narebska, A., koter, S., and Kujowski, W. (1990): Conversion of Osmotic Energy in Systems with Charged Membranes. *Journal Non-Equilibrium Thermodynamics*, 15, 1 - 10.

20. Brydges, T.G., and Lorimer, J.W. (1983): The Dependence of Electro-Osmotic Flow on Current Density and Time. *Journal of Membrane Science*, 13, 291-305.

21. Kruissink, C.H.A. (1983): The effect of Electro-Osmotic Water Transport on Current Efficiency and Cell Performance in Chlor-Alkali Membrane Electrolysis. *Journal of Membrane Science*, 14, 331-366.

22. Hidalgo-Alvarez, R., de las Nieves, F.J. and Pardo, G. (1984): Anamalous Electro-Osmotic Flow through a Heteroporous Ion-Exchange Membrane - A Test Based upon the Reciprocity Relations. *Journal of Non-Equilibrium Thermodynamics*, 9, 157-1643.

23. Ceynowa, Josef (1983): Electro-Osmosis in the System Ion-Exchange Membrane-Sulphuric Acid Solution. *Die Angewandte Makromolekulare Chemie,* 116, 165-174 (No 1824).

24. Tombalakion, A.S., Barton, H.J., Graydon, W.F. (1962): *Journal Physical Chemistry,* 66, 1006.

25. Rueda, C., Ruiz-Bauza, C., and Agular, J. (1977): Electro-Osmotic Permeability of Cellulose Acetate Membranes. *Journal Physical Chemistry,* 61, 789.

26. Tasaka, Masayasu., Tamura, Staoski., and Takemura, Naota (1082): Concentration Dependence of Electro-Osmosis and Streaming Potential across Charged Membranes. *Journal of Membrane Science,* 12, 169-182.

27. Oda, Goshio., and Yawataya, Tadaski (1957): On the Distribution and Behaviour of Water in Cation-Exchange Resin Membranes. *Bulletin of the Chemical Society of Japan,* 30,(3), 213.

28. Narebska, A., Koter, S., and Kujowski, W. (1984): Ions and Water Transport Across Charged Nafion Membranes. Irreversible Thermodynamic Approach. *Desalination,* 51, 3 - 17.

29. Narebska, A. and Koter, S. (1987): Conductivity of Ion-Exchange Membranes - Convection Conductivity and Other Components. *Electro-Chimica Acta,* 32, (3), 449 - 453.

30. Narebska, A., Kujowski, W., and Koter, S. (1987): Irreversible Thermodynamics of Transport Across Charged Membranes, Part II - Ion-Water Interactions in Permeation of Alkali. *Journal of Membrane Science,* 30, 125 - 140.

31. Narebska, A., Koter, S., and Kujowski, W. (1985): Irreversible Thermodynamics of Transport Across Charged Membranes. 1. Macroscopic Resistance Coefficients for a System with Nafion 120 Membrane. *Journal of Membrane Science,* 25, 153 - 170.

32. Koter, S., and Narebska, A. (1987): Conductivity of Ion-Exchange Membranes. *Electrochimica Acta,* 32, (3), 455 - 458.

33. Kononov, A.N., Ponomarev, M.I., Shkaraputa, L.N., Grebenyuk, V.D., and Sklyar, V.T. (1984): Removal of Hydrochloric Acid from Waste Waters Containing Organic Synthesis Products. *Khimiya i Teckhnologiya Vody,* 6, (1), 66-68.

34. Korngold, E. (1978): Concentration of sulphuric and Hydrochloric Acids. *Electrodialysis in Advanced Waste Water Treatment,* 24, 129-139.

35. Laskorin, B.M., Smirnova, N.M., Tisov, Y., Gorina, G.N., and Borisov, A.V. (1973): Use of Electrodialysis with Ion-Selective Membranes for Concentrating Carbonate Solutions. *Zhurnal Prikladnoi Khimii,* 46, (9), 2117-2119.

36. Smagin, V.N., and Chukkin, V.A. (1975): Concentration of Brines of Desalination Plants with Electrodialysis. *5th International symposium on Fresh Water from the Sea,* 3, 139-148.

37. Urano, K., Ase, T., and Naito, Y. (1984): Recovery of Acid from Wastewater by Electrodialysis. *Desalination,* 51, 213-226.

38. Itoi, S., Nakamura, I., and Kawahara, T. (1980): Recovery of Metals from Plating Rinse Waters. *Desalination,* 32, 383.

39. Schoeman, J.J. (1985): The Status of Electrodialysis Technology for Brackish and Industrial Water Treatment. *Water SA,* 11, (2), 79-86.

40. Lakshminarayanaih, N. (1962): Electro-Osmotic Permeability of Ion-Exchange Resin Membranes. Proceedings Indian Academy, Sci., A55, 200.

41. Demarty, M., Maurel, A., and Selegny, E. (1974). *Journal Chim. Phys., Phys. Chim. Biol.,* 71, 811.

42. Mauritz, K.A., and Hopfinger, A.J. (1982): Structural Properties of Membrane Ionomers, In: *Modern Aspects of Electrochemistry,* 14, J.O.M. Bockris, B.E. Conway, and R.E. White, Eds., Plenum Publishing Corp., Ch.6.

43. Narebska, A., and Wodzki, R. (1982): Swelling Equilibria and Structure Variations of Nafion and Polyethylene (Polystyrene Sulphonic Acid) Membranes at High Electrolyte Concentrations and Increased Temperature. *Die Angewandte Makromolekulare Chemie,* 107, 51 - 60 (No. 1679).

44. Narebska, A., Wodzki, R., and Erdmann, K. (1983): Properties of Perflurosulphonic Acid Membranes in Concentrated Sodium Chloride and Sodium Hydroxide Solutions. *Die Angewandte Makromolekulare Chemie,* 111, 85 - 95 (No. 1711).

45. Lakshminarayanaih, N. (1969): Transport Phenomena In Membranes. Academic Press, Inc. 111 Fifth Avenue, New York, New York 10003.

46. Kressman, T.R.E., and Tye, F.L. (1956): *Discussions Farady Soc.* 21, 185.

47. Lakshminarayanaih, N., and Subrahmanyan, V. (1964): *J Polymer Sci. Pt. A* 2, 4491.

48. Boudet-Dumy, M., Lindheimer, A., and Gavach, C. (1991): Transport Properties of Anion-Exchange Membranes In Contact with Hydrochloric Acid Solutions. Membranes for Acid Recovery by Electrodialysis. *Journal of Membrane Science,* 57, 57-68.

49. Cherif, A.T., and Gavach, C. (1988): Sulphuric Acid Concentration with an Electrodialysis Process, *Hydrometallurgy,* 21, 191.

50. Huang, T.C., and Juang, R.S. (1986): Recovery of Sulphuric Acid with Multi-Compartment Electrodialysis. *Ind. Eng. Chem. Processes Des. Dev.,* 25, 537.

51. Nott, B.R. (1981): Electrodialysis for Recovering Acid and Caustic from Ion-Exhange Regeneration Wastes. *Ind. Eng. Chem. Prod. Res. Dev.,* 20, 170.

52. Grebenyuk, V.D., Penkalo, I.I., and Chalaya, L.M. (1986): Desalination of Water with Simultaneous Production of Alkali and Acid. *Khim. Teknol. Vody,* 8, 76.

53. Leitz, F.B. (1976): Electrodialysis for Industrial Water Clean-Up. *Environ. Sci. Technol.,* 10, 136.

54. Eisenmann, J.L. (1979): Membrane Processes for Metal Recovery from Electroplating Rinse Water. Second Conference on Advanced Pollution Control for the Metal Finishing Industry, E.P.A., Cincinnati, OH, 99.

55. Hanley, T.R., Chiu, H.K., and Urban, R.J. (1985): Phosphoric Acid Concentration by Electrodialysis. AIChE Symp. Ser., 82, 121.

56. McRae, W.A. (1983): In Desalination Technology, Developments and Practice (A. Porteous, ed), *Applied Science*, Chapter 8.

57. Iaconelli, W.B. (1973): The Use of Electrodialysis in the Food Industry, Paper presented at the IFT Annual Meeting.

58. Reed, P.B., (1984): *Chem. Eng. Prog.*, 47.

59. Barney, J.J., and Hendrik, J.L., (1878): *Chem. Prod. Res. Dev.*, 17, 17.

60. Bhagat (1980): *Water Pollution Control*, 11, 118.

61. Melzer, J., and Van Deventer, D. (1983): Electrodialysis Used for Desalination of Waste Water in an Eskom Power Station. Presented at a Symposium on Desalination: New Developments and Industrial Application, CSIR Conference Centre, Pretoria, 27 October 1983.

62. Gering, K.L., and Scamehorn, J.F. (1988): Use of Electrodialysis to Remove Heavy Metals from Water. *Separation Science and Technology*, 23, (14 & 15), 2231-2267.

63. Goldman, D.E. (1943): Potential, Impedance and Rectification in Membranes. *J. Gen. Physiol.*, 27, 37.

64. Kirkwood, J.G. (1954): **In** Ion Transport Across Membranes (H.T. Clarke, ed), Academic, New York, 119.

65. Miller, D.G. (1960): Thermodynamics of Irreversible Processes. *Chem. Rev.*, 60, 15.

66. Kedem, O., and Katchalsky, A. (1958): Thermodynamic Analysis of the Permeability of Biological Membranes to Non-Electrolytes. *Biochim. Biophys. Acta.* 27, 229.

67. Krämer, H., and Meares, P. (1969): Correlation of Electrical and Permeability Properties of Ion-Selective Membranes. *Biophys. J.*, 9, 1006.

68. Kedem, O., and Essig, A. (1965): Isotope Flows and Flux Ratios in Biological Membranes. *J. Gen. Physiol.*, 48, 1047.

69. Coster, H.G.L. and George, E.P. (1968): A Thermodynamic Analysis of Fluxes and Flux-Ration in Biological Membranes. *Biophys. J.*, 8, 457.

70. Mazur, P. and Overbeek, J.T. (1951): On Electro-Osmosis and Streaming-Potentials in Diaphragms. *Rec. Trav. Chim.*, 70, 83.

71. Spiegler, K.S. (1958): *Trans. Faraday Soc.*, 54, 1408.

72. Kedem, O. and Caplan, S.R. (1965): Degree of Coupling and its Relation to Efficiency of Energy Conversion. *Trans. Faraday Soc.*, 61, (9), 1897.

73. Kedem, O., and Perry, M. (1977): Proc. Symp. on the Behaviour of Ions in Macromolecular and Biological Systems, Colston, England, 134.

74. Caplan, S.R. (1965): The Degree of Coupling and Efficiency of Fuel Cells and Membrane Desalination Processes. *J. Phys. Chem.*, 69, 3801.

75. Lee, K.H., Baker, R.W., and Lonsdale, H.K. (1981): Membranes for Power Generation by Pressure Retarded Osmosis. *Jour. Membrane Science*, 8, 141.

76. Donnan, F.G. (1924): *Chem Rev.* 1, 73.

77. Hale, D.K., and McCauley, D.J. (1961): *Trans. Faraday Soc.* 57, 135.

78. Lakshminarayanaiah, N. (1965): *Chem. Rev.* 65, 531.

79. Lakshminarayanaiah, N. (1969): *J. Phys. Chem.* 73, 97.

80. Oda, Y., and Yawataya, T. (1956): *Bull. Chem. Soc. Japan.* 29, 673.

81. Harned, H.S., and Owen, B.B. (1958): "The Physical Chemistry of Electrolytic Solutions", 3rd ed., p. 359. Reinhold, New York.

82. Spiegler, K.S., and Kedem, O. (1966): Thermodynamics of Hyperfiltration (Reverse Osmosis): Criteria for Efficient Membranes. *Desalination*, 1, 311-326.

83. Ionics Pamphlet on EDR (1987).

84. Katz, W.E. (1977): The Electrodialysis Reversal (EDR) Process. Presented at the International Congress on Desalination and Water Reuse, Tokyo, November/December 1977. Published by Ionics, Inc., 65 Grove Street, Watertown, MA, USA 02172 (Bulletin TP. 307).

85. Leitz, F.B. and Eisenmann, J.L. (1981): Electrodialysis as a Separation Process. A.I.Ch.E. Symposium Series 77, 204-209.

86. Tani, Y. (1981): Energy Saving Electrodialyzer for Seawater Desalination. Technical Proceedings, Ninth Annual Conference, National Water Supply Improvement Association, Washington, D.C. Published by NIWSA, 26 Newbury Road, Ipswich, NA, USA, 01938.

87. Urano, K. (1977): Present Status of Electrodialysis Process in Japan. *Desalination,* 20, 365.

88. Wirth, J.R. and Westbrook, G. (1977): Cooling Water Salinity and Brine Disposal Optimized with Electrodialysis Water Recovery/Brine Concentration System. *Combusion,* May, 33-37.

89. Lakshminarayanaih, N. (1965): *Chem. Revs.* 65, 494.

90. Friedlander, H.Z. and Rickles, R.N. (1966): *Anal, Chem.* 37, 27A.

91. Molau, G.E. (1981): Heterogeneous Ion-Exchange Membranes. *Journ. of Membrane Science,* 8, 309-330.

92. Korngold, E., De Körösy, F., Rahav, R. and Taboch, M.F. (1970): Fouling of Anion-Selective Membranes in Electrodialysis. *Desalination,* 8, 195.

93. Van Duin, P.J. (1973): Poisoning of Electrodialysis Membranes. Proceedings of 4th International Symposium on Fresh Water from the Sea, 3, 253-259.

94. Katz, W.E. (1982): Desalination by ED and EDR-State-of-the-Art in 1981. *Desalination,* 42, 129.

95. Fraivillig, J.B. (1983): Reverse Osmosis/Electrodialysis Reversal Comparison. Permasep Products (Du Pont), Maylands Avenue, Hemel Hampstead, Herts, HP2-7DP.

96. Miva, T. (1977). Desalting by Electrodialysis. *Desalination,* 20, 375.

97. Song, Shi and Pei-Qi Chem (1983): Design and Field Trials of a 200 m^3/day Seawater Desalination by Electrodialysis. *Desalination,* 46, 191.

98. Parsi, E.J., Prato, T.A. and P'Donoghue, K. (1980): Status of High Temperature Electrodialysis. Presented at the Eighth Annual Conference of the National Water Supply Improvement Association, San Francisco, 6-10 July.

99. Brown, D.R. (1981): Desalting High Salinity Water Using 10-Stage EDR. Proceedings of the Ninth Annual Conference and International Trade Fair of the National Water Supply Association, 2.

100. Elyanow, D., Parent, R.G. and Mahoney, J. (1980): Parametric Tests of an Electrodialysis Reversal System with Aliphatic Anion Membranes. Report to WRT, US Department of the Interior (Contract No. 14-34-0001-9510),Washington, D.C.

101. Katz, W.E. (1971): Electrodialysis for Low TDS Waters. *Ind. Water Engng.,* June/July (Bulletin TP.301).

102. Highfield, W.H. (1980): Electrodialysis in Industrial Water Treatment. Presented at the 41st Annual Meeting of the International Water Conference, Pittsburgh, Pennsylvania, October, 1980. (Bulletin TP.316).

103. Itoi, S. (1979): Electrodialysis of Effluents from Treatment of Metallic Surfaces. *Desalination* 28, 193.

104. Trivedi, D.S., and Prober, R. (1972): On the Feasibility of Recovering Nickel from Plating Wastes by Electrodialysis. *Ion Exch. Membr.,* 1, 37.

105. Eisenmann, J.T. (1977): Recovery of Nickel from Plating Bath Rinse Waters by ED. *Plat. Surf. Finish.,* 64 (11), 34.

106. Jordan, D.R., Bearden, M.D. and McIhenny, W.R. (1975): Blowdown Concentration by Electrodialysis. *Chem. Engineering. Prog.,* 71(7), 77.

107. Jordan, D.R., McIhenny, W.F., and Westbrook, G.T. (1976): Cooling Tower Effluent Reduction by Electrodialysis. American Power Conference.

108. Westbrook, G.T. and Wirth, L.F. Jr. (1976): Water Reuse by Electrodialysis. *Ind. Water Engng.*, April/May 8.

109. Smirnova, N.M., Laskorin, B.N., Mishukova, J.S. and Borisov, A.V. (1983): The Application of Electrodialysis with Ion-Exchange Membranes for Treatment of Sodium Sulphate Solutions. *Desalination,* 46, 197.

110. Nott, B.R. (1981): Electrodialysis for Recovering Acid and Caustic Soda from Ion-Exchange Regeneration Wastes. *Ind. Engng. Chem. Product Des. and Dev.*, 20, (1).

111. Schoeman, J.J. and Botha, G.R. (1981): Behandeling van Industriële Uitvloeisels met Elektrodialise. Presented at a Symposium on Industrial Effluents, 23 November, Pretoria.

112. Oren, G. and Litan, J. (1974): The State of the Solution Membrane Interface during Ion Transport Across and Ion-Exchange Membrane. *Journ. Physical Chemistry,* 78, 1805.

113. Simon, G.P. and Calmon, C. (1986): Experimental Mehtods for the Determination of Non-Transport Properties of Membranes. *Desalination,* 59, 106, 103.

114. Kneifel, K., and Hattenbach, K. (1980): Properties and Long-Term Behaviour of Ion-Exchange Membranes. *Desalination,* 34, 77.

115. Schoeman, J.J., Hill, E., Enslin, G.M. and MacLeod, H. (1990): Electro-Osmotic Pumping of Salts, Acids and Bases. Contract Report to the Water Research Commission.

116. Schoeman, J.J. and Enslin, G.M. (1989): Evaluation of Sealed-Cell Electrodialysis for Industrial Effluent Treatment. Contract Report to the Water Research Commission.

117. Kedem, O. (1992): Private Communication.

APPENDIX A

1. DEFINITION OF TRANSPORT NUMBERS

a) Transport number of ion i, t_i:

$$t_i = (z_i J_i F/I)_{\Delta c = 0}, \quad i = 1,2 \tag{A1}$$

where I is the electric current, J_i is the flux of species i, z_i is its charge, and F is the Faraday constant.

b) Reduced transport number of species i (6), t_i^r.

For ions (i = 1,2):

$$t_i^r = \frac{1}{z_i} t_i = \left(\frac{FJ_i}{I}\right)_{\Delta c = 0}$$

For water:

$$t_w^r = t_w = \left(\frac{FJ_w}{I}\right)_{\Delta c = 0} \tag{A2}$$

APPENDIX B

1. DERIVATION OF THE FORMULA FOR THE CURRENT EFFICIENCY (Eq. 3.5.3, Fig. 3.5.1)

At t = 0 the concentrations of the anode (i = a) and the cathode (i = c) solutions are

$$c_i^\circ = n_i^\circ / V^\circ, \qquad i = a, c \tag{B1}$$

where n_i° is the number of moles of an electrolyte in the "i" solution. The volumes of both solutions are equal and denoted by V°. After passing the current I during time Δt, the concentrations in both compartments change to

$$c_i^t = (n_i^\circ + \Delta n_i) / (V^\circ + \Delta V_i), \quad i = a, c \tag{B2}$$

where Δn_i and ΔV_i are the changes of the amount of an electrolyte and of the volume in the "i" compartment, respectively. Assuming $\Delta V_i << V^\circ$, from eqs. (B1) and (B2) we obtain

$$\Delta c_c^t - \Delta c_a^t = (\Delta n_c - \Delta n_a - c_c^\circ \Delta V_c + c_a^\circ V_a)/V^\circ \tag{B3}$$

For the standard system (Fig. 3.5.1), the changes of ΔV_i and Δn_i are as follows:

Real membrane:

$$\begin{aligned} \Delta n_i &= z_i(\Delta n^m + \Delta n^{mid}) \\ &= z_i \omega J_1 / v_1 \Delta t \text{ (moles of } Av_1Bv_2) \end{aligned} \tag{B4}$$

$$\begin{aligned} \Delta V_i &= z_i(\Delta V^m + \Delta V^{mid}) \\ &= z_i \omega (\bar{v}_s J_1 / v_1 + \bar{v}_w J_s 1)\Delta t, \quad i = a \text{ or } c \end{aligned} \tag{B5}$$

where $z_a = 1$, $z_c = -1$

Δn^m and ΔV^m denote changes in the amounts of ions and of volume due to the transport across the investigated membrane, respectively

$$\Delta n^m = \omega J_1 \Delta t / v_1 (Av_1Bv_2) + x\,/|\,z_2\,|(B^{z_2}) \tag{B6}$$

$$\Delta V^m = \left(\omega \bar{v}_s J_1 / v_1 + \bar{v}_w J_w + \frac{\bar{v}_2}{|z_2|}\,\frac{I}{F}\right)\Delta t \tag{B7}$$

Δn^{mid} and ΔV^{mid} denote analogical effects of transport across ideal membranes surrounding the investigated membrane

$$\Delta n^{mid} = -x/|z_2|(B^{z_2}) \tag{B8}$$

$$\Delta V^{mid} = -\frac{\bar{v}_2}{|z_2|}x \tag{B9}$$

$$x = I\Delta t/F \tag{B10}$$

$$J_1 = -\omega\bar{t}_1^r I/F + v_1 J_s \tag{B11}$$

$$J_w = -\omega\bar{t}_w I/F + J_w^{os} \tag{B12}$$

Ideal membrane ($\bar{t}_2$, $\bar{t}_w$, J_s, $J_w^{os} = 0$):

Equations (B4) and (B5) are simplified to

$$\Delta n_I = -z_I\frac{1}{z_1 v_1}x \tag{B13}$$

$$\Delta V_I = -z_I\frac{\bar{v}_s}{z_1 v_1}x \tag{B14}$$

By substituting eqs. (B13), (B14) and (B3) into eq. (5), we obtain :

$$(\Delta c^t - \Delta\bar{c}^\circ)_{ideal} = \frac{2(1 - \bar{v}_s\bar{c}^\circ)x}{z_1 v_1 V^\circ} \tag{B15}$$

By substituting eqs. (B4) and (B5) through eqs. (B3) and (B15) in the formula defining the current efficiency (eq. 3.5.1), we obtain:

$$CE = \frac{z_1 v_1 F}{I}\left[\frac{J_1}{v_1} - \frac{c^\circ\bar{v}_w}{1 - \bar{v}_s\bar{c}^\circ}J_w\right] \tag{B16}$$

By introducing eqs. (B11) and (B12) into eq. (B16), we finally obtain:

$$CE = z_1 v_1 \left[\frac{\bar{t}_1^r}{v_1} - \left(\frac{\bar{c}_s}{c_w} \right) \bar{t}_w - \omega \left(J_s - \left(\frac{\bar{c}_s}{c_w} \right) J_w^{os} \right) F/I \right] \quad \text{(B16a)}$$

where

$$\left(\frac{\bar{c}_s}{\bar{c}_w} \right) = \frac{\bar{v}_w \bar{c}^\circ}{1 - \bar{v}_s \bar{c}^\circ} = 0{,}018\tilde{m} \quad \text{(B17)}$$

$$\bar{c}^\circ = (c_a^\circ + c_k^\circ)/2 \quad \text{(B18)}$$

2. THE SYSTEM WITH ELECTRODE REACTIONS

In practice, in any system there are electrodes and electrode reactions which cause additional variations in the concentrations in mol/dm^3 of the solutions. Consequently, the differences Δn_i^{cor} and ΔV_i^{cor} will appear:

$$\Delta n_i^{mid} = z_i \Delta n^{mid} = \Delta n_i^{el} + \Delta n_i^{cor}, \quad i = a, c \quad \text{(B19)}$$

$$\Delta V_i^{mid} = z_i \Delta V^{mid} = \Delta V_i^{el} + \Delta V_i^{cor}, \quad i = a, c \quad \text{(B20)}$$

where Δn_i^{el} and ΔV_i^{el} denote changes of amount of ions and volume due to electrode reactions.

By substituting eqs. (B19) and (B20) through eqs. (B3) and (B5) into eq. (6), we obtain:

$$CE = \frac{z_1 v_1}{2(1 - \bar{v}_s \bar{c}^\circ)} \left[\frac{V^\circ F}{I} \left(\frac{\Delta c_c^t}{\Delta t} - \frac{\Delta c_a^t}{\Delta t} \right)^{pract} \underbrace{+ \Delta \bar{n}_c^{cor} - \Delta \bar{n}_a^{cor} - c_c^\circ \Delta \bar{V}_c^{cor} + c_a^\circ \Delta \bar{v}^{cor}}_{\text{correction}} \right] \quad \text{(B21)}$$

where $\Delta \bar{n}_i^{cor} = \omega \Delta n_i^{cor}/x$; $\Delta \bar{V}_i^{cor} = 1 - \omega \Delta V_i^{cor}/x$, $i = a, c$

$\Delta \bar{n}_i^{cor}$ and $\Delta \bar{V}_i^{cor}$ for some systems are presented in Table 1. Substitution in the right-hand term of eq. (B21) gives the necessary corrections[17].

Table 1: **Δn_i^{cor} and ΔV_i^{cor} for different electrode/electrolyte/membrane systems (eq. B21).**

	Cation-exchange membrane		Anion-exchange membrane ($z_2 = z$)	
	$i = a, c;\ z_a = 1;\ z_c = -1$			
Electrode	$\Delta \bar{n}_i^{cor}$	ΔV_i^{cor}	Δn_i^{cor}	ΔV_i^{cor}
Ag/AgCl Solute: $MeCl_z$	0	$z_i(\bar{v}_{Ag} - \bar{v}_{AgCl})$	z_i/z_2	$z_i(\bar{v}_s/z_2 + \bar{v}_{Ag} - \bar{v}_{AgCl})$
Pt Solute: $Me(OH)_z$	0	c: $\bar{v}_w$ a: $-0.5\bar{v}_w$	z_i/z_2	c: $-\bar{v}_s/z_2 + \bar{v}_w$ a: $\bar{v}_s/z_2 - 0.5\bar{v}_w$
Pt Solute: H_2SO_4	$-z_i/2$	c: $0.5\bar{v}_s$ a: $-0.5(\bar{v}_s - \bar{v}_w)$	0	c: 0 a: $0.5\bar{v}_w$

APPENDIX C

Table 1: **Electrodialysis desalination/concentration results of an approximately 1 000 mg/ℓ NaCl solution with Ionac MA-3475 and MC-3470 membranes at 0,5 V/cp (4 v/8 cp; 10V total).**

Time min	Current amp	Cf mS/m	Cf mg/ℓ	Cb mS/m	Cb mg/ℓ	pH feed	pH brine
0	0,18	170	992			7,1	
15	0,17	151	880	1 197	7 855	6,6	7,2
30	0,16	139	809	1 610	10 709	6,8	7,3
45	0,15	128	744	1 980	11 429	7,0	7,3
60	0,14	118	685	2 340	14 675	7,4	7,3
75	0,13	109	632	2 660	17 560	7,5	7,1
90	0,12	101	585	2 910	19 814	7,5	7,0
105	0,11	93,6	542	3 180	22 248	7,6	6,9
120	0,10	86,3	499	3 320	23 511	7,6	6,8
135	0,09	79,0	456	3 500	25 133	7,8	7,1
150	0,09	73,1	420	3 610	26 125	7,8	6,8
165	0,08	68,2	392	3 720	27 117	7,6	6,9
180	0,08	62,2	357	3 760	27 478	7,7	6,8
195	0,07	58,5	335	3 770	27 568	7,5	6,8
210	0,07	55,5	317	3 770	27 568	7,6	6,9
225	0,06	48,0	273	3 760	27 478	7,4	6,9
240	0,06	44,3	251	3 760	27 478	7,5	6,9
255	0,05	41,5	235	3 760	27 478	7,3	7,0
270	0,05	37,6	212	3 640	26 396	7,0	7,0

Cross sectional area of diluating chamber is:

13 cm x 0,2 cm = 2,6 cm^2

For a linear flow rate of 1 cm/s:

2,6 cm^2 x 1 cm/s = 2,6 cm^3/s (flow rate)

Therefore, for 10 diluating chambers, the flow rate must be 1 560 mℓ/min.

Flow rate used	:	1 350 mℓ/min
∴ Linear flow velocity	:	0,87 cm/s
Feed volume (beginning)	:	12 ℓ
Product volume (end)	:	11,25 ℓ
Brine volume (end)	:	230 mℓ
Brine conductivity	:	3 150 mS/m
Brine concentration	:	21 981 mg/ℓ

$\int f(x)\,dx$ = 15/2 (I1 + 2 (I_2 + I_3 + + In-1) + In)

= 7,5 (3,69)

= 27,675 amp.min

= 1660,5 amp.s (coulombs).

Salt equivalents removed:

Beginning: 12 ℓ x 992 mg/ℓ = 11 904 mg

i.e. $\frac{11\ 904}{58,44}$ = 203,7 me

End : 11,77 x 212 mg/ℓ = 2 495,24 mg

i.e. $\frac{2495,24}{58,44}$ = 42,7

∴ me removed = 161 me

= 0,161 ge

Current efficiency (%) = $96\ 500\ \frac{C}{ge} \times 0,161\ ge \times 100$

$10\ cp \times 1660,5\ C$

= 93,57%

Electrical energy consumption:

$$p = V \times I \times h \text{ (across membranes only)}$$

$$= 5 \times \frac{27,675}{60}$$

$$= 2,306 \text{ wh}$$

$$= 0,002306 \text{ kwh}$$

$$\text{Energy consumption/m}^3 = \frac{0,00231}{0,012}$$

$$= 0,19219 \text{ kwh/m}^3 \text{ feed}$$

$$\text{\% water recovery} = \frac{11,77 \times 100}{12}$$

$$= 98,08 \%$$

$$\text{\% Brine volume} = \frac{0,23 \times 100}{12}$$

$$= 1,92 \%$$

$$\text{Concentration factor} = \frac{21\ 981}{992}$$

$$= 22,16$$

$$\text{Water yield} = \frac{0,01177 \text{ m}^3 \times 1\ 440 \text{ min}}{0,169 \text{ m}^2 \times 270 \text{ min} \quad \text{d}}$$

$$= 0,369 \text{ m}^3/\text{m}^2\text{-d}$$

(**Note:** membrane area is 169 cm^2, but there are 10 membrane pairs, therefore total membrane area is 0,169 m^2).

Table 2: **Electrodialysis concentration/desalination results of an approximately 3 000 mg/ℓ HCl solution with Selemium AAV and CHV membranes at 2 V/cp (16 V/8 cp).**

Time min	Current amp	Vo V	Cf M	Cf mg/ℓ	Cb M	Cb mg/ℓ	V-Vo 10 cp	CD mA/cm²	Rcp	Specific resis-tance ohm·cm
0	3,48	1,08	0,091	3318			1,892	20,6	91,9	28
15	3,56	1,65	0,076	2771	1,7	61982	1,835	21,1	87,1	32
30	3,46	1,38	0,067	2463	2,1	76566	1,862	20,5	91,0	35
45	3,18	1,39	0,061	2224	2,2	80212	1,861	18,8	98,9	40
60	2,83	1,32	0,055	2005	2,25	82035	1,868	16,8	112	44
75	2,49	1,21	0,047	1714	2,25	82035	1,879	14,7	128	49
90	2,19	1,20	0,045	1641	2,1	76566	1,880	13,0	145	53
105	1,92	1,23	0,036	1313	2,0	72920	1,877	11,4	165	63
120	1,68	1,27	0,034	1240	1,95	71097	1,874	9,9	189	69
135	1,49	1,28	0,029	1057	1,85	67451	1,872	8,8	212	80
150	1,32	1,32	0,026	948	1,75	63805	1,868	7,8	239	85
165	1,16	1,42	0,022	802	1,65	60159	1,858	6,9	271	99
180	1,03	1,62	0,019	692	1,60	58336	1,838	6,1	302	111
195	0,93	1,86	0,018	656	1,50	54690	1,814	5,5	330	126
210	0,84	1,73	0,017	602	1,40	51044	1,827	5,0	368	139
225	0,75	1,83	0,014	510	1,35	49221	1,812	4,4	409	156
240	0,67	2,13	0,013	474	1,30	47398	1,787	4,0	451	174
255	0,61	2,13	0,012	419	1,2	43752	1,787	3,6	495	193

Linear flow velocity : 0,87 cm/s

Feed volume (beginning) : 12 ℓ

Product Volume (end) : 11,32 ℓ

Brine Volume (end) : 680 mℓ

Brine molarity : 1, 9 M

$\int f(x)\,dx = 15/2\,(I_1 + 2\,(I_2 + I_3 + \quad + In\text{-}1) + In)$

$= 7{,}5\,(63{,}09)$

$= 473{,}175$ amp·min

$= 28390,\ 5$ amp·s (coulombs)

Acid equivalents removed:

Beginning : $12\ \ell \times 3318\ mg/\ell = 39816\ mg$

i.e. $\frac{39816}{36,46} = 1092,05\ me$

End : $11,32\ \ell \times 419\ mg/\ell = 4743,08\ mg$

i.e. $\frac{4743,08}{36,46} = 130,09\ me$

$\therefore$ me removed $= 1092,05 - 130,09$

$= 961,96\ me$

$= 0,96196\ ge$

Current efficiency (%) $= \frac{96500\ C \times 0,96196\ ge \times 100}{ge}$

$\frac{}{10\ cp \times 28390,5\ C}$

$= 32,7\ \%$

Energy Consumption (P) $= V \times I \times h$

$= 20 \times \frac{473,175}{60}$

$= 157,725\ Wh$

$= 0,157725\ kwh$

$\therefore$ Energy Consumption/m^3 $= \frac{0,157725}{0,012}$

$= 13,15\ kwh/m^3\ feed$

% Water recovery $= \frac{11,32 \times 100}{12}$

$= 94,3\%$

% Brine volume $= \frac{0,68 \times 100}{12}$

$= 5,7\ \%$

Concentration factor $= \frac{69274}{3318}$

$= 20,9$

Water yield $= \frac{0,01132 \times 1440}{0,169 \times 255}$

$= 0,38\ m^3/m^2 \cdot d$

APPENDIX D

PUBLICATIONS BY J J SCHOEMAN

(a) Full length articles in specialist journals

Author(s)	Title	Year	Detailed reference
Schoeman, J J	Ontsouting van brakwaters en konsentrering van industriële uitvloeisels deur middel van elektrodialise	1983	Die Suid-Afrikaanse Tydskrif vir Natuurwetenskap en Tegnologie, 2 (4)
Schoeman, J J and Botha, G R	An evaluation of the activated alumina process for fluoride removal for drinking water and some factors influencing its performance	1985	Water S.A. 11 (1)
Schoeman, J J	The status of electrodialysis technology for brackish and industrial water treatment	1985	Water S.A. 11 (2)
Schoeman, J J	An evaluation of a South African clinoptilolite for ammonia-nitrogen removal from an underground mine water	1986	Water S.A. 12 (2)
Schoeman, J J	Rapid determination of the fouling of Electrodialysis membranes by industrial effluents	1987	Water S.A. 12 (12)
Schoeman, J J	An investigation of the performance of two newly installed defluoridation plants in South Africa and some factors affecting their performance	1987	Water Sci. Tech. 19
Schoeman, J J	The effect of particle size and interfering ions on fluoride removal by activated alumina	1987	Water S.A. 13 (4)
Schoeman, J J Buys, I J M Schutte, I B and McLeod, H	Pilot investigation on the treatment of fertilizer manufacturing process effluent using lime and electrodialysis reversal	1988	Desalination, 70
Schoeman, J J and Van Staden, J F	Evaluation of sealed-cell electrodialysis for industrial effluent treatment	1991	Water S.A. 17 (4)
Schoeman, J J, Van Staden, J F, Saayman, H M and Vorster, W A	Evaluation of reverse osmosis for electroplating effluent treatment	1992	Submitted for publication to Water Sci. Tech.
Schoeman, J J and Van Staden, J F	Electro-osmotic pumping of salts, acids and bases in a conventional electrodialysis stack	1992	Submitted for publication to Water S.A.